Design, Formulation and Evaluation of Liposomes Co-loaded with Human Serum Albumin and Rifampicin

A thesis submitted to Rhodes University in fulfilment of the requirements for the degree of

Master of Science (Chemistry)

By

ALAIN MURHIMALIKA BAPOLISI

B. Pharm. (Official University of Bukavu)

Supervised by Professor RUI WERNER MAÇEDO KRAUSE

January 2020

DEDICATION

*To my late father, Pharmacist **Pius Burhonyi Bapolisi**. I will always be proud to have had you as father and role model. May your soul rest in eternal peace Dad.*

ACKNOWLEDGEMENTS

I would like to acknowledge the support from all the wonderful people who made the completion of this work possible.

In a particular way, I would like to express my sincere gratitude to the following:

Professor Rui Werner Maçedo Krause, my supervisor and Head of the Chemistry Department, without his thorough and supportive guidance this work would not have been possible;

The NGO Förderverein Uni Kinshasa e.V./Else-KroenerFresenius Stiftung & Holger- Poehlmann Foundation, for all the intellectual and financial support throughout my studies;

Dr Christian Nkanga, for mentoring me since day one, for his thoughtful advices and for being a trusted friend;

Professor Roderick Bryan Walker, from the Pharmaceutics Division at Rhodes University, for all the useful scientific discussions and some material support provided;

The staff members of the Chemistry Department at Rhodes University;

The Chemistry Lab F22 and Pharmacy lab S12 mostly members for being good collaborators;

My family, especially my mother Léocadie Ntampaka, my brothers and sisters: Wyvine and Christian Birihanze, Carine and Achille Bapolisi, Nondine and Nérée Bapolisi, Odile and Olivier Mosimba, Emery Bapolisi, Daniella Bapolisi;

My unconditional friends and companions, Mugoli Kasole, Sylvia Pöhlmann, Justin Bazibuhe, Urbain Ndagano, Yolande Ikala, Mihlali Stoffels, Siphamandla Ruiters, Beli Bulambo, Christian Irenge, Gracien Misenga;

My BEBUC and CVX communities.

ABSTRACT

Tuberculosis (TB) is a devastating infectious disease caused by *Mycobacterium tuberculosis* and is the leading cause of death from a single infectious agent. The high morbidity and mortality rates of TB are partly due to factors such as the lengthy regimen (of 6–24 months), the development of drug resistance, and the pathogen location within the macrophages. These, with poor physiochemical properties of existing drugs hamper the effectiveness of the treatment despite the existence of potent antibiotics such as Rifampicin (Rif). Hydrophobicity plagues many drugs, including Rif, which are then particularly affected due to inherently poor intracellular availability. Novel drug delivery approaches are therefore needed in order to optimize the cytotoxic potential of said antitubercular drugs.

To improve the bioavailability of hydrophobic drugs, numerous delivery strategies have been developed. Amongst these, the coordination of cytotoxic drugs to therapeutic proteins have shown some success for improved efficacy in the management of illnesses including infectious diseases. Of therapeutic proteins, Human Serum Albumin (HSA) is an attractive drug carrier with interesting benefits such as low immunogenicity, antioxidant properties and improving cellular uptake of drugs through HSA-specific binding sites which are expressed on most cells including macrophages, where *M. tuberculosis* often resides. Hence, combination of Rif to HSA (Rif-HSA) seems a promising approach for improved intracellular delivery of Rif.

However, the *in vivo* stability of colloidal protein-based therapeutics is mostly challenging and an effective vehicle is needed to control the biological fate of such conjugates. Liposomes seem to be appropriate carriers for the Rif-HSA complex due to their reputable applicability for encapsulating diverse materials (i.e., hydrophobic and hydrophilic compounds or small and complex molecules) and preventing chemical and biological degradation of the cargo.

Therefore, the main objective of this study was to simultaneously encapsulate Rif and HSA in liposomes, which, to the best of our knowledge, has not been done before. The dual liposomes (Rif-HSA-lip) were made by a modified “Reverse Phase Evaporation” method (REV), following a Design of Experiments (DOE) approach to determine which factors impact the formulation. In addition, liposomes were made from crude soybean lecithin (CSL), rather than expensive and highly purified lipids.

The liposomes were fully characterised, and the encapsulation efficiency (%EE) was monitored using high-performance liquid chromatography (HPLC). The results were correlated with factors such as organic and aqueous phase composition, as well as the *in vitro* release profile of Rif.

Transmission electron microscopy (TEM) results confirmed the formation of spherical dual liposomes nanoparticles of roughly 200 nm. Dynamic light scattering (DLS) and Zeta potential measurements showed a negative charge (<–45 mV) and with satisfactory polydispersity (PDI<0.5).

HSA dramatically improved the aqueous solubility of Rif (from1.9 mg/ml in water to around 4.3 mg/ml in HSA 10% solution) mainly due to Rif-HSA hydrophobic interactions. This resulted in a good %EE of almost 60% for Rif, despite the presence of bulky HSA in the lipid bilayer. These details were confirmed using proton nuclear magnetic resonance (^{1}H NMR) and Fourier-transform infrared spectroscopy (FTIR).

Furthermore, energy dispersive X-ray (EDX) and DLS data suggested the presence of HSA poking out on the surface of liposomes, which is encouraging for potential targeted delivery in the future.

The *in vitro* release studies also depicted a substantial improvement in the diffusion of Rif in dual liposomes versus free Rif, from 65% after 12 hours for free Rif to 95% after only 5 hours for Rif-HSA-lip.

Finally, stability studies conducted over 30 days at room temperature, showed that the freeze-dried formulations of Rif-HSA-lip exhibited good shelf stability over liposomes with no HSA.

This study represents an illustrative example of co-loading of antibiotics and proteins into liposomes, which could encourage further development of novel nanoparticulate tools for the effective management of both drug-susceptible and -resistant infectious diseases such as TB.

GRAPHICAL ABSTRACT

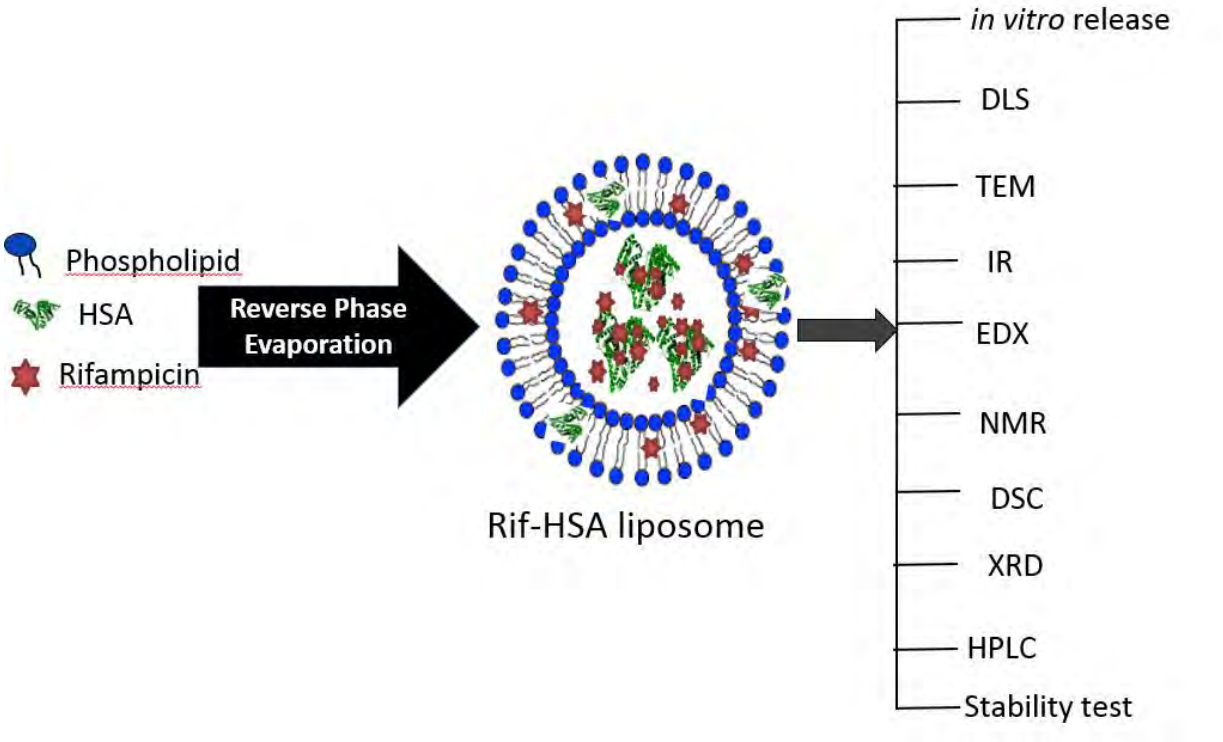

Co-loading and characterization of HSA and Rif in liposomes

TABLE OF CONTENTS

LIST OF FIGURES

LIST OF TABLES

Chapter One

General Introduction

Part of this chapter (particularly the liposomes section) has been published as a book chapter:

- *Christian I. Nkanga, Alain M. Bapolisi, Nnamdi I. Okafor, and Rui W.M. Krause; "General perception of liposomes: formation, manufacturing and applications". Book Chapter, in the Book under the working title: Liposomes - Advances and Perspectives, ISBN 978-1-78984-495-5. Editor Angel Catala, IntechOpen, London, England,* ***2019****.*
  DOI: http://dx.doi.org/10.5772/intechopen.84255

1. GENERAL INTRODUCTION

1.1. Tuberculosis

1.1.1. Epidemiology

Tuberculosis (TB) is an ancient disease that has affected humans for thousands of years. Its cause was only revealed in 1882, when Dr Robert Koch discovered the *Mycobacterium tuberculosis* complex. It is primarily a pulmonary (lungs) infection (85% of cases) but can also be extra-pulmonary (spine, brain, etc.) (WHO 2019; Pai et al. 2016). The World Health Organization (WHO) reported 10.0 million annual incidences of TB cases and 1.2 million deaths among HIV-negative populations in 2018. TB is one of the top 10 causes of global death and is presently recognised for outranking the human immunodeficiency virus (HIV) infection as the leading cause of death from a single infectious agent (WHO, 2019).

The high morbidity and mortality of TB are partly attributable to health-related risk-factors such as diabetes, smoking, alcohol abuse, undernourishment and HIV infection. HIV is a remarkable risk factor for progression of TB infection to active TB disease due to the considerable reduction of $CD4^+$ T cells (Pai et al. 2016). In 2018, it was globally reported that 8.6% of all TB cases were people living with HIV and an average of 251 000 deaths from TB among HIV-positive people (i.e. 33% of the total number of deaths caused by HIV/AIDS) (WHO, 2019).

TB disease affects both genders in all age groups, but men aged ≥ 15 years old represented the highest-burden with 57% of TB cases in 2018, while women accounted for 32% and children under 15 years old for 11%. The WHO classifies TB among the poverty-related diseases. TB affects predominantly developing regions in South-East Asia (44%), Africa (24%) and Western Pacific (18%) (WHO, 2019).

Figure 1.1 presents the estimated number of incident cases in 2018 for countries with at least 100 000 cases. India is the country with the highest-burden of TB with 27% of the global total cases of TB, followed by China and Indonesia with 9% and 8% respectively. In Africa, Nigeria (4%) and South Africa (3%) are the two most affected countries (WHO, 2019).

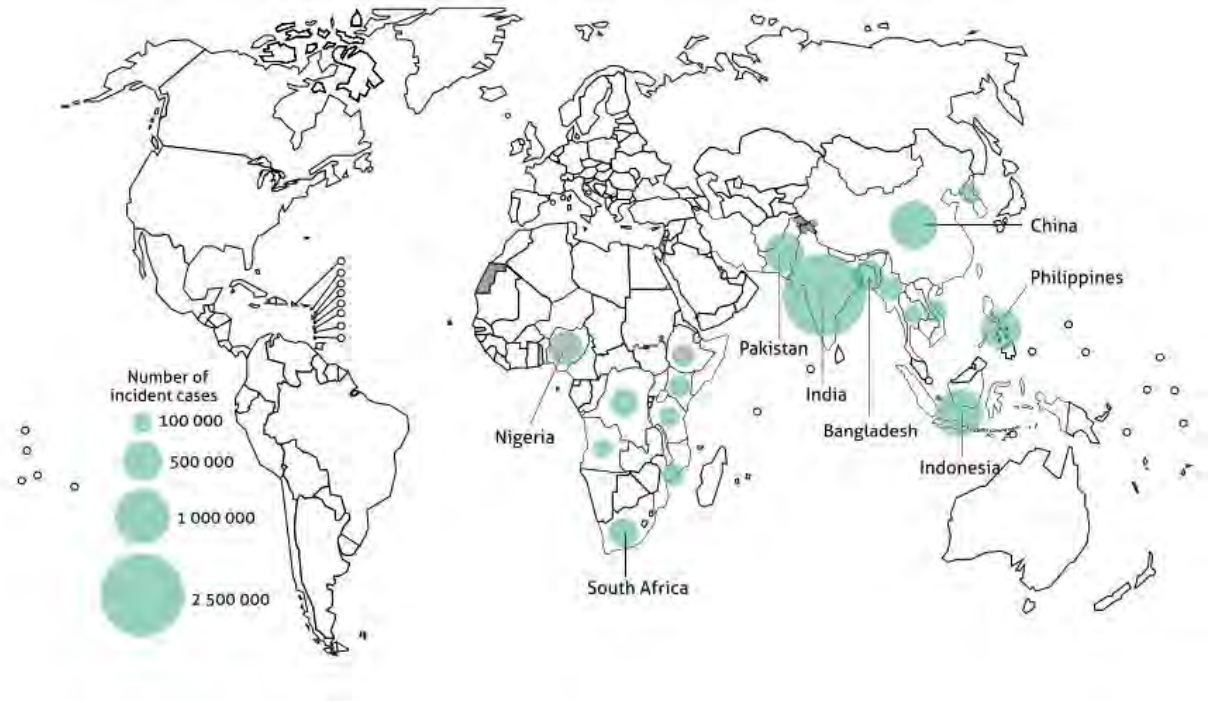

Figure 1.1: *Estimated TB incidence in 2018 (WHO, 2019)*

The United Nations Sustainable Development Goals (SDGs) include ending the TB epidemic by 2030 (under Goal 3). However, most WHO regions and countries with a high TB burden are failing to meet the 2020 milestones of the End TB Strategy. In fact, looking at the state of current indicators globally, the cumulative reduction of incidences between 2015 and 2018 was only 6.3% (while it is expected to be 20% by 2020) and the reduction of death was of 11% for the same period (although it is expected to reach 35% in 2020). In addition, TB-affected families face catastrophic costs. Intensive research and development are pivotal in order to meet the SDG and End TB Strategy targets for 2030 (WHO 2019; Stop TB partnership 2015).

1.1.2. Pathogen and pathogenesis

1.1.2.1.Pathogen

The genus *Mycobacterium* belongs to the family of Mycobacteriaceae, suborder of Corynebacterineae, order of Actinomycetales, phylum of Actinobaceria and kingdom of bacteria (Velayati and Farnia 2017). In general, TB is caused by *Mycobacterium tuberculosis* complex, an

aerobic bacillus that comprises diverse species including *Mycobacterium tuberculosis, Mycobacterium africanum, Mycobacterium bovis, Mycobacterium bovis* BCG, *Mycobacterium microti, Mycobacterium canettii, Mycobacterium caprae, Mycobacterium pinnipedii, Mycobacterium suricattae, Mycobacterium mungi, Mycobacterium dassie, and Mycobacterium oryx* (Velayati and Farnia 2017; Ingen et al. 2012). These species are identical at the nucleotide level, but they differ widely in terms of their host tropisms, phenotypes and pathogenicity. *M. tuberculosis* is the most dangerous species to humans; it affects humans and animals in contact with humans. *M. bovis* has the broadest spectrum, affecting humans, domestic and wild bovines and goats. The *M. bovis* BCG, also known as Calmette Guérin, is an attenuated strain of *M. bovis* and used as a TB vaccine (Velayati and Farnia 2017).

M. tuberculosis has an unusual composition of the cell wall, incorporating the characteristics of both Gram-positive and Gram-negative bacterium. It possesses multilayered peptidoglycan combined with arabinogalactan and reflects the characteristics of a Gram-positive bacterium. In addition, it has a significant amount of lipid components (especially mycolic acid) which are combined with surface glycolipids and form a pseudo lipid bilayer more related to the outer bilayer in a Gram-negative cell wall (Fu and Fu-Liu 2002). Unlike other bacteria, the cell wall of *M. tuberculosis* does not adsorb the Gram stain. Alternatively, acid-fast stains (Ziehl-Neelsen) or fluorescent stains (auramine) are used for revelation of the bacteria in microscopy (Cudahy and Shenoi 2016). *Mycobacteria* are nitrate and niacin positive but they require weeks for growth to be detected due to their very slow division rate every 12–24 hours (Wanger et al. 2017).

1.1.2.2.Pathogenesis

M. Tuberculosis is an airborne bacterium transmitted by inhalation of infectious droplet nuclei which are formed when a patient with active pulmonary TB disease coughs, sneezes or sings. The bacteria upon translocation to the lower respiratory tract infect the alveolar macrophages. In normal conditions, *M. tuberculosis* is eliminated either by innate or adaptive immune responses. Failure to eliminate the pathogen leads to its persistence in a quiescent state. The bacteria internalized in the alveolar macrophages outsmart the immune system and block the phagosome-lysosome fusion. Subsequent to the colonization of the macrophage by the bacteria, a multicellular host response called granuloma (consisting of macrophages, dendritic cells, monocytes, B cells, T cells) is generated to contain the infection. This stage of infection is called latent TB infection,

which is a controlled and asymptomatic infection. However, the bacteria consider the phagocytes forming the granuloma as a shelter and potential growing collection for their replication if the immune system fails to contain the infection under suppressed immune condition. When the bacterial load becomes important after replication the bacteria will disseminate to other organs throughout the body, enter the bloodstream and re-enter the respiratory tract. This stage is the active TB disease and the infected host is now infectious and symptomatic (Pai et al. 2016; Heemskerk et al. 2015). **Figure 1.2** depicts the pathophysiology of latent and active tuberculosis infections.

Clinically, three stages of TB infection can be differentiated: the latent TB infection (LTBI), the active TB disease and the subclinical TB. The LTBI is an asymptomatic and non-contagious state of TB infection. People with LTBI are at risk to develop active TB disease. The active TB disease is symptomatic and a transmissible state of the infection for which culture-based and molecular diagnostic are positive. The characteristic symptoms of active TB disease are fever, general fatigue, anorexia, weight loss and persistent cough and in the advanced state, haemoptysis. If not treated TB disease can cause death. The subclinical TB is a TB case for which the culture is positive but there is no signs or symptoms of the active TB disease (Pai et al. 2016).

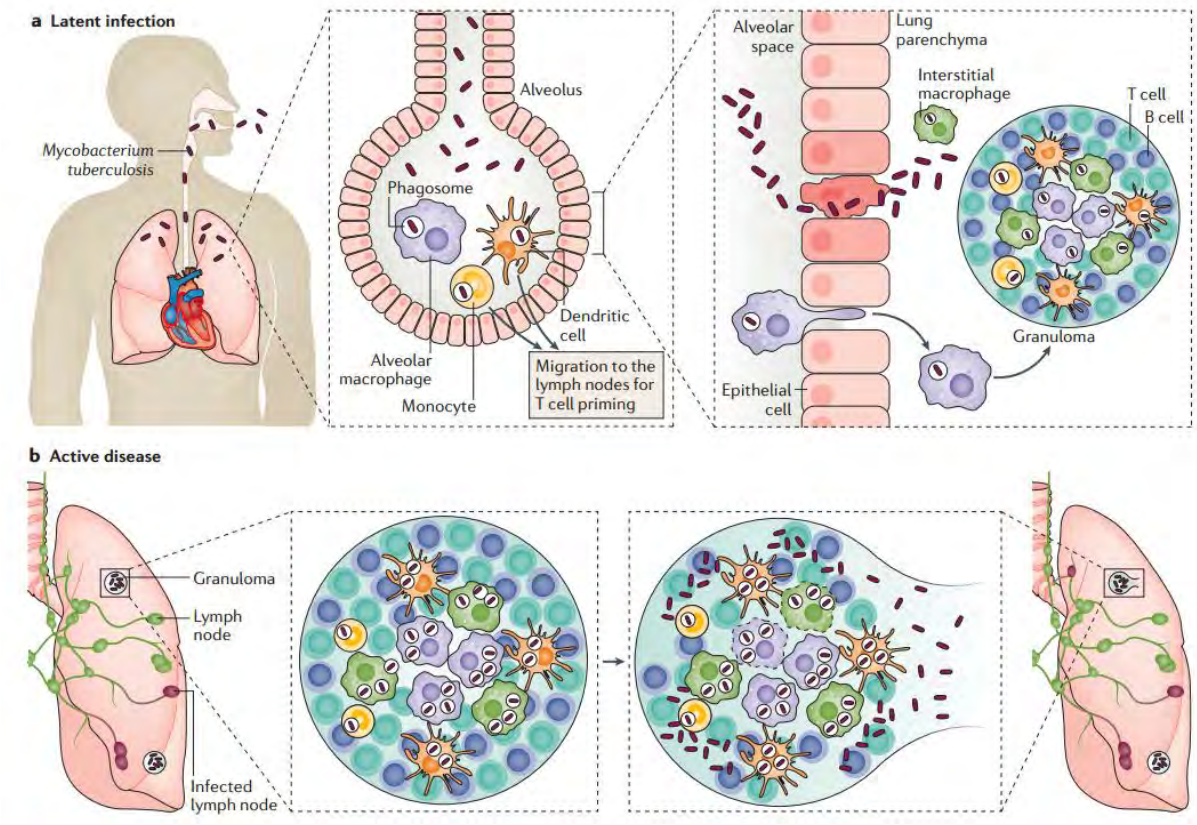

Figure 1.2 : *Pathophysiological representation of M. tuberculosis infection* (Pai et al. 2016)

1.1.3. Drug resistant TB

Drug resistant TB occurs as a result of gene mutations in *M. tuberculosis* that causes the bacteria to become resistant to most common anti-TB drugs. Human behaviour has been implicated as a source of the development of drug resistance and the main cause is non-compliance to the treatment regimens (Palomino and Martin 2014).

Worldwide, drug susceptibility testing plays an important role in drug resistance surveillance. It essentially consists of observing either the growth or the metabolic inhibition of *M. tuberculosis* in a medium containing the anti-TB drug. The genetic mutations related to the drug action can also be screened by molecular techniques (Kim 2005). The susceptibility testing is fairly reliable for isoniazid, rifampicin, fluoroquinolones and injectable agents such as streptomycin, amikacin and kanamycin (WHO, 2010).

Four types of drug-resistant TB can be distinguished: rifampicin-resistant TB (RR-TB); isoniazid resistant, rifampicin-susceptible TB (Hr-TB); multidrug resistant TB (MDR-TB); and extensively drug-resistant TB (XDR-TB). While RR-TB indicates TB strains resistant to rifampicin and may be susceptible or resistant to isoniazid, Hr-TB refers to TB strains that are resistant to isoniazid but are still susceptible to rifampicin. The term MDR-TB refers to TB strains that are resistant to both rifampicin and isoniazid. In 2018, half a million new RR-TB cases were detected, of which 78% were MDR-TB. XDR-TB refers to MDR-TB strains that, in addition to rifampicin and isoniazid resistance, are characterized by a resistance to at least one fluoroquinolone and a second line injectable agent (WHO, 2019, 2016).

Rapid molecular tests, culture methods and sequencing technologies are the main bacteriological confirmation techniques used to diagnose MDR/RR-TB (WHO, 2019).

1.1.4. Diagnosis

A timely diagnosis of TB is a key element in the disease management. LTBI can be tested either by the tuberculin skin test (TST) or the interferon-gamma release assay (IGRA) (WHO, 2018). The TST, also called the Mantoux skin test, consists of a transdermal injection of tuberculin units which activates immune reactions resulting in a delayed-type hypersensitivity response. The size of the induration at the site of injection after 48 to 72 hours determines the outcome of the test. However, the TST has limitations related to its low specificity and lack of sensitivity, particularly in immunosuppressed individuals (WHO 2019; Huebner et al. 1993).

The IGRAs measure the release of Interferon-γ (IFN-γ) from T lymphocytes after stimulation of the cells with *M. tuberculosis*-specific antigens, and can be performed using the enzyme-linked immunosorbent assay (ELISA)-based whole-blood method or the enzyme linked immunosorbent spot (ELISPOT) assay. Unlike the TST, the IGRAs are useful for testing the latent TB infection in BCG-vaccinated individuals (WHO, 2019; Zijenah, 2018). Nevertheless, both TST and IGRA have low predictive values since positive results might still be found due to the memory of T cell responses in individuals who successfully eliminate *M. tuberculosis* (Pai et al. 2016).

The risk population that should be identified for LTBI testing and eventually for treatment are people living with HIV, HIV-negative household contacts with bacteriologically confirmed

pulmonary TB, HIV-negative patients initiating anti-TNF treatment, receiving dialysis or preparing for an organ or haematological transplant, and patients with silicosis (WHO, 2018).

Several diagnostic tools have been approved by the WHO for active TB disease diagnosis. Pulmonary TB disease is commonly diagnosed using the sputum smear microscopy method, which is based on direct examination of sputum for acid-fast bacilli. It is a simple, cheap, rapid and highly specific method widely used in countries with a high TB burden. The loop-mediated isothermal amplification can also be used to diagnose pulmonary TB after processing of the sample and detection under ultraviolet light. The Gene Xpert MTB/RIF assay based on polymerase chain reaction offers the advantage of rapid simultaneous detection of *M. tuberculosis* Deoxyribonucleic (DNA) and rifampicin resistance from unprocessed sputum. The gold standard for TB diagnosis and drug resistance testing is culture examination and it should be performed to confirm the diagnosis of the disease. However, in the absence of a positive culture, signs and symptoms can be important to diagnose the TB disease in resource-limited conditions (Zijenah 2018).

Improved diagnostic techniques are being developed and have reached advanced stages in the diagnostic pipeline for active TB disease and drug resistance detection. For instance, the WHO (2019) currently recommends the lateral flow lipoarabinomannan (LF-LAM) assays for the diagnosis of TB in all HIV patients with symptoms of TB. The WHO is conducting evaluations of many new and improved diagnostic methods/settings such as the centralized high-throughput testing platforms based on polymerase chain reaction (The Real-Time MTB, the Roche Cobas MTB assay, the FluoroType MTBDR assay, Max MDR-TB assay), rapid tests for the detection of TB disease and drug resistance (the Xpert MTB/RIF Ultra (Ultra), the GeneXpert® Omni® (Omni), the Truenat MTB assays®) , computer-aided detection systems (chest X-ray), the Microbroth dilution method for drug Susceptibility testing (DST), and Critical concentrations of anti-TB medicines used for DST (WHO, 2019).

1.1.5. Therapeutic management and limitations

Preventive treatment of TB disease encompasses treatment of people with LTBI, prevention and control of *M. tuberculosis* transmission to high risk health persons (TB exposed individuals) and vaccination of children (WHO, 2019).

The preventive treatment of LTBI can be achieved mainly by using antibiotics from the group of rifamycins alone or in combination with other antimycobacterial agents. The regimen currently recommended by WHO (2019) for successful management of LTBI is summarized in **Table 1.1**.

Table 1.1*: WHO (2019) recommended regimen for LTBI*

Dosage	**Drug combination**	**Duration of the treatment**	**Regimen code**
A weekly dose	Rifapentine + Isoniazid	3 months	3HP
A daily dose	Rifampicin + Isoniazid	3 months	3RH
A daily dose	Rifampicin	3–4 months	4R
A daily dose	Isoniazid	6 months	6H

The Bacille Calmette-Guérin (BCG) is the only vaccine currently on the market that prevents severe forms of TB infections in children. BCG vaccination is now part of the national childhood immunization programs in countries epidemiologically affected by TB. However, currently there is no effective TB vaccine for adults (WHO, 2019).

The main objectives of TB disease therapy are (i) to reduce the propagation of the bacteria in patients by preventing death and stopping transmission of *M. tuberculosis*; (ii) to eradicate persisting bacilli so as to prevent relapse after completion of therapy; and (iii) to prevent development of drug resistance during treatment (Nahid et al. 2016).

The chemotherapeutic arsenal currently available for the management of TB disease comprises two categories of drugs, first line and second line drugs. First line drugs (group 1) constitute the basic treatment of TB diseases with drugs such as rifampicin, isoniazid, pyrazinamide, ethambutol and streptomycin. However, in most cases where first line drugs fail to cure the disease, due to development of drug resistance, the use of second line drugs is required. Second line drugs can be subdivided into further groups, namely injectable agents (group 2), fluoroquinolones (group 3), oral bacteriostatic agents (group 4) and other new agents with an unclear role in the management of TB (WHO, 2010). **Table 1.2** summarizes the five different groups of anti-TB drugs including available formulations, daily dosages and adverse events for each drug.

***Table 1.2**: Group of anti-TB drugs with preparation form and strength, dose and adverse effects (adapted from Heemskerk et al., 2015; WHO, 2010)*

Drug name	Form (strength)	Adult daily dose/kg weight (typical daily dose)	Main adverse effects
GROUP 1: FIRST LINE DRUGS			
Isoniazid	Tablets (50, 100, 300 mg), aqueous solution (100 mg/mL) for IV or IM injection.	5 mg/kg (300 mg)	Hepatitis; peripheral neuropathy
Rifampicin (Rifampin)	Capsules (150, 300 mg), powder for suspension, aqueous solution for IV injection	10 mg/kg (600 mg)	Hepatitis, orange discoloration of secretions; drug-drug interactions
Rifabutin	Capsules (150 mg)	5 mg/kg (300 mg)	Neutropenia, urine discoloration
Rifapentine	Tablets (150 mg film coated)	10–20 mg/kg (1200 mg)	Neutropenia
Pyrazinamide	Tablets (500 mg)	20–30 mg/kg	Hepatitis; arthralgia
Ethambutol	Tablets (100, 400 mg)	(400 mg)	Visual disturbance (acuity, color vision)
Streptomycin	Aqueous solution (1 g vials) for IM or IV injection	15 mg/kg (1000 mg)	Auditory nerve damage
GROUP 2: SECOND LINE DRUGS- INJECTABLE			
Kanamycin/ Amikacin	Aqueous solution (500 mg and 1 g vials) for IM or IV injection	15–20 mg/kg (1000 mg)	Renal failure
Capreomycin	Aqueous solution (1g vials) for IM or IV injection	15–20 mg/kg (1000 mg)	Nephrotoxicity, tubular dysfunction, azotemia, proteinuria, urticarial, maculopapular rash
GROUP 3: FLUOROQUINOLONES			
Levofloxacin	Tablets (250, 500, 750 mg), aqueous solution (500 mg vials) for IV injection	(500–1000 mg)	Generally well tolerated
Moxifloxacin	Tablets (400 mg), aqueous solution for IV injection	(400 mg)	
Ofloxacin	Tablets (200, 300, 400 mg)	(1000 mg)	
GROUPE 4: ORAL BACTERIOSTATIC SECOND LINE AGENTS			
Ethionamide	Tablets (250 mg)	15–20 mg/kg (1000 mg)	Severe gastrointestinal intolerance
Prothionamide	Tablets (250 mg)	15–20 mg/kg (1000 mg)	
Terizidone	Capsules (250 mg)	15–20 mg/kg (900 mg)	Neurological and psychiatric disturbances
Cycloserine	Capsules (250 mg)	10–15 mg/kg (250–500 mg)	Neuropathy and central nervous system disturbances
Para-amino salicylic acid	Granules (4 g packets), tablets (500 mg), solution for IV injection	(8–12 g)	Gastro-intestinal intolerance, hypothyroidism
GROUP 5: AGENTS WITH UNCLEAR ROLE IN THE TREATMENT OF DRUG RESISTANT TB			
Clofazimine	Capsules (100 mg)	(100 mg)	Ichthyosis and dry skin, brownish-black discoloration of skin, cornea, retina and urine, anorexia and abdominal pain
Linezolid	Tablets (600 mg)	(600 mg)	Gastrointestinal and vision disturbances, anaemia
Bedaquiline	Tablets (100 mg)	(400 mg)	Gastrointestinal disturbance, QT prolongation
Delaminid	Tablets (50 mg)	(200 mg)	QT prolongation

The recommended regimen for treatment of drug-susceptible tuberculosis consists of a combination of four first line TB drugs, isoniazid, pyrazinamide, ethambutol and rifampicin. Noteworthy, the incorporation of rifampicin, which is the most effective TB medicine in the late 1970s, has considerably shortened the TB treatment from 18–24 months to 6 months. The regimen of six months consists of first 2 months of intensive phase of treatment with isoniazid, rifampicin, pyrazinamide and ethambutol, followed by the continuation phase of 4 months of rifampicin and isoniazid treatment. Pyridoxine should be administered with isoniazid to all patients at risk of neuropathy (Nahid et al. 2016; Heemskerk et al. 2015). The treatment efficacy and progress can be monitored with the help of diagnostic techniques such as repeat sputum smears, cultures and X-rays (Pai et al. 2016). Whilst the success rate in the classical treatment of drug-susceptible TB is at least 85%, the success rate for MDR-TB treatment is merely 56%. The treatment of RR-TB and MDR-TB is generally longer and expensive and more toxic with more severe adverse events (WHO, 2019).

Generally, a treatment with second line TB drugs is required, and drugs for which there is possibility of cross-resistance should be avoided for MDR/RR-TB. Several regimens with different combinations are possible but each regimen should be carefully designed and frequently monitored by the use of culture to enable timely detection of a failing MDR-TB regimen and fast action (WHO, 2019, 2010). The WHO currently recommends an oral regimen lasting 18–20 months for most MDR/RR-TB patients, generally composed of a combination of fluoroquinolone, bedaquiline and linezolid plus at least one effective agent. The selection of medicines should be given based on the balance between relative benefits and potential harms. A standardised shorter regimen of 9–12 months for MDR-TB can be envisaged but under specific conditions such as the incorporation of a daily injectable agent for at least 4 months. A 6 month regimen of rifampicin, ethambutol, pyrazinamide and levofloxacin can be used for the treatment of Hr-TB (WHO, 2019, 2016).

However, the TB regimen is subject to various limitations, partly due to the long duration of the treatment, which results in toxic effects in some patients. Mild increases in the level of liver enzymes, skin rash, gastrointestinal intolerance, neuropathy and arthralgia are the common adverse events which can be handled without interruption of the treatment. Patients can also develop serious adverse events such as severe hepatitis, immune thrombocytopenia, agranulocytosis,

hemolysis, renal failure, optic neuritis, and ototoxicity. In such cases, discontinuation of the treatment and alternative regimens might be considered. The risk of treatment failure, relapse and development of drug resistance are higher due to high dosage frequency regimen and poor patient adherence to conventional therapies (Pai et al. 2016; Forget and Menzies 2006).

Therefore, novel drug delivery strategies are needed in order to improve TB drug efficacy, lessen the adverse effects, shorten the frequency of the regimen and consequently improve the patient compliance and prevent drug resistance. To achieve this, researchers have tried to encapsulate TB drugs in diverse drug carriers such as liposomes, niosomes, micelles, nano-emulsions, solid lipid nanoparticles, polymer based microparticles and nanoparticles, implants, etc. (Hussain et al. 2019).

Current efforts in research and development of TB drugs in the pharmaceutical sector are commendable. According to the last WHO TB report of 2019, 23 drugs in various combinations and 14 vaccine candidates were in clinical trials as of August 2019, and a vaccine candidate, M72/AS01$_{E,}$ showed promising results with protective effect among individuals with latent TB infection (WHO, 2019).

1.1.6. Rifampicin drug profile

In this work, rifampicin was chosen as the model drug for encapsulation studies firstly because it is the most effective anti-TB drug and secondly because of its poor aqueous solubility and lastly because of the unfortunate rapid development of RR-TB.

1.1.6.1.Physicochemical and molecular aspects

Molecular formula: $C_{43}H_{58}N_4O_{12}$

Molecular weight*:* 822.9 g/mole

Structure:

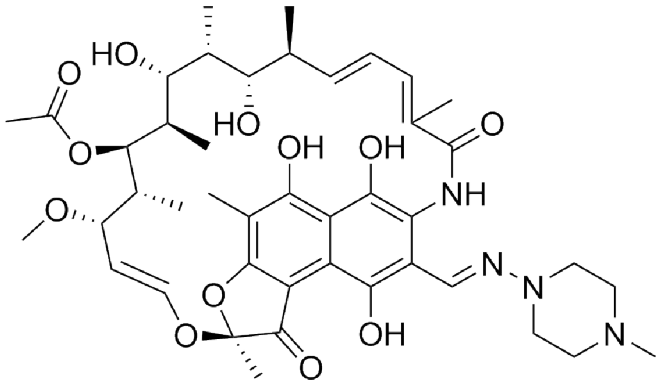

Figure 1.3 *: Molecular structure of rifampicin*

Systematic name (IUPAC):

[(7*S*,9*E*,11*S*,12*R*,13*S*,14*R*,15*R*,16*R*,17*S*,18*S*,19*E*,21*Z*)-2,15,17,27,29-pentahydroxy-11-methoxy-3,7,12,14,16,18,22-heptamethyl-26-[(*E*)-(4-methylpiperazin-1-yl)iminomethyl]-6,23-dioxo-8,30-dioxa-24-azatetracyclo[23.3.1.$1^{4,7}$.$0^{5,28}$]triaconta-1(29),2,4,9,19,21,25,27-octaen-13-yl] acetate.

Selected Depositor-supplied Synonyms

Rifampicin; Rifampin; Rifadin; Rimactane; Rimactan; Rifamycin AMP; Rifaldazine; Rifampicinum; Rifaprodin; Riforal; Tubocin; Rifa; Archidyn; Rifoldin; Rifoldine; Rimactizid; Rifagen; Rimazid; Arficin; Benemicin; Doloresum; Eremfat; Fenampicin; Rifaldazin; Rifaldin; Rifamor; Rifinah; Rifobac; Rimactazid; Sinerdol; Arzide; Rifcin; Rifam; Abrifam; Rifamsolin; Dipicin; Rimycin,; Rifamicin AMP, RIF, 3-([(4-Methyl-1-piperazinyl)imino]methyl)rifamycin SV (PubChem 2019).

Production

Rifampicin is among semisynthetic rifamycin derivatives. Rifamycins are antibiotics produced from a bacterium called *Amycolatopsis mediterranei* (previously known as *Nocardia mediterranei* or *Streptomyces mediterranei*). The bacterial fermentation in presence of added diethylbarbituric acid predominantly produces rifamycin B. Rifamycin B can be converted chemically, enzymatically or by biotransformation into rifamycin SV, which has more potent activity and clinical application. By semi-synthesis, different analogues of rifamycin SV can be produced, among them rifampicin, with N-amino-N'-methylpiperazine, which shows better activity against

Gram-positive and Gram-negative bacteria and particularly against mycobacteria. Other rifampicin derivatives also used in clinical application are rifabutin and rifapentin (**Figure 1.4**) (Floss and Yu 2005; Sensi 1983).

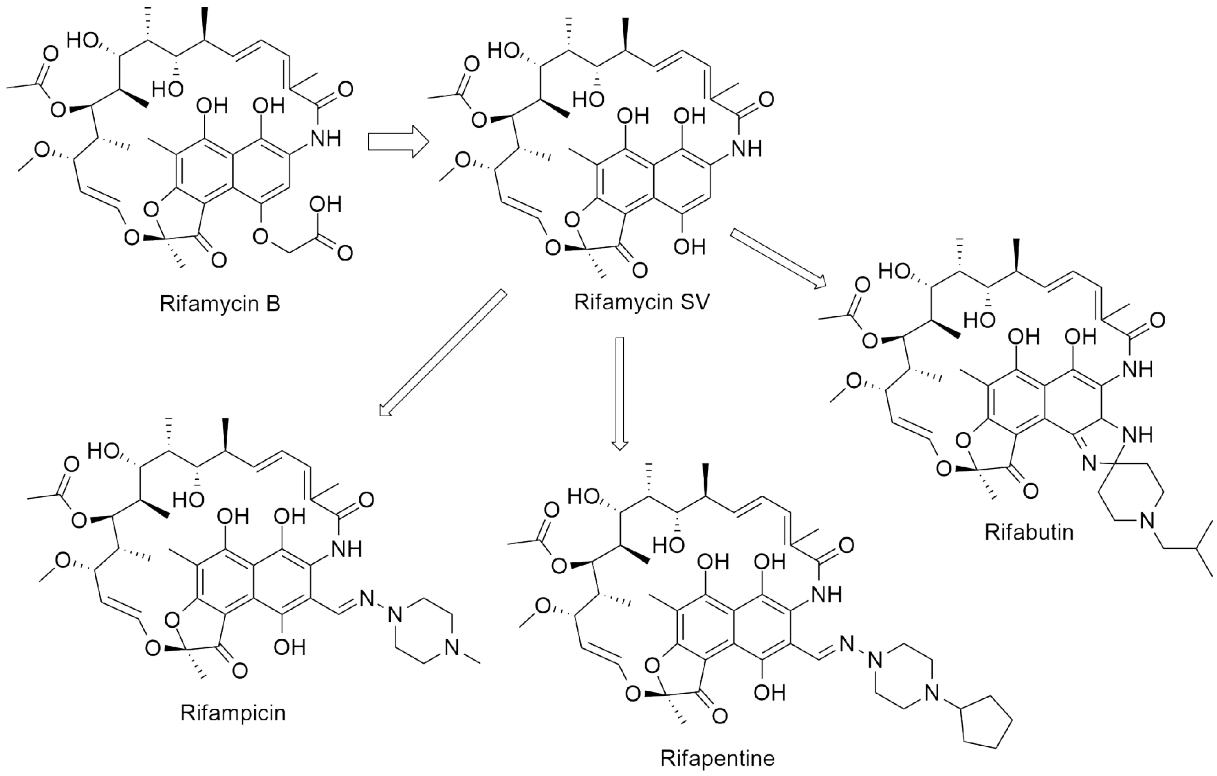

***Figure 1.4**: Conversion of rifamycin B into rifamycin SV and clinically used derivatives (adapted from Floss and Yu, 2005)*

Organoleptic characters

Rifampicin is an odourless orange-brown to red-brown crystalline powder (PubChem 2019).

Melting point: 183°C–188°C

Solubility

Freely soluble in methyl chloride, dimethyl oxide, chloroform, soluble in ethyl acetate, methanol and tetrahydrofuran, slightly soluble in water (pH less than 6), acetone, and carbon tetrachloride. In water, rifampicin solubility is 1.4mg/ml at 25°C (PubChem 2019).

Stability

Very stable in dimethyl sulfoxide, unstable in water, light, heat air and moisture (PubChem 2019). Not chemically stable in acidic conditions. Rifampicin can degrade by hydrolysis of the azomethine imine linkage to liberate 1-amino-4-methylpiperazine (Arca et al. 2018).

1.1.6.2.Pharmacological aspects

Drug class: antimycobacterial agents

Available dosage forms

Tablets, capsules, powder for suspension for oral administration and aqueous solution for intravenous injections.

Daily dose

8–12 mg/kg of body weight for adults and 10–20 mg/kg of body weight for children. Maximum dose: 600 mg per day.

Mechanism of action

Rifampicin blocks RNA transcription of the bacteria by binding to the pocket of DNA-dependent RNA polymerase located at the β subunit encoded by the *rpoB* gene, and therefore prevents elongation of RNA chains and consequently hinders bacterial protein synthesis (Floss and Yu 2005; Levin and Hatfull 1993).

Rifampicin resistance

Rifampicin is recommended for use in drug combinations (most commonly with isoniazid) because pathogens develop rifampicin resistance at a high rate. The predominant mechanism of rifamycin resistance is by mutation of the *rpoB* gene, which is the drug target. Another mechanism of resistance development is the inactivation of rifampicin by some bacteria such as the *Rhodococcus* species and *Mycobacterium smegmatis* through an inducible mechanism requiring *de novo* protein synthesis. However, this last mechanism is not likely to be clinically significant for *M. tuberculosis* infections (Floss and Yu 2005). The remarkable emergence of Rifampicin resistance strains underlines the urgent need for promoting targeted delivery of Rifampicin to drug-susceptible strains to avoid sub-dosing exposition, which encourages resistance development.

Thus, extensive research is underway to attempt controlled and targeted Rifampicin delivery at bacterial sites, achieving site-specific drug concentration and significant reduction of bacterial loads.

Pharmacokinetics

After oral administration, Rifampicin is rapidly absorbed and well distributed throughout the body. The half-life of rifampicin for a daily recommended single dose (600 mg) is about 2.5 hours In the hepatocyte, rifampicin is likely to be metabolized and undergo deacetylation. The resulting microbiologically active desacetylrifampicin is more polar than rifampicin and is easily excreted in the bile. Rifampicin can be excreted in the bile and the urine. The peak serum concentration is around 10 μg/ml within 2 hours. The amount of drug transported in the blood that binds to plasma proteins (mainly albumin) is roughly 80% (Acocella 1978). This illustrates high interactions between albumin-type proteins and Rifampicin and explains why formulation scientists are currently investigating Rif-Albumin complexes as a potent delivery system.

Therapeutic indications

Rifampicin is indicated in the treatment of drug susceptible TB infections (LTBI, pulmonary and extra-pulmonary TB diseases, Hr-TB). It is recommended for use in combination with other antimycobacterial agents. Rifampicin can also be used to treat other diseases such as leprosy (WHO 2010; Floss and Yu 2005).

Contraindications

Known hypersensitivity to Rifampicin and hepatic diseases.

Adverse effects

In most cases Rifampicin taken at the recommended dose is well tolerated by patients, but can cause gastrointestinal disturbance (abdominal pain, nausea, vomiting) and pruritus with or without rash. Fever, influenza-like syndromes and thrombocytopenia are more likely to occur with intermittent administration. In some patients, a 3 times' weekly regimen can induce temporary oliguria, dyspnea and hemolytic anemia. Dose-related hepatitis can potentially be fatal when the maximum recommended daily dose (600 mg) is exceeded (WHO, 2010). The relative toxicity of

rifampicin as well as its frequent side effects are part of the reasons why this drug makes a good candidate for drug delivery studies.

Drug interactions

As rifampicin induces hepatic enzymes, an increase in the dosage should be considered for some drugs metabolized in the liver such as some anti-infectives (including certain antiretroviral drugs), hormone therapy (i.e. norethindrone, tamoxifen, and levothyroxine), oral contraceptives, methadone, warfarin, cyclosporine, corticosteroids, anticonvulsants, cardiovascular drugs, theophylline, sylphonylurea hypoglycemic, and so on. The interaction of some antiretroviral drugs (non-nucleoside reverse transcriptase inhibitors and protease inhibitors) with rifampicin may lead to the ineffectiveness of antiretroviral drugs, failure of treatment of TB or an increased risk of adverse effects (WHO, 2010).

As with drug resistance and adverse effects, drug interactions also justify the need for Rifampicin encapsulation studies, since new delivery strategies are required to prevent such drug-drug interactions. To this effect, numerous studies have attempted to encapsulate Rifampicin in polymeric, lipid-based or proteins.

1.2. Therapeutic proteins

Proteins are the most abundant biological macromolecules of living cells. They are responsible for performing various vital functions in the immune, circulatory and homeostatic processes of the organism by acting as enzymes, hormones, regulatory, transport and structural molecules (Murray et al. 2017). The therapeutic potential of peptides and proteins against some life-threatening diseases and syndromes and advances in the pharmaceutical biotechnology industry have increased the value and number of protein-based products in the market and in the development pipeline. Antibodies, antibody-drug conjugates, vaccines, enzymes, cytokines, interferons and recombinant proteins are used for different purposes including diagnosis, prophylaxis, disease management and/or cure of various diseases such as cancer, inflammatory diseases, genetic disorders and infectious conditions (Lagassé et al. 2017; Akash et al. 2015; Dimitrov 2012).

1.2.1. Protein structure and function relationship

The structure of a functional protein is generally described in terms of four hierarchical levels of organization, primary, secondary, tertiary and quaternary structure. The formation of the primary structure is the first step to the actual synthesis of a protein. The monomeric units that form the linear polymer are 23 proteinogenic amino-acids, of which 20 are commonly referred to as standards amino acids (**Table 1.3)**. The basic structure of amino acids (**Figure 1.5**) consists of an alpha carbon covalently bonded to a hydrogen, a carboxylic carbon, an amine nitrogen and an amino acid-specific side chain (R'). The primary structure or polypeptide chain is produced from condensation reactions between amino acids. The bond formed between two amino-acids, called a peptide bond, results from the reaction between the carboxyl group of one amino acid and the amino group of the other amino acid. Proteins in their primary structure differ from one another in the sequence of their amino acids. The information dictating the sequence of amino acids to produce the needed protein primary structure is found in the genetic material, DNA (Murray et al. 2017).

The secondary structure of the protein is governed by the polarity of the amino acids which constitute its primary structure. In an aqueous environment, hydrophilic polar and charged side chains will easily interact with water through hydrogen bonding while the hydrophobic non polar side chains interact through Van der Waals forces and create a hydrophobic core in the folding-in of the protein. The polypeptide chain can adopt the shape either of alpha helices, beta strands, turns or random coils stabilized by the hydrogen bonding interactions between the N-H and C=O groups in the polypeptide backbone. The tertiary structure of protein is the resulting three-dimensional (3D) form that is adapted when the polypeptide folds into itself. Under physiological conditions, a stable fold or tertiary structure is required for a polypeptide to function as a protein. The tertiary structure is stabilized by hydrophobic interactions between nonpolar side chains and by disulfide bonds. Many proteins are composed by association of the folded chains of more than one polypeptide existing in their tertiary structure; this constitutes the quaternary structure (Murray et al. 2017; Petsko and Ringe 2004; Lodish et al. 2000).

Table 1.3: *List of proteinogenic amino acids*

N°	*Amino Acid Name*	*Abbreviation*
Nonpolar, hydrophobic, aliphatic		
1	Glycine	Gly
2	Alanine	Ala
3	Valine	Val
4	Leucine	Leu
5	Methionine	Met
6	Isoleucine	Ile
Nonpolar, hydrophobic, aromatic		
7	Phenylalanine	Phe
8	Tryptophan	Trp
Polar, uncharged, hydrophobic, aromatic		
9	Tyrosine	Tyr
Polar, uncharged, hydrophilic		
10	Serine	Ser
11	Threonine	Thr
12	Cysteine	Cys
13	Asparagine	Asn
14	Glutamine	Gln
15	Proline	Pro
Polar, negatively charged		
16	Aspartate	Asp
17	Glutamate	Glu
Polar, positively charged		
18	Lysine	Lys
19	Histidine	His
20	Arginine	Arg
Nonstandard proteinogenic amino acids		
21	Pyrrolysine	
22	Selenocysteine	
23	N-formylmethionine	

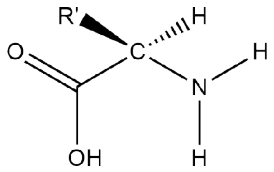

Figure 1.5*: General structure of amino acids*

1.2.2. Classification of therapeutic proteins

Leader et al., (2008) suggested a competent classification of therapeutic proteins into four groups based on the functions and applications of certain US Food and Drug Administration (FDA)

approved therapeutic proteins. **Table 1.4** summarizes classification of the four groups with subgroups and random examples of clinical applications.

Table 1.4: *Functional classification of protein therapeutics (adapted form Leader et al., 2008)*

Group	Subgroup	Drug examples (clinical use)
Group I: **Protein therapeutics with enzymatic or regulatory activity**	**Ia:** Replacing a protein that is deficient or abnormal	Insulin (diabetes); factor VIII (hemophilia A); β-Gluco- cerebrosidase (Gaucher's disease), Human albumin (hypoproteinemia)
	Ib: Augmenting an existing pathway	Erythropoietin (anemia), Human follicle-stimulating hormone (assisted reproduction) interferon-β1a (sclerosis); urokinase (pulmonary ambolism); trypsin (decubitus ulcer)
	Ic: Providing a novel function or activity	Botulinum toxin type A (cervical dystonia); L-asparaginase (acute lymphocytic leukemia)
Group II: **Protein therapeutics with special targeting activity**	**IIa:** Interfering with a molecule or organism	Bevacizumab (colorectal cancer), trastuzumab (breast cancer), infliximab (rheumatoid arthritis); Enfuvirtide (HIV infection)
	IIb: delivering other compound or proteins	Denileukin diftitox (persistent or recurrent cutaneous T-cell lymphoma whose malignant cells express the CD25 component of the Interleukin 2 receptor
Group III: **Protein vaccines**	**IIIa:** Protecting against a deleterious foreign agent	Hepatitis B surface antigen (Hepatitis B vaccination)
	IIIb: Treating autoimmune disease	Anti-Rhesus immunoglobulin G (Immunization in Rh(D)-negative women)
	IIIc: Treating cancer	*(in clinical trials)*
Group IV: **Protein diagnostics**		Recombinant purified protein derivative (Diagnosis of tuberculosis exposure derivative)

1.2.3. Protein-drug conjugates

Researchers have ingeniously exploited the propensity of small drugs to bind to proteins to design a novel therapeutic concept of protein-drug conjugates, which has shown promising development in the past decades. Some proteins such as albumin, IgG, IgM, transferrin, gelatin, human haptoglobin, hemoglobin A and fibrinogen have been successfully used for the development of protein conjugates. On conjugation to a high molecular weight protein, small drugs inherit certain physiological characteristics of proteins such as extended circulation time and selective

distribution to specific/targeted tissues. The pharmacokinetics behaviour and targeted potential of drugs can therefore be improved and the unwanted toxicity can be diminished (Vhora et al. 2015).

The recent development of Antibody-Drug Conjugates (ADCs), with improved efficacy and a better therapeutic index, seems to be promising for the management of life threatening diseases such as cancer (Diamantis and Banerji 2016; Casi and Neri 2012). For example, Trastuzumab emtansine (T-DM1) is an approved antibody drug conjugate for HER-2 positive breast cancer which was developed by linking a potent antimicrotubule agent, DM1, to the HER2-specific monoclonal antibody, trastuzumab (Krop and Winer 2014). The ability of antibodies to specifically bind to targeted antigens and their conjugation to cytotoxic drugs has gained considerable attention for potential therapeutic applications (Weiner 2015; Panowski et al. 2014). Additionally, it has been reported that the improvement in conjugation techniques of antibodies to small anti-infectious molecules could lead to successful therapies for infectious diseases (Meulen 2011) such as staphylococcus infections and TB (Mariathasan and Tan 2017). Lehar et al., (2015) have recently developed an Antibody-Antibiotic Conjugate (AAC) against intracellular *Staphylococcus aureus*, which was found to be superior to vancomycin for the treatment of bacteraemia.

In drug delivery sector, peptides and proteins are also used in the design of peptide- and protein-nanoparticle conjugates. They play a key role in improving, controlling and defining the performance of nanoparticles (Spicer et al. 2018). Among the therapeutic proteins, albumin-type proteins are among the most commonly investigated macromolecules for drug delivery application; which is one of the reasons why Human Serum Albumin was used in this study.

1.2.4. Albumin protein profile

Albumin is the most extensively used protein in clinical and biomedical research, mainly due to its versatility. It possesses advantageous intrinsic properties such as biocompatibility, low immunogenicity, biodegradability and nontoxicity (Tao et al. 2019; Kudarha and Sawant 2017; Larsen et al. 2016). The most common types of albumin that can be found commercially are ovalbumin (OVA), bovine serum albumin (BSA), and human serum albumin (HSA), which are produced from egg white, bovine serum and human serum respectively (Kudarha and Sawant 2017).

1.2.4.1.Human serum albumin profile

HSA is a large molecule (66.5 KDa) made of a sequence of 585 amino acids. It contains single tryptophan residue (Trp 214) and one free cysteine (Cys 34) and high amounts of glutamic acid (Glu), arginine (Arg) and lysine (Lys) (**Figure 1.6**). Produced in the liver (10–15 g daily), it is the most abundant protein in the plasma of human blood (35–50 g/L human serum), where it plays a vital role in maintaining the colloid osmotic pressure of the plasma. (Tao et al. 2019; Larsen et al. 2016). HSA is a negatively charged and highly water soluble protein with a long half-life of about 19 days, which is mainly due to the recycling of the protein through interaction with cellular receptors, notably the neonatal Fc Receptor (FcRn) mediated recycling, and the Megalin/Cubilin complex rescue from renal clearance (Larsen et al. 2016).

X-ray crystallography shows that HSA is a heart shaped monomeric globular protein. It contains 17 disulfide bridges that provide stability to the macromolecule. As shown in **Figure 1.7**, the 3D structure of HSA **s**uggests that the macromolecule consists of three homologous domains I, II, and III, and each domain contains two separate helical sub-domains A and B with 4 and 6 α-helices, respectively. HSA has two primary binding sites called Sudlow sites (I and II). The site I is located in subdomain IIA and is known to be the binding site for heterocyclic anions such as the anticoagulant drug warfarin. The site II is found in the subdomain IIIA and known as the binding site for carboxylates such as benzodiazepine and diazepam. In addition to the two Sudlow sites, the HSA has other binding sites such as fatty acid binding sites and a Cys34 binding site. Cys 34 is the binding site for Au (I), Hg (II) and complex Pt (II) in the form of cisplatin, nitric oxide (Kudarha and Sawant 2017; Larsen et al. 2016).

HSA is an outstanding protein which is resistant to changes in pH (stable in the pH range of 4–9), heat (can be heated up to 60°C) and exposure to organic solvents (Sleep 2015; Elzoghby et al. 2012).

	5	10	15
1	Asp - Ala - His - Lys - Ser - Glu - Val - Ala - His - Arg - Phe - Lys - Asp - Leu - Gly -		
16	Gly - Glu - Asn - Phe - Lys - Ala - Leu - Val - Leu - Ile - Ala - Phe - Ala - Gln - Tyr -		
31	Leu - Gln - Gln - Cys - Pro - Phe - Glu - Asp - His - Val - Lys - Leu - Val - Asn - Glu -		
46	Val - Thr - Glu - Phe - Ala - Lys - Thr - Cys - Val - Ala - Asp - Glu - Ser - Ala - Glu -		
61	Asn - Cys - Asp - Lys - Ser - Leu - His - Thr - Leu - Phe - Gly - Asp - Lys - Leu -Cys -		
76	Thr - Val - Ala - Thr - Leu - Arg - Glu - Thr - Tyr - Gly - Glu - Met - Ala - Asp - Cys -		
91	Cys - Ala - Lys - Glu - Gln - Pro - Glu - Arg - Asn - Glu - Cys - Phe - Leu - Gln - His -		
106	Lys - Asp - Asp - Asn - Pro - Asn - Leu - Pro - Arg - Leu - Val - Arg - Pro - Glu - Val -		
121	Asp - Val - Met - Cys - Thr - Ala - Phe - His - Asp - Asn - Gln - Glu - Thr - Phe - Leu -		
136	Lys - Lys - Tyr - Leu - Tyr - Glu - Ile - Ala - Arg - Arg - His - Pro - Tyr - Phe - Tyr-		
151	Ala - Pro - Glu - Leu - Leu - Phe - Phe - Ala - Lys - Arg - Tyr - Lys - Ala - Ala - Phe -		
166	Thr - Glu - Cys - Cys - Glu - Ala - Ala - Asp - Lys - Ala - Ala - Cys - Leu - Leu - Pro -		
181	Lys - Leu - Asp - Glu - Leu - Arg - Asp - Glu - Gly - Lys - Ala - Ser - Ser - Ala - Lys -		
196	Gln - Arg - Leu - Lys - Cys - Ala - Ser - Leu - Gln - Lys - Phe - Gly - Glu -Arg - Ala -		
211	Phe - Lys - Ala - Trp - Ala - Val - Ala - Arg - Leu - Ser - Gln - Arg - Phe - Pro - Lys -		
226	Ala - Glu - Phe - Ala - Glu - Val - Ser - Lys - Leu - Val - Thr - Asp - Leu - Thr - Lys -		
241	Val - His - Thr - Glu - Cys - Cys - His - Gly - Asp - Leu - Leu - Glu - Cys - Ala - Asp -		
256	Asp - Arg - Ala - Asp - Leu - Ala - Lys - Tyr - Ile - Cys - Glu - Asn - Gln - Asp - Ser -		
271	Ile - Ser - Ser - Lys - Leu - Lys - Glu - Cys - Cys - Glu - Lys - Pro - Leu - Leu - Gly -		
286	Lys - Ser - His - Cys - Ile - Ala - Glu - Val - Glu - Asn - Asp - Glu - Met - Pro - Ala -		
301	Asp - Leu - Pro - Ser - Leu - Ala - Ala - Asp - Phe - Val - Glu - Ser - Lys - Asp - Val -		
316	Cys - Lys - Asn - Tyr - Ala - Glu - Ala - Lys - Asp - Val - Phe - Leu - Gly - Met - Phe -		
331	Leu - Tyr - Glu - Tyr - Ala - Arg - Arg - His - Pro - Asp - Tyr - Ser - Val - Val - Leu -		
346	Leu - Leu - Arg - Leu - Ala - Lys - Thr - Tyr - Glu - Thr - Thr - Leu - Glu - Lys - Cys -		
361	Cys - Ala - Ala - His - Asp - Pro - Tyr - Glu - Cys - Ala - Ala - Lys - Val - Phe - Asp -		
376	Glu - Phe - Lys - Pro - Leu - Val - Glu - Glu - Pro - Gln - Asn - Leu - Ile - Lys - Gln -		
391	Asn - Cys - Glu - Leu - Phe - Glu - Gln - Leu - Gly - Glu - Tyr - Lys - Phe - Gln - Asn -		
406	Ala - Leu - Leu - Val - Arg - Tyr - Thr - Lys - Lys - Val - Pro - Gln - Val - Ser - Thr -		
421	Pro - Thr - Leu - Val - Glu - Val - Ser - Arg - Asn - Leu - Gly - Lys - Val - Gly - Ser -		
436	Lys - Cys - Cys - Lys - His - Pro - Glu - Ala - Lys - Arg - Met - Pro - Cys - Ala - Glu -		
451	Asp - Tyr - Leu - Ser - Val - Val - Leu - Asn - Gln - Leu - Cys - Val - Leu - Glu - His -		
466	Lys - Thr - Pro - Val - Ser - Asp - Arg - Val - Thr - Lys - Cys - Cys - Thr - Glu - Ser -		
481	Leu - Val - Asn - Arg - Arg - Pro - Cys - Phe - Ser - Ala - Leu - Glu - Val - Asp - Glu -		
496	Thr - Tyr - Val - Pro - Lys - Gln - Phe - Asn - Ala - Glu - Thr - Phe - Thr - Phe - His -		
511	Ala - Asp - Ile - Cys - Thr - Leu - Ser - Glu - Lys - Glu - Arg - Gln - Ile - Lys - Lys -		
526	Gln - Thr - Ala - Leu - Val - Glu - Leu - Val - Lys - His - Lys - Pro - Lys - Ala -Thr -		
541	Lys - Glu - Gln - Leu - Lys - Ala -Val - Met - Asp - Asp - Phe - Ala - Ala - Phe - Val -		
556	Glu - Lys - Cys - Cys - Lys - Ala - Asp - Asp - Lys - Glu - Thr -Cys - Phe - Ala - Glu -		
571	Glu - Glu - Lys - Lys - Leu - Val - Ala - Ala - Ser - Gln - Ala - Ala - Leu - Gly - Leu		

Figure 1.6 *: Complete amino acid sequence of HSA (adapted from Meloun et al., 1975)*

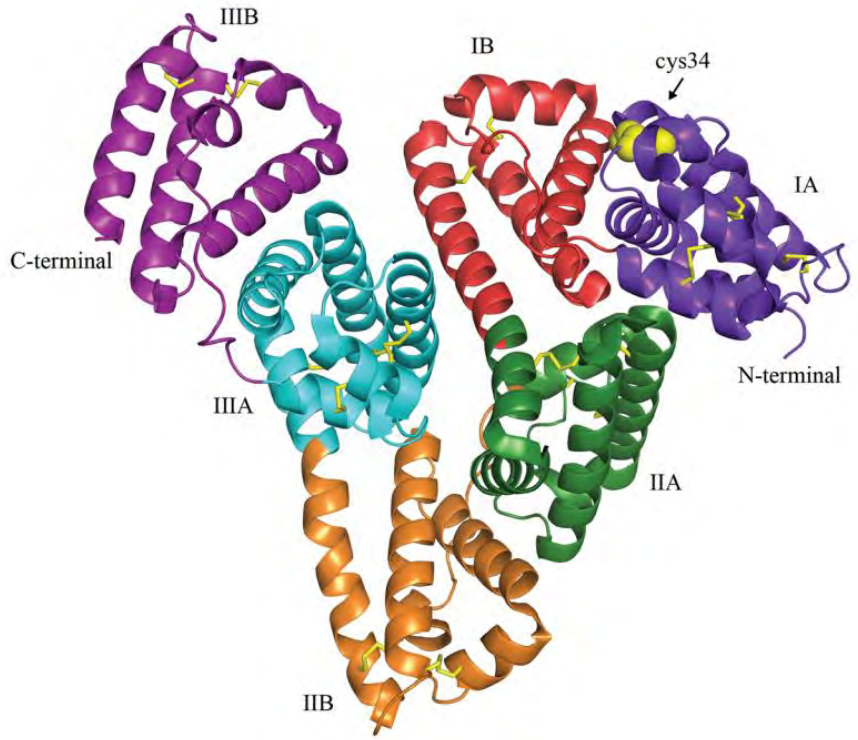

Figure 1.7: *Crystal structure of HSA* (Larsen et al. 2016)

1.2.4.2.Albumin applications

In clinical treatment, HSA is prescribed as a drug to increase circulating plasma osmolarity in order to maintain the blood homeostasis in various medical conditions such as hypoproteinemia, nephrotic syndrome, hypovolemia, hyperbilirubinemia (Tao et al. 2019; Leader et al. 2008).

Albumin has been used as a versatile carrier for drugs, genes, hormones, peptides and several other molecules due to its natural properties such as the transport function, the multiple ligand binding sites and the cellular interactions. Moreover, it has the potential to extend the half-life of the drug when used as a carrier (Kudarha and Sawant 2017; Larsen et al. 2016). Albumin can be used for the targeted delivery of drugs as tumour and inflamed tissues are known to preferentially uptake albumin. Albumin is also used as coating agent in order to enhance the biocompatibility of nanoparticles and biomedical devices and improve their targeted and trafficking features during drug delivery (Tao et al. 2019). Other benefits to albumin in drug delivery include assisting with release though the action of proteases, targeting albumin-specific binding sites, and using albumin fragments as intrinsic drug-release stimuli (Tao et al. 2019; Sleep 2015; Kratz 2008).

Albumin nanoparticles are generally biodegradable and easy to prepare. They can be fabricated by various nanotechnological methods such as desolvation, emulsification, thermal gelation and more specialized techniques such as nano-spray drying, nab-technology and self-assembly (Elzoghby et al. 2012).

Albumin-drug conjugates have been widely explored in cancer research and offer additional functionalization possibilities. PEGylation of the albumin conjugates can be expected to impart hydrophilicity and to improve the bloodstream circulation of the conjugates. Targeting ligands such as cyclic or acyclic RGD, lactosamine and folate can also be coupled in order to empower the conjugate with targeting potential (Vhora et al. 2015). In the management of infectious diseases such as TB, the ability to conjugate a second line TB drug P-Amino salicylic acid (PAS) to maleylated bovine serum albumin has significantly improved the uptake of the complex by the macrophage and consequently increased the intracellular anti-TB activity of PAS (M. Kaur et al. 2016).

1.2.5. Challenges of therapeutic proteins

The formulation of therapeutic proteins is more challenging than the formulation of conventional small chemicals. In fact, the preservation of stability of a protein is a critical factor for its functionality in biological media. Proteins are highly susceptible to degradation under variation of conditions such as temperature, solvent, pH, salt type and concentration, co-solutes, preservatives or surfactants. Therefore, appropriate physical and chemical conditions and excipients must be carefully selected in order to assure efficacy of the therapeutic proteins in formulations and minimize possible drug incompatibility and/or instability (Akash et al. 2015; Chi et al. 2003).

Although therapeutic proteins have proven clinical potentials, their efficacy is mitigated by limited therapeutic index, acquired resistance, individual patient variation and inefficient delivery (Kintzing et al. 2016).In addition to considering stability issues, a suitable vehicle and route of administration of therapeutic proteins should be envisaged, taking into consideration their hydrophobicity/hydrophilicity, large molecular size, rapid elimination and enzymatic degradation. Biodegradable polymers and nontoxic nanostructured materials such as liposomes have been intensively evaluated for successful delivery of therapeutic proteins (Akash et al. 2015)

1.3. Liposomes

1.3.1. General consideration of liposomes

Liposomes are artificial lipid-based bilayered vesicles firstly described by Bangham et al., (1965) as swollen phospholipid systems, which they named Banghasomes. Liposomes are small sphere-shaped vesicles, with sizes varying from a few nanometers to several micrometers. They consist of one or more phospholipid bilayers encapsulating an aqueous compartment, which makes them versatile carriers that can encapsulate materials of various polarities and natures (Lila and Ishida 2017; Bozzuto and Molinari 2015; Akbarzadeh et al. 2013).

Liposomes offer a wide range of applications across the pharmaceutical and cosmetic to food industries. In the biomedical sector liposomes are the most successful delivery system due to their multiple advantages. In addition to their co-loading capabilities, liposomes are biocompatible, biodegradable, nontoxic and non-immunogenic carriers that offer improved drug solubility and controlled distribution as well as the possibility of targeted delivery of the payload through surface modification. Liposomes can also prevent chemical and biological degradation of the encapsulated drugs (Nisini et al. 2018; Panahi et al. 2017; Lila and Ishida 2017; Pattni et al. 2015). Currently, several liposomal formulations have been clinically approved for various indications such as cancer therapy, fungal infections, photodynamic therapy, pain management and viral infections, and many more are under development and at advanced stages of clinical trials (Bulbake et al. 2017).

Although liposomes have provided some success in drug product development, the limitations identified in liposomal technology have remained almost stagnant over decades. The most common drawbacks of liposomes arise partly from poor stability under shelf and *in vivo* conditions. This is mostly due to potential lipid oxidation and hydrolysis, leakage and loss of hydrophilic cargoes, as well as particles fission and fusion. Some of these problems can be circumvented by playing around formulation adjuvants, such as anti-oxidants, or post-preparation processing, such as freeze-drying (Pattni et al. 2015; Akbarzadeh et al. 2013; Randles and Bergethon 2013).

1.3.2. Liposomes formation and classification

1.3.2.1.Liposomes formation

The main chemical constituent of liposomes are phospholipids. Phospholipids are amphiphilic molecules characterized by a hydrophilic head that consists of a charged phosphate moiety and hydrophobic tails corresponding to two acyl chains of fatty acids which can be saturated or unsaturated (Kalepu and Betha 2013; Mozafari 2010). In aqueous media, phospholipid molecules self-assemble into a bilayered structure. Within the bilayer phospholipid polar groups line up to form a water-attracting surface while their lipophilic chains face each other to yield a water-free zone. On mechanical shaking or heating, phospholipid bilayers continuously enclose the dispersing aqueous medium and form a vesicular system. In this system, hydrophilic groups of phospholipids are oriented towards the inner and outer aqueous phases, while their hydrophobic tails are centred within the bilayer (Lila and Ishida 2017; Pattni et al. 2015). This architecture underlines the ability of liposomes to readily encapsulate hydrophilic and hydrophobic materials inside the inner aqueous core and the lipid bilayers, respectively, as illustrated in **Figure 1.8**.

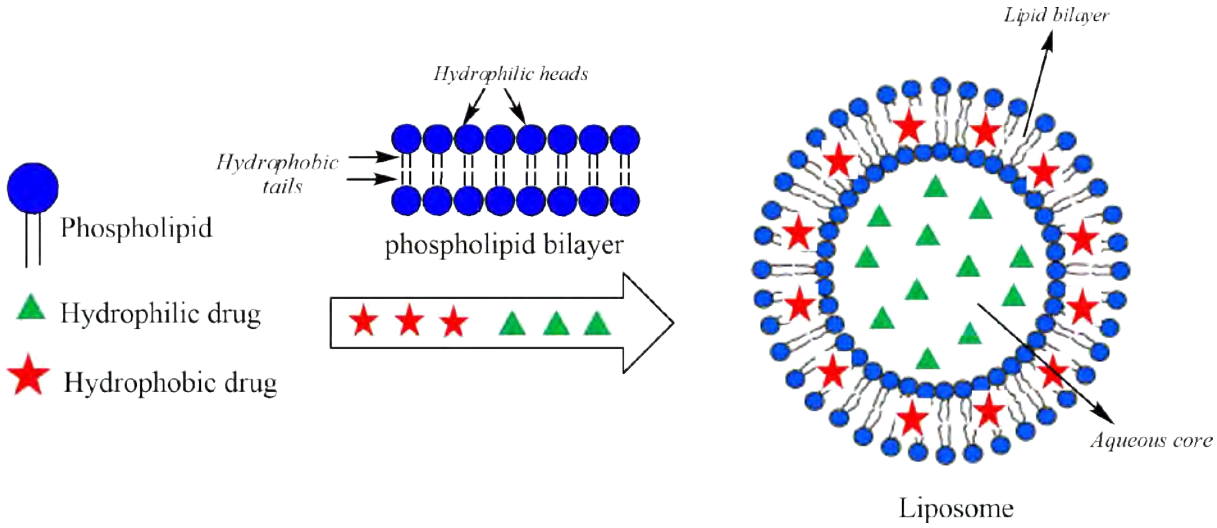

***Figure 1.8**: Flowchart illustrating liposome formation and encapsulation of drug molecules.*

1.3.2.2.Liposomes classification

Depending on the particle size and number of bilayers forming the vesicles (lamellarity), liposomes can be categorized into the following classes (Pattni et al. 2015; Rani 2013):

- Small unilamellar vesicles (SUV), size range 20–100 nm;
- Large unilamellar vesicles (LUV), size >100 nm;
- Giant unilamellar vesicles (GULV), size >1000 nm;
- Oligolamellar vesicles (OLV), size range 100–1000 nm;
- Multilamellar large vesicles (MLV), with size >500 nm;
- Multivesicular vesicles, size from 1000 nm to several thousand nanometers.

Based on their composition, liposomes can be classified as conventional, long circulating, cationic, stimuli-responsive or immunoliposomes. The differences between these categories will be highlighted in section **1.3.3.2** when discussing the composition and evolution of liposomes.
There are also many other vesicular systems also considered to be liposome-type vesicles. These include emulsomes, enzymosomes, sphingosomes, transfersomes, ethosomes, pharmacosomes and virosomes, which are lipid-based liposomes analogous. The non-lipid-based liposomes analogous are aquasomes, bilosomes and niosomes (Kamboj et al. 2013; Rani 2013). All the liposome-type systems are briefly presented in **Table 1.5**.

Table 1.5: *Presentation of liposome-type systems*

Vesicle designation	Main components	Illustrative application
Emulsomes	A mixture of fats and triglycerides stabilized by high proportion of lecithin	Emulsomes loaded with Amphotericin B for the treatment of visceral leishmaniasis (Kamboj et al. 2013)
Enzymosomes	Complexes of lipids and enzymatic proteins	Encapsulation and delivery of superoxide dismutase for oxidative stress management (Kamboj et al. 2013)
Sphingosomes	Sphingolipids containing amide and ether bonds	Sphingosomes loaded with vincristine (Marqibo®) for lymphoblastic leukemia therapy (Kamboj et al. 2013; Silverman and Deitcher 2013)
Transfersomes	A mixture of single chain surfactant, phospholipids and ethanol (10%)	Transfersomes loaded with diclofenac for improved topical delivery/retention (Ghanbarzadeh and Arami 2013)
Ethosomes	Phospholipids and ethanol (20–40%)	Mitoxantrone-loaded ethosomes for the treatment of melanoma (X. Yu et al. 2015)
Pharmacosomes	Conjugate of drug and phospholipid	Pharmacosomes loaded with diclofenac for enhanced the bioavailability and reduced toxicity (Kamboj et al. 2013)
Virosomes	Viral glycoproteins	Virosome containing HIV-1 gp41-subunit antigens for protection against vaginal simian-HIV (Bomsel et al. 2011)
Aquasomes	Tin oxide, diamonds or brushite core covered with oligomeric film	PEG-lipid coated aquasomes containing interferon-$_{\alpha}$-2b for prolonged and enhanced cytotoxicity (K. Kaur et al. 2015)
Bilosomes	Bile salts and acids (deoxycholic acid)	Bilosomes loaded with diphtheria toxoid for systemic and mucosal immunization (Shukla et al. 2011)
Niosomes	Non-ionic surfactants (span and tween)	Niosomes based formulation for enhanced oral bioavailability of candesartan cilexetil (Yuksel et al. 2016)

1.3.3. Liposomes composition and evolution

1.3.3.1.Liposomes composition

Liposomes consist of physiologically acceptable natural or synthetic phospholipids found in the lipid bilayer membranes of human cells. The main natural sources of phospholipids include vegetable oils from soybean, cotton seed, corn, sunflower, rapeseed and animal tissues such as egg yolk and bovine brain. The most common phospholipids used for liposomes preparation are

phosphatidylcholines (PC), phosphatidylethanolamines (PE), phosphatidylserines (PS), phosphatidylglycerols (PG), phosphatidic acid (PA), phosphatidylinositol (PI) and cardiolipin (CL) (Li et al. 2015). The basic molecular structures and characteristics of these biocompatible lipids are shown in **Figure 1.9**.

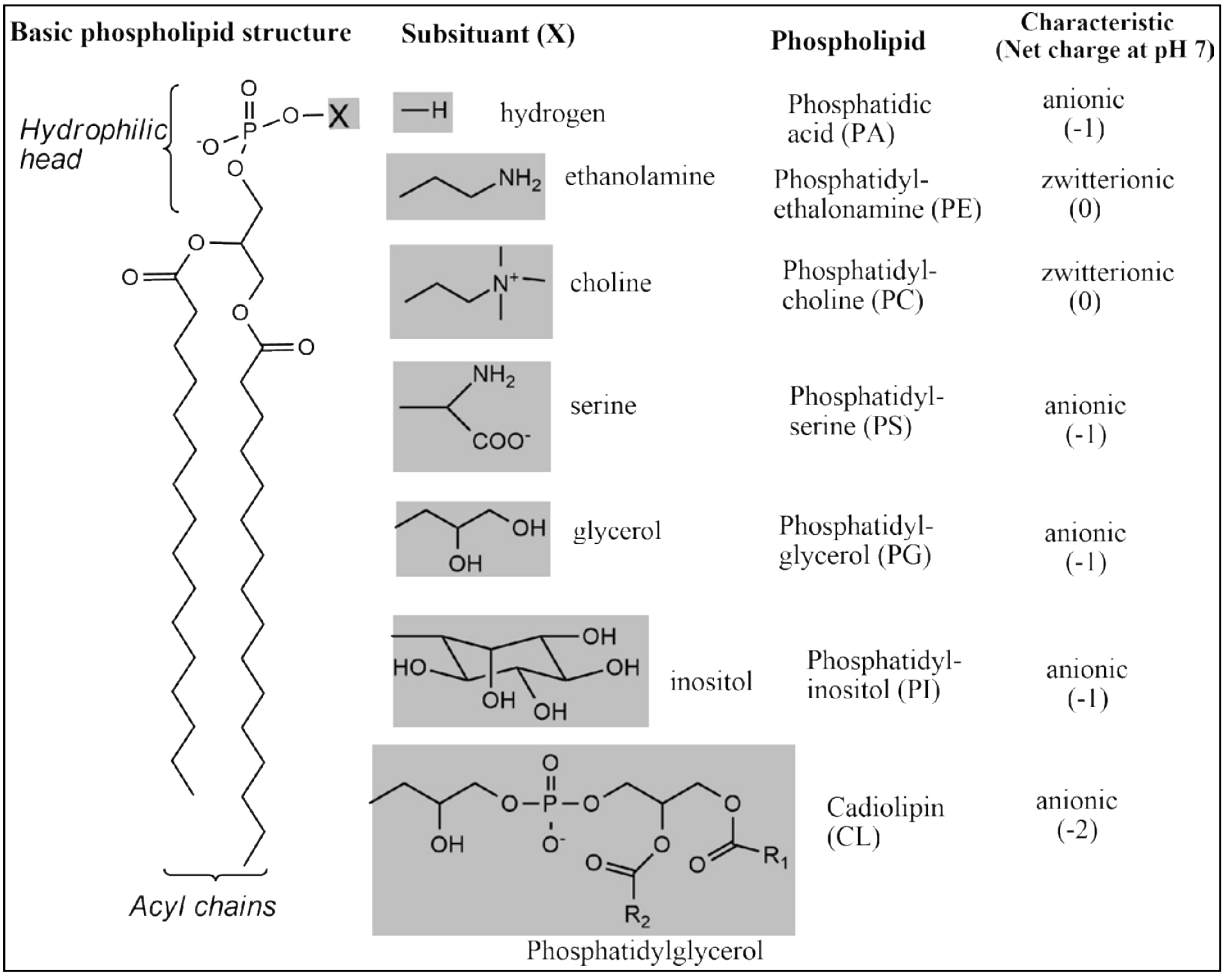

Figure 1.9: *General structure of phospholipids and common head groups (adapted from Li et al. 2015; Aktas et al. 2014)*

In liposomal technology, considerable attention is given to the transition temperature (Tt) phase of these phospholipids. The Tt refers to the temperature above which phospholipids exist in liquid crystalline phase. In this fluid state, hydrophobic tails of phospholipids are randomly oriented but ready to form closely continuous bilayered vesicles (liposomes). Below the Tt, phospholipids exist in gel state, where the hydrophobic tails are completely expanded and well packed, thus not able to form liposomes (Pattni et al. 2015; Patel and Panda 2012).

As most of the phospholipids used for liposomes formulation have a Tt close to the physiological temperature (37°C), the addition of cholesterol has been adopted as a strategy to stabilize the liposomal vesicles in physiological media. This is especially significant for phospholipids that can undergo phase transition and leakage at room temperature, which can lead to the premature release of the liposome cargo. In fact, due to its high hydrophobicity, cholesterol was found to be efficient in strengthening the packing of phospholipid bilayers, thereby reducing membrane permeability. Numerous studies have reported the ability of cholesterol to impact liposome properties and functionality, including encapsulation efficiency and release characteristics (Vemuri and Rhodes 1995; Taylor et al. 1990; Kruyff, Demel, and Deenen 1971). The work by Kirby et al., (1980) demonstrated that increasing cholesterol content can prevent leakage and improve *in vivo* stability of liposomes. Later, Lopez-Pinto et al., (2005) observed a direct correlation between cholesterol content and liposome sizes. These observations have established cholesterol content as a key parameter in liposome formulation.

Like cholesterol, there are many other ingredients that can affect liposome behaviour and afford the desired encapsulation or delivery profiles. Additive agents such as oleic acid and N-[1(2,3-dioleoyloxy) propyl]-N,N,N-trimethylammonium chloride (DOTAP) are useful for the preparation of negatively and positively charged liposomes, respectively. These charged liposomes offer the advantage of great liposomal stability during storage, as charged particles repel each other and reduce aggregation tendencies. While the cell internalization of positively charged liposomes (cationic liposomes) is promoted by their electrostatic interaction with cell membranes (which are negatively charged), liposomes bearing negative charges are subject to poor cell internalization due to the corresponding repulsive forces. Cationic liposomes are used in gene therapy due to their ability to successfully encapsulate nucleic acids by electrostatic forces (Pattni, Chupin, and Torchilin 2015; Paecharoenchai et al. 2012).

In addition, some special lipids such as cholesteryl hemisuccinate (CHEMS) and 1,2-dioleoyl-sn-glycero-3-phosphoethanolamine (DOPE) have been widely used to prepare liposomes with pH-dependent release features. CHEMS can exhibit pH-sensitivity either alone or in the presence of other lipids. In ionized forms at basic or neutral pH, CHEMS stabilizes the lamellar form of DOPE in lipid-based vesicles. However, the protonated or molecular CHEMS formed at acidic pH promotes the hexagonal phase of this lipid, which leads to the disruption of the vesicular systems and release of the encapsulated materials (H. Xu et al. 2008; Hafez and Cullis 2000). Tocopherol

hemisuccinate (THS) has shown a similar pH-responsiveness as CHEMS, due to its molecular similarity (H. Xu et al. 2012).

The composition of liposomes appears to be a broad topic, but is crucial for the desired product development. However, the nature and costs of the liposome components used in previous decades, particularly the synthetic or highly purified natural phospholipids, have been reported to be among the factors negatively affecting the universal implementation and affordability of liposome technology (Li et al. 2015; Yokota et al. 2012). The review by Machado et al., (2014) discussed the feasibility of using crude soybean and rice lecithin for liposomal encapsulation of food ingredients. The authors demonstrated that these naturally occurring phospholipid mixtures could be useful for liposomes preparation regardless of the intended area of application. Nkanga et al., (2017) recently investigated liposomal encapsulation of isoniazid using crude soybean lecithin. The formulated liposomes exhibited much better encapsulation efficiency than purified soybean lecithin. This study proposed crude soybean lecithin for liposomal encapsulation of drug molecules. However, the complexity of this lipid mixture might be a bottleneck for some biomedical applications, where molecular architecture of the lipid bilayer must be explored to obtain insights into potential cell membrane permeability. The versatility of crude soybean lecithin liposomes (soy-liposomes) is therefore limited, considering the wide range of applications that the liposomal systems usually cover.

1.3.3.2.Liposomes evolution

Based on the composition, liposomal systems can be considered to have evolved from conventional, long circulating, targeted and immune-liposomes to stimuli-responsive liposomes. The liposomes composed purely of phospholipids with or without cholesterol (conventional liposomes) have shown some limitations due to their uptake by the cells of the mononuclear phagocytic system (MNPS), such as macrophages that ensure liposomes clearance through phagocytosis. This biological fate makes conventional liposomes appropriate vehicles for targeted drug delivery to infected MNPS cells, as is the case of alveolar macrophages where *Mycobacterium tuberculosis* often resides. However, the uptake by the MNPS cells decreases liposomes half-life and exposes to high risk of therapeutic failure when the site of interest is beyond the MNPS (Lila and Ishida 2017).

Extensive studies conducted in liposome technology have led to the identification of some astute strategies for addressing the issue of MNPS' attack, namely, liposome downsizing and surface modification. In this regard, it was observed that the physiological clearance of larger liposomes (MLV) was much quicker than that of smaller liposomes (SUL), which describe long-circulating profiles with increased half-lives (Immordino et al. 2006). The stealth strategy arising from surface modification involves grafting or coating hydrophilic polymers such as polyethylene glycol (PEG) and chitosan, which prevents detection of liposomes by the MNPS cells. While stealth behaviour allows liposomes to achieve a much longer circulation time (hence the name 'long circulating liposomes'), this strategy comes with poor targeting efficiency due to the wider distribution of liposomes in the body. Due to this limitation, further developments have led to the introduction of targeted liposomes. These liposomes are characterized by surface decoration with glycoproteins, polysaccharides or specific receptor ligands to achieve narrowed distribution and accumulation at the site of interest (Kamboj et al. 2013; Torchilin 2005) . The observation that ligand-decorated liposomes could provide selective drug accumulation inspired further design of antibody-functionalized liposomes (immunoliposomes) as well as stimuli-responsive liposomal systems for controlled drug delivery (Nisini et al. 2018). **Figure 1.10** shows the trend in the development of 'intelligent' liposomes for site-specific delivery, from conventional liposomes, stealth liposome, targeted liposomes, immunoliposomes to stimuli-responsive liposomes.

Stimuli-responsive liposomes are smart liposomal systems that exhibit rapid release of the cargo due to changes in some physicochemical or biochemical stimuli, such as pH, temperature, redox potentials, enzyme concentrations, ultrasound, electric or magnetic fields (Karanth and Murthy 2007; Drummond et al. 2000).

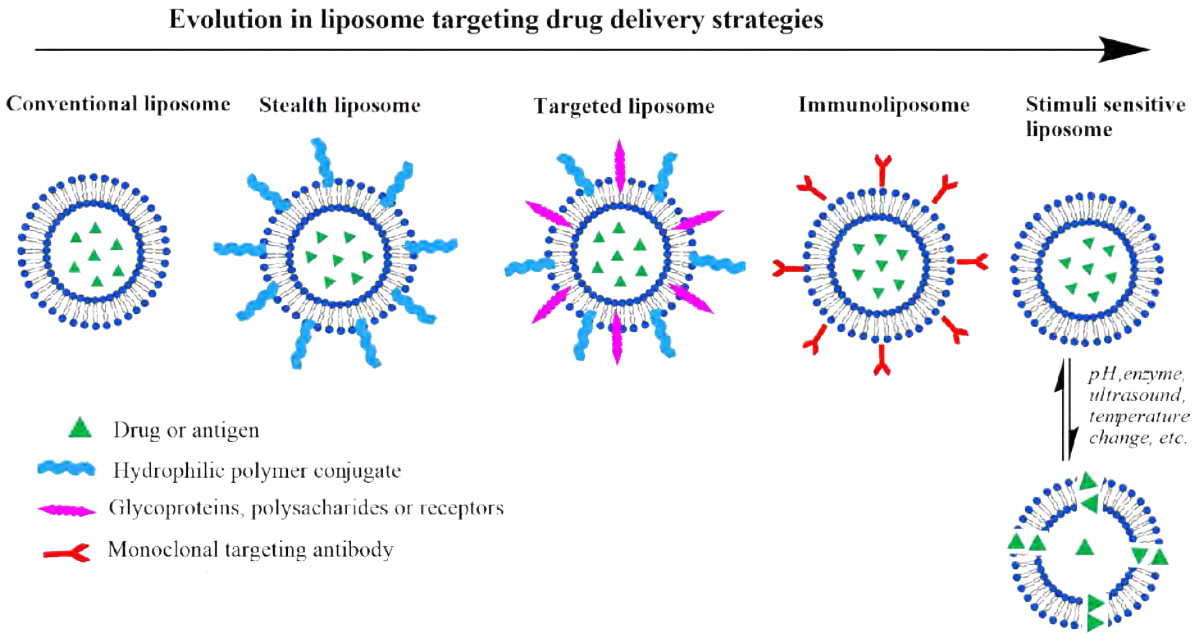

***Figure 1.10**: Schematic representation of the trend in liposome improvements for site specific delivery (adapted from Nisini et al. 2018)*

1.3.4. Liposomes preparation and characterization

1.3.4.1.Preparation methods

Liposomes can be prepared using a wide range of methods that involve a combination of lipids with aqueous media which affect liposome characteristics such as size, lamellarity and encapsulation efficiency (EE). The recently reported methods can be categorized as conventional, which mostly involve approaches that are easy to use at laboratory scale, and advanced methods that appear to be more useful for up-scale production but require some special equipment (Pattni et al. 2015).

- **Conventional methods**

The most commonly used methods for the formulation of liposomes share the following fundamental stages, (i) lipid dissolution in organic solvents, (ii) drying of the resultant solution, (iii) hydration of dried lipid (using various aqueous media), (iv) isolation of the liposomal

vesicles, and (v) quality control assays (Akbarzadeh et al. 2013). While sharing these basic stages, the conventional preparation methods have different advantages and disadvantages that are comparatively presented in **Table 1.6**. The specific technological details of these methods are separately discussed in the following paragraphs.

Table 1.6: *Advantages and disadvantages of conventional methods (adapted from Maherani et al. 2011)*

Method	Advantages	Drawbacks
Film hydration (Bangham method)	Simple process	Require organic solvent and mechanical agitation, production of large particles with no control on size, poor encapsulation efficiencies of hydrophilic materials, time consuming, sterilization issue
Reverse phase evaporation	Simple design, high encapsulation efficiency	Not applicable to fragile payloads due to large quantity of organic solvent use, time consuming, sterilization issue
Solvent injection	Simple process	Traces of organic solvent as residue, possible nozzle blockage in ether system, time consuming, sterilization issue
Detergent removal	Simple design, homogenous product, control of particle size	Presence of organic solvent, detergent residue, time consuming, low entrapment efficiency, poor yield, sterilization issue
Heating method	Simple and fast process, organic solvent free, no need for sterilization, possible up-scale production	High temperature required

.

- **Film hydration**

Also known as the Bangham method, film hydration represents the simplest and oldest method used in liposome technology. In this method, lipids are first dissolved in a suitable organic solvent, and dried down to yield a thin film at the bottom of the flask. The obtained lipid film is hydrated using an appropriate aqueous medium to produce liposomal dispersion. The structural organization of the formed vesicles can be affected by the hydration conditions. A gentle hydration of the lipid film forms giant unilamellar vesicles (GULV), whereas a harsh hydration gives rise to multilamellar vesicles (MLV) with poor size homogeneity, which requires an additional downsizing step. The most commonly used sizing methods are probe and bath sonication, which

yield small unilamellar vesicles (SUV). Despite its higher effectiveness, probe sonication is often blamed for potential contamination (with titanium from the titanium-based nozzle used for mechanical agitation), and the production of local heat that can affect lipid and drug stability. Although the two sonication methods produce liposomes with identical characteristics, the use of bath sonication remains a better option due to easy control of operational parameters. Another technique used for liposome sizing is the consecutive extrusion of the liposomal formulation through polycarbonate filters of defined pore sizes. In this method, the number of extrusion cycles is the key parameter to control for effective homogenization (Pattni et al. 2015; Akbarzadeh et al. 2013).

- **Reverse phase evaporation**

Reverse phase evaporation method (REV) is an alternative method to film hydration that involves the formation of water-in-oil emulsion between the aqueous phase (containing hydrophilic materials) and the organic phase (containing lipids and any hydrophobic materials). A brief sonication of this mixture is required for system homogenization. The removal of the organic phase under reduced pressure yields a milky gel that subsequently turns into a liposomal suspension. The liposomes can be isolated from the dispersion using centrifugation, dialysis or sepharose 24 column (Machado et al. 2014). By REV, liposomes can be produced from various lipids or mixture of lipids and are generally LUV and OLV with high aqueous-to-lipid ratios that are four times higher than MLV and are advantageous for the entrapment of hydrophilic materials with a high encapsulation yield. This method has proven to be suitable for the encapsulation of small, large and macromolecules and for encapsulation of thermolabile materials as it does not require any heating. The main drawback of the method is the use of organic solvents and the brief sonication time that may denature some proteins. In addition, organic solvents commonly employed in REV, namely diethyl ether, isopropyl ether and chloroform, may remain as traces in the resulting liposomes and may be hazardous for human health and liposome stability. To circumvent this, several vortex-evaporation cycles can be used to minimize the amount of residual organic solvents, and alternative solvent systems such as ethanol and ethyl acetate can be used. (Akbarzadeh et al. 2013; Cortesi et al. 1999; Szoka and Papahadjopoulos 1978).

- **Solvent injection**

Solvent injection involves the quick injection of the lipid solution (in ethanol or diethyl ether) into an aqueous medium. The experiment is performed either at room or at higher temperature (e.g., 60°C), depending on whether the organic solvent is water-miscible or not. The liposomes prepared by solvent injection process are mostly polydispersed and highly contaminated by organic solvents, especially ethanol, due to the formation of an azeotrope mixture with water. As presented in **Table 1.6**, solvent injection suffers from several drawbacks including continuous exposure of the therapeutic agents to high temperature and organic solvents which might affect both the stability and safety of the liposomal products (Machado et al. 2014; Maherani et al. 2011).

- **Detergent removal**

In the detergent removal method, phospholipids are dissolved in an aqueous solution containing detergents at critical micelle concentrations (CMC). Upon detergent removal, the reaction medium frees individual phospholipid molecules that self-assemble into bilayered structures. Detergent removal is mostly achieved by means of a dialysis bag, polystyrene-based absorber beads or Sephadex columns (gel permeation chromatography). Dilution of the resultant mixture with some appropriate aqueous medium leads to the restructuring of the formed micelles that evolve into liposomes (Pattni et al. 2015; Akbarzadeh et al. 2013).

- **Heating method**

Of all the conventional methods, the heating method is known to be the most attractive method for liposomes preparation due to its organic solvent-free characteristics. In the heating method, lipids are hydrated for 1 hour, and heated for another hour above the transition temperature of the phospholipids in the presence of a hydrating agent (glycerin or propylene glycol 3%). When cholesterol is part of the formulation, the reaction medium is heated up to 100°C because of its high melting point. Being prepared under heating conditions, the resultant liposomes can be readily used without any further sterilization treatments, which minimizes both formulation complexity and timing. In addition, there is no need for further removal of the hydrating agents employed, since these represent physiologically acceptable ingredients that are well-established for pharmaceutical applications. Moreover, the observation that these hydrating agents can prevent particle coagulation and sedimentation makes them much more attractive as stabilizer and isotonizing additives. The hydroxyl groups of these hydrating agents provide a cryoprotective

effect that makes the heating method an efficient one for the formulation of inhalable liposomes (Laouini et al. 2012; Mozafari 2005).

- **Advanced preparation methods**

  - **Microfluidic channel method**

Microfluidic methods include all the advanced techniques that make use of microscopic channels (in the size range of 5–500 μm). In this method, lipids are dissolved in an appropriate organic solvent (ethanol or isopropanol) and the resultant solution is propelled perpendicularly or in the opposite direction to the aqueous medium within the micro-channels. The continuous axial mixing of the organic and aqueous solutions leads to liposome formation due to the local diffusion of phospholipids in the aqueous phase, which encourages the self-assembly process. Among many others, the micro hydrodynamic focusing method represents the most commonly used microfluidic method for liposomes formulation. This method produces small and large unilamellar vesicles, 40–140 nm, with good size homogeneity (mono dispersed feature). The other microfluidic techniques include the microfluidic droplets and the pulsed jet flow microfluidic methods. The microfluidic droplets method involves dissolution of phospholipids in hexane for preparation of giant liposomes (4–20 μm). In the pulsed jet flow microfluidic method, the conventional film hydration method has been modified by drying the lipid solution in microtubes. The resultant lipid film is hydrated within the microtubes through a perfusion process that produces much larger vesicles, 200–534 μm, with remarkable encapsulation efficiency (Pattni et al. 2015; Y. P. Patil and Jadhav 2014). As a common advantage, the microfluidic methods offer the possibility of production of vesicles with desired size, due to the versatility and flexibility of the methods. The disadvantages of these methods include the use of organic solvent and intense agitation, as well as difficulty for large scale production (Maherani et al. 2011).

  - **Supercritical fluidic method**

While it is considered equivalent to the conventional REV, the supercritical fluidic technique makes use of a supercritical fluid, such as carbon dioxide (CO_2), maintained under supercritical conditions (supercritical temperature and pressure). In this state, CO_2 is an excellent solvent for the lipids. A high-performance liquid chromatography (HPLC) pump provides a continuous flow of the aqueous phase into a flow cell that contains the supercritical lipid solution, allowing phase

transition of the dissolved phospholipids. On a sudden decrease in pressure, the CO_2 is completely removed and the phospholipids self-assemble into a bilayered vesicular system. The supercritical fluidic method affords LUV (100–1200 nm) with a 5-fold higher encapsulation efficiency than the equivalent conventional method. Apart from being organic solvent-free, the supercritical fluidic method offers many other advantages such as the use of CO_2 as a cheap and environmentally harmless solvent, the possibility of controlling particle size, in-situ sterilization and large-scale production in industrial settings. However, the disadvantages of the supercritical fluidic technique include its high cost, low yield and use of high pressures (200–350 bar) which require special infrastructures and restrict their universal applications for wider developments of liposomal technology (Pattni et al. 2015; Y. P. Patil and Jadhav 2014; Maherani et al. 2011).

1.3.4.2.Post-preparation treatments

- **Freeze-thawing**

The freeze-thawing treatment involves freezing the liposome dispersion in liquid nitrogen, and subsequently thawing it at the temperature above the phase transition temperature of the lipids used for formulation. After freeze-thawing, the liposomal vesicles are subjected to fusion as the lipid bilayers become fluid and highly permeable, allowing extensive diffusion of hydrophilic molecules, which leads to cryoconcentration. These structural modifications encourage encapsulation of hydrophilic materials that are poorly loaded in liposomes when conventional methods are used (Costa et al. 2014; Sriwongsitanont and Ueno 2011).

- **Freeze-drying**

Commonly known as lyophilization, freeze-drying is a post-preparation treatment for liposomes that is applied in both laboratory and industrial settings to preserve the characteristics of liposomal products. Freeze-drying involves the freezing of the aqueous samples and subsequent removal of ice by sublimation. Freeze-drying represents a very useful treatment for shelf stability of liposomal suspensions, as water molecules can trigger some chemical reactions and lead to modification of the cargo or excipients in the formulation. Freeze-drying appears to be of great interest when the prepared formulation contains thermos-sensitive materials such as proteins, nucleic acids, which might undergo fast degradation when subjected to heat-drying. The use of freeze-drying has

gained considerable attention in liposome technology due to the improved storage stability of liposomal products. Because of potential leakage of liposomes during freeze-drying, the addition of hydrophilic compounds, commonly called cryoprotective agents (such as carbohydrates), has been established to ensure good stability and quality of the final product. The cryoprotectants commonly used include mannitol, lactose, sucrose and trehalose. Among these, trehalose is the most reputed cryoprotecting agent since it preserves liposome stability during and after freeze-drying treatment (Akbarzadeh et al. 2013).

1.3.4.3. Characterization techniques

After production, liposome formulations are subjected to extensive characterization, evaluating the physicochemical properties of liposomes that affect their shelf stability and biological performance. The most routinely investigated parameters in liposome characterization include vesicle size and size distribution (or polydispersity), surface charge (or Zeta potential), shape and morphology, lamellarity, encapsulation efficiency, phase behaviour (or polymorphism) and *in vitro* release profile (Pattni et al. 2015; Prathyusha et al. 2013). **Table 1.7** indicates the techniques used for evaluation of liposome characteristics. The most frequently used methods are briefly discussed in the following paragraphs.

Table 1.7: *Analytical methods commonly used for liposomes characterization*

Parameters	Analytical techniques
Particle size	Dynamic light scattering (DLS)
	Size exclusion chromatography (SEC)
	Field-flow fractionation (FFF)
	Microscope technologies: transmission electron microscopy (TEM), cryogenic-TEM (Cryo-TEM), and atomic force microscopy (AFM)
Zeta potential /Surface charge	DLS
	Electrophoretic mobility
Particle shape / morphology	Microscopic techniques such as TEM, Cryo-TEM and AFM
Lamellarity	Cryo-TEM
	Nuclear magnetic resonance spectroscopy of the 31-phosphorus (^{31}P-NMR)
Phase behaviour	X-ray diffraction (XRD)
	Differential scanning calorimetry (DSC)
	Thermogravimetric analysis (TGA)
Encapsulation efficiency	Centrifugation, dialysis or column separation for liposomes isolation, followed by drug content determination
Drug release	Dialysis or centrifugation, followed by drug quantification using analytical method, such as UV–Vis spectrophotometry, fluorescence spectrometry, enzyme- or protein-based assays, gel electrophoresis, HPLC, UPLC, LC-MS

- **Dynamic light scattering (DLS)**

Also known as photon correlation spectroscopy or quasi-elastic light scattering, DLS represents the most commonly used method for determination of liposome size, size distribution (polydispersity) and Zeta potential (surface charge). DLS is done by an instrument called a Zetasizer Nano. The standard operational principle of DLS is based on the continuous motion of dispersed particles due to their bombardment by solvent molecules (Brownian motion). This phenomenon causes remarkable scattering of the applied light. Since the extent of fluctuation in light intensity is associated with the diffusion rate of the suspended particles, which is related to

particle diameter (smaller particles diffusing faster than the larger ones), the particle size is automatically deducted from the estimated amount of scattered light. When addressing Zeta potential measurements, DLS allows surface charge determination by accessing changes in the scattered light intensity caused by particle motion due to the electric field applied. In other words, for surface charge (Zeta potential) evaluation, changes in the intensity of the scattered light are governed by the applied electric field (which causes extensive motion of charged particles), in contrast to size measurements where Brownian motion is the key factor (Pattni et al. 2015; Braun et al. 2011). Apart from being a simple, fast and reliable method for routine analyses, DLS offers many other advantages including the fact that the measurement is taken from a native environment, and a wide size range can be evaluated (from a few nanometers to several micrometers). However, DLS shows some limitations such as the difficulty of differentiating individual particles from aggregates and high sensitivity to contaminants (Fissan et al. 2014). In addition, DLS is technically unable to provide true particle size, but rather hydrodynamic diameter due to particle solvation. Water layers on the particle surface can lead to false readings of particle diameters in aqueous media (Eaton et al. 2017).

- **Transmission electron microscopy (TEM)**

Microscopic observation provides direct visualization of the liposomal vesicles as individual particles, which allows for effective analysis of shape and morphology as well as a precise and reliable size reading. In this context, TEM techniques are commonly used in liposome technology for structural characterizations. In TEM experiments, the liquid sample is spotted onto a copper grid, and the solvent dried prior to the microscopic analysis. Under a TEM instrument, liposomal vesicles mostly appear as black spherical particles on a white background. For a variant TEM technique such as negative staining TEM, liposomes appear as bright spherical spots on a black background since the spotted sample is treated with uranyl acetate or phosphotungstic acid (as negative staining agent). Due to its effectiveness, TEM appears to be a powerful complementary technique to DLS for confirmation of the liposomal structure. Unlike DLS, TEM offers the advantage of differentiating individual vesicles from aggregates, allowing critical assessment of the liposome population. However, TEM presents several limitations due to sample preparation. Apart from being time-consuming, sample pre-treatments in TEM analyses may cause

considerable changes in liposomal shape or morphology, such as potential vesicle shrinkage, swelling or artefact formation (Pattni et al. 2015; Chetanachan et al. 2008).

To overcome these limitations, Cryo-TEM was developed to minimize liposome disruption by making use of a flash freezing treatment for direct particle visualization in solid-state (without solvent removal). Currently, CryoTEM is the most reliable technique for visual determination of liposome structure, including lamellarity. However, Cryo-TEM also has a limitation in that it works perfectly only with very small particles. This has led to the development of atomic force microscopy (AFM) for direct particle analysis in native environments. Although AFM offers the advantage of higher particle resolution at three-dimensional level, the use of this technique is mostly limited by the high cost of the instrument, which compromises its universal availability and accessibility (Bozzuto and Molinari 2015; Pattni. et al 2015).

- **Differential scanning calorimetry (DSC) and X-ray diffraction (XRD)**

DSC and XRD are complementary techniques that evaluate the thermal behaviour and crystallinity, respectively, and provide valuable information for the characterization of loaded liposomes (Singh et al. 2015; Omwoyo et al. 2014; Prathyusha et al. 2013). DSC evaluates the differences in heat flow (electric power) between a sample and a reference. In DSC experiments, the sample and the reference are subjected to a programmed heating, cooling or isothermal treatment in a controlled atmosphere (mostly saturated with nitrogen gas). The heating treatment is achieved either by the same heater (heat flux DSC) or by separate heaters (power compensated DSC). The experiment is conducted in specialized metal pans made of aluminium, tin, zinc or indium. Throughout the experiment, frequent electric power adjustments occur upon material phase transition (melting or crystallization), ensuring thermal equilibrium between the sample and the reference. This phenomenon is described and expressed by the plot of heat capacity against temperature or time (heat flow curve). The heat flow curve provides the respective transition temperature and enthalpy, which permits the identification of the nature of thermal events, i.e., endo- or exothermic (Giron 2002; Ohline et al. 2001; Koyama et al. 1999). DSC represents the most useful thermal analysis technique in the study of lipid-based materials (Castelli et al. 2005; Ohline et al. 2001; Koyama et al. 1999).

Unlike DSC where sample recovery is not possible, XRD is a non-destructive analytical tool that allows structural investigations of crystalline materials. XRD makes use of X-rays that deeply

penetrate solid materials and provide useful information at atomic structure level. Although relatively expensive, an XRD instrument is an environmentally and user-friendly device that is easy to use. A wide range of materials such as powders, crystals and liquids can be quickly assessed by XRD. Its other advantages include high resolution, reliability, relatively cheap maintenance, and easy data collection, processing and interpretation. The phase transitions and polymorphism determined by XRD represent valuable information in pharmaceutical development and the production of both excipients and biologically active materials (Chauhan and Chauhan 2014; Dorofeev et al. 2012; Kirtansinh, Piyushbhai, and Natubhai 2011).

- **Lamellarity assays**

The lamellarity of liposomes is part of their structural characteristics which can have an impact on the intended applications. The number of lipid bilayers can be evaluated using chemically labelled or radiolabelled agents that can be distributed in the bilayer membranes. However, this technique is limited as these reagents might be distributed only on the outer lipid membrane and lead to false readings. To date, Cryo-TEM is the most commonly used technique for the determination of lamellarity by visualization (Pattni et al. 2015). The nuclear magnetic resonance spectroscopy of the 31-phosphorus (^{31}P-NMR) is also currently used to estimate the lamellarity of liposomes. This technique estimates the ratio of phospholipids in the outer layers to that of the inner layers (Fröhlich et al. 2001). The ^{31}P-NMR spectrum with a broad peak indicates the presence of MLV while a narrow peak corresponds to SUV. The addition of paramagnetic ions such as Mn^{2+}, Co^{2+}, and Pr^{3+} shifts the respective peaks to either downfield or upfield due to ionic interactions with the phosphate backbone. By comparing the spectroscopic profile with and without the paramagnetic ion, the lamellarity of liposomes can be estimated. Other techniques such as small-angle X-ray scattering (SAXS) and trapped volume determination can be used to estimate liposome lamellarity (Pattni et al. 2015; Bouwstra et al. 1993).

- **Encapsulation Efficiency**

The Encapsulation Efficiency (EE), also referred as ‘incorporation efficiency’ or ‘trapping efficiency’, is in most cases expressed as percent encapsulation and is typically defined as the total amount of the encapsulant (drug) found in liposome solution versus the total initial input of encapsulant solution. The EE depends mainly on the ability of the liposome to entrap the

encapsulant molecules (depending on the organic/aqueous phase composition, or liposome lamellarity), the preparation procedure used and the initial concentration of encapsulant loaded. Prior to determination of EE, pre-treatment methods such as dialysis, centrifugation, ultrafiltration, size exclusion chromatography or solid-phase extraction must be used to separate the un-encapsulated (free) drug from the liposomal formulation. The EE can be determined either indirectly by quantification of the free drug or directly by evaluation of the entrapped drug. The direct method requires extraction of the entrapped drug from the liposomes. To achieve this, lipid bilayers can be disrupted by replacing the aqueous media with an organic phase such as acetonitrile, ethanol, methanol or a surfactant such as Triton X-100. Depending on the physicochemical characteristics of the drug, several quantitative analytical techniques such as UV spectroscopy, fluorescence spectroscopy, enzyme- or protein-based assays, and gel electrophoresis, HPLC, UPLC or LC-MS can be used to determine the drug content (Pattni et al. 2015; Edwards and Baeumner 2006).

- ***In vitro*** **release assays**

The profile of release for the liposomal cargoes is commonly estimated *in vitro* using dialysis. This method implies trapping the liposomal dispersion into a dialysis bag of specific molecular weight cut off. The resultant tubing membrane is placed in a simulated physiological fluid (release medium) that is often a buffer maintained under well-defined conditions, such as specific temperature and speed of stirring/shaking. At predetermined time intervals, an aliquot is withdrawn from the release medium and an equal volume of the fresh buffer is replaced to maintain sink conditions. In the withdrawn sample aliquots, the released cargo is quantified using certain routine analytical techniques such as UV-Vis spectrophotometry, HPLC and UPLC, adapted to the molecular species under evaluation. The release profile is obtained by plotting the cumulative release percentage against the chosen time intervals (Pattni et al. 2015). Data from the *in vitro* release study are considered to be part of the rational development of formulations for controlled release, since they allow effective prediction of *in vivo* performance of the delivery systems (Rani 2013). Mathematical models can be used to determine the release processes of encapsulated molecule(s) in function of time. The main-release kinetic models include zero order, first order, Higuchi, Hixson–Crowell, Korsmeyer–Peppas, Baker–Lonsdale, Weibull, Hopfenberg, and Gompertz (Bruschi 2015; Dash et al. 2010).

1.3.5. Applications

Liposomes have evolved significantly from mere experimental tools of research to industrially established products for clinical and veterinary use. They have a proven ability to improve the physicochemical features of the cargoes and ferry them to the sites of interest. The concepts of liposomal encapsulation have been applied in several fields of life science. Liposomes are frequently used for the delivery of drug, gene, vaccine and diagnostic products; but other applications encompass encapsulation of food and cosmetic ingredients as well as routine analysis of chemical substances (Lila and Ishida 2017; Bozzuto and Molinari 2015).

1.3.5.1.Application in drug delivery

Liposomes are used in drug delivery to modify the pharmacokinetics of drugs to improve the therapeutic efficacy while minimizing potential toxicity (Akbarzadeh et al. 2013). Liposomes can alter the spatial and temporal distribution of the entrapped drug molecules *in vivo*, leading to controlled delivery at the site of interest and reduced off-target adverse effects (Daraee et al. 2016). The liposomal systems have been extensively investigated for the delivery of existing and emerging drugs at various research levels, from basic stages related to research and development to preclinical and clinical applications. Currently, liposomes represent the most clinically established drug vehicles for human diseases (Bozzuto and Molinari 2015; Bulbake et al. 2017). Liposomal formulations have been used to address a wide range of pathological conditions through different administration routes including dermal, transdermal, oral, pulmonary and parenteral routes. The clinical areas commonly explored in liposome research encompass skin disorders, cancers and infectious diseases (Pattni et al. 2015).

Cancer therapy appears to be in the forefront of liposome delivery research, due to the poor bioavailability and side effects of most current anti-cancer drugs. In addition, several infectious diseases, most especially where the pathogen is hosted by the MNPS (i.e., tuberculosis, leishmaniasis and fungal infections), have been reported to be good candidates for liposome application, taking advantage of the spontaneous liposome uptake by the cells of MNPS (Lila and Ishida 2017). Apart from the nature and localization of the disease, the design and development of liposomes depend on the intended administration route, as different anatomical and physiological characteristics can be encountered from one route to another (Prathyusha et al. 2013).

Furthermore, the application of liposomes in drug delivery is highly dependent on their colloidal and physiochemical features, i.e., vesicle size, surface charge and system stability (Çağdaş et al. 2014). For instance, small liposomes (SUV) are good candidates for Parkinson's and Alzheimer's diseases, due to the need for crossing the brain blood barrier to achieve brain targeted delivery. Large liposomes are preferred for macrophage-targeted delivery of antimicrobials when pathogens are located inside the MNPS cells (e.g., tuberculosis, leishmaniasis), taking advantage of the passive liposome cell uptake (Lila and Ishida 2017; Pattni et al. 2015; Prathyusha et al. 2013). This underlines the need for thorough exploration of process and formulation parameters at early stages of product development to produce liposomes with desired characteristics, making the technology for liposome manufacturing key to future therapeutic research and development.

1.4. Study background and rationale

Tuberculosis (TB) is an infectious disease caused by *Mycobacterium tuberculosis*. TB represents a serious threat to global health as the leading cause of death from a single infectious agent (WHO, 2019). The high morbidity and mortality rate of TB is partly due to the lack of effective therapeutic treatments. In fact, the current recommended treatment, which is a lengthy medication of 6–24 months with multiple drug combinations, poses problems of frequent side effects and poor patient compliance which has promoted the development of multidrug resistance and extensively drug resistance tuberculosis (WHO 2019; Nasiruddin et al. 2017; Zumla et al. 2013). The rapid development of antimicrobial resistance (AMR) is a serious concern for TB, particularly as novel antibacterial compounds, including those already commercially available, are also subject to AMR. The WHO (2019) reported that 3.4% of new TB cases and 18% of previously treated cases globally in 2018 were multi-drug resistant TB/Rifampicin resistant TB cases.

In addition to the crucial issue of resistance to TB antibiotics, the development of new TB vaccines faces important challenges (Pai et al. 2016), and there is currently no TB vaccine effective in adults (WHO, 2019). Moreover, the location of the pathogen within the granuloma hampers existing treatment and justifies the need for targeted therapeutic approaches (Ekins 2014). Novel drug delivery systems are needed in order to improve TB drug efficacy, lessen the adverse effects, shorten the duration of the regimen and consequently improve the therapy success and patient compliance, and prevent drug resistance. To achieve this, researchers have tried to encapsulate TB

drugs in diverse drug carriers such as liposomes, niosomes, micelles, nano-emulsions, solid lipid nanoparticles, polymer based microparticles and nanoparticles and implants (Hussain et al. 2019).

Liposomes are minute lipid-based systems reported to be the most successful drug carriers for improved drug delivery. As versatile phospholipid-containing vesicles, liposomes can encapsulate a diverse range of biologically active compounds including compounds of different hydrophilicity (hydrophilic, amphiphilic or hydrophobic substances) and molecular sizes *viz*., small and simple chemicals or large and complex molecules such as proteins. The evolution in formulation and functionalization of liposomes, as versatile nanostructures, has expanded their application with improved features such as biocompatibility, biodegradability, low toxicity, controlled release and targeted delivery, increased solubility, bioavailability and stability of encapsulated active pharmaceutical ingredients (Nisini et al. 2018; Panahi et al. 2017). Liposomes are therefore suitable for the delivery of hydrophobic antibiotics such as rifampicin that are mostly affected by poor and variable bioavailability. Although rifampicin is the most effective anti TB drug, its effectiveness is handicapped by the high dose daily required (600 mg) in most regimens due to the limitations of the conventional forms such as instability at gastric pH, limited solubility at neutral pH, polymorphism and stimulation of its own metabolism (Acra et al. 2018; Bhise et al. 2010; Milán-Segovia et al. 2010).

In addition, the encapsulation of antimicrobials in liposomes permits selective targeted delivery and enhances activity against both extracellular and intracellular pathogens (Yadav et al. 2017). The rapid uptake of liposomes by the mononuclear phagocytic system cells, particularly by the alveolar macrophages where the *Mycobacterium tuberculosis* often resides, makes liposomes appropriate vehicles for targeted drug delivery (Lila and Ishida 2017). Passive and active targeting techniques have been explored in order to improve delivery of active substances to target cells. Passive targeting can be achieved by controlling the nanoparticulate characteristics of liposomes, most especially size, shape and surface charge. Active targeting can be achieved by grafting targeting ligands on the surface of liposomes to facilitate site specific delivery of therapeutic liposomes through receptor mediated mechanisms. Proteinaceous molecules such as peptides or antibodies have been extensively used as targeting ligands due to their biological activity (Riaz et al. 2018; Caracciolo 2015).

Therapeutic proteins, such as antibodies, are recognized as the first natural antimicrobial therapeutics prior to antibiotics. An important trend in the biopharmaceutical sector includes the exploration of the natural properties of proteins by conjugating them to cytotoxic chemicals or other drug carrier systems in order to improve therapeutic potential and targeted delivery of drugs. Protein-drug conjugates have proven to be revolutionary in the treatment of a wide range of diseases including cancer, inflammatory disease, genetic disorders and infectious conditions (Lagassé et al. 2017; Mariathasan and Tan 2017; Vhora et al. 2015; Dimitrov 2012).

Of the therapeutic proteins, albumin is attractive due to its interesting features such as abundance in human plasma, antioxidant properties and its role in the transport of nutrients and drugs. These roles of albumin are due, in part, to its extended circulation half-life, cellular interactions and multiple binding sites. Albumin is an amphiphilic protein with high water-solubility but has many hydrophobic binding pockets, which are able to host different ligands such as fatty acids, steroids or drugs naturally. Albumin has been used as a drug carrier particularly because of its low immunogenicity (Ahmed et al. 2019; Liu et al. 2017; Larsen et al. 2016). However, the *in vivo* stability of colloidal protein-based therapeutics is challenging. In order to overcome this bottleneck, the incorporation of albumin based nanoparticles into liposomes has been investigated and proven to be effective (Ruttala and Ko 2015).

Researchers have successfully loaded hydrophobic antibiotics into liposomes or albumin-based nanoparticles, for example rifampicin was encapsulated in liposomes either alone or in combination with another drug (Gomez et al. 2019; Nkanga et al. 2019; Gaur et al. 2010; Zaru et al. 2009). Ge et al. (2018) attempted to develop Rifampicin-loaded albumin-based nanoparticles. In other studies, liposomal encapsulation of complex proteins such as albumin has been achieved with some success (Okamoto et al. 2018; Brgles et al. 2008; J. Colletier et al. 2002). In addition, Ruttala and Ko (2015).) have loaded paclitaxel-albumin-nanoparticles into liposomes with a resulting improved anticancer efficacy.

To the best of our knowledge, the possibility of co-loading anti TB drugs and proteins into a single liposome formulation has not been studied extensively. To achieve this, I hypothesized that the reverse phase evaporation (REV) would be the appropriate formulation method, mainly because it produces ULV and OLV and is in theory suitable for the encapsulation of amphiphilic and large proteins (such as albumin). Moreover, the method is reported to be suitable for achieving higher

liposomal loading efficiency for highly hydrophobic antibiotics such as rifampicin (Gomez et al. 2019).

1.5. Study objectives

The aim of this work was to evaluate the possibility of achieving simultaneous encapsulation of a hydrophobic anti-TB drug, rifampicin (Rif), with a typical large therapeutic protein, Human Serum Albumin (HSA), into liposomes by REV and to investigate the physicochemical properties of the resulting dual liposomes.

The specific objectives of the study were:

(1) To design, formulate and optimize liposomes made of crude soybean lecithin using REV
(2) To evaluate and compare the solubility of Rif in water and in different solutions of HSA
(3) To simultaneously load Rif and HSA into liposomes using REV
(4) To evaluate the effects of lipid composition and HSA on the loading of Rif
(5) To optimize the simultaneous encapsulation of Rif and HSA in liposomes using REV
(6) To conduct an extensive characterization of Rif-HSA co-loaded liposomes.

Chapter Two

Materials and Methods

2. MATERIALS AND METHODS

2.1. Materials

2.1.1. Chemicals

Soybean lecithin was purchased from Health Connection Wholefoods (USA) and Cholesterol from Carlo Erba/Divisione Chimica (Italy). Rifampicin ≥ 97% purity (HPLC grade) powder and rifampicin VETRANAL™ analytical standard were purchased from Sigma Aldrich (Germany). Albumin human fraction V No A-1653 was purchased from Sigma (USA). HPLC grade acetonitrile, chloroform, orthophosphoric acid and diethyl ether were sourced from Merck (Germany). Ultra-pure water was HPLC grade (18 mega Ohm), prepared using a Milli-Q academic A10 water purification system (Millipore® Bedford, MA, USA), or purchased as LCMS-quality water from Merck. All these chemicals were used without further purifications.

2.1.2. Equipment

A rotary evaporator (Heidolph Hei-VAP Value, Germany), vortex mixer (Deluxe Vortex Mixer Chiltern MT19) and bath sonicator (Digital Ultrasonic Cleaner PS-10A, China) were used for the liposome formulation and manufacturing process. An Eppendorf 5414 micro centrifuge, MSE Mistral-1000 and Beckam Coulter Allegra 64 Centrifuge were used for centrifugation of the test formulations. A Lyo Lab 3000 lyophilizer Apollo Scientific CC (South Africa) was used to freeze-dry the samples. An Agilent 1100 Liquid Chromatography series equipped with a quaternary pump (G1311A), degasser (G1322A), diode array detector (G1315B) and manual injector (G1328B) was used for HPLC analysis with a Luna® LC column (5 µm C18, 100 Å, 250 x 4.6 mm i.d.). A PerkinElmer Spectrum 100 FT-IR Spectrometer was used for recording IR spectra and PerkinElmer DSC-6000 instrument was used for thermal analyses. An XRD D8 Discover instrument (Bruker, USA) was used for the assessment of crystallinity of materials. Particle size distribution and Zeta Potential were determined using a Zetasizer nano ZEN–3600 MAL1043132 from Malvern Instruments (UK). A Zeiss Libra–120KV TEM (Germany) was used for microscopic observation of particles shape. An INCA PENTA FET coupled to VAGA TESCAM was used for energy dispersive X-ray spectroscopy (Germany) and proton nuclear magnetic

resonance (^{1}H-NMR) spectra were recorder on a Bruker AMX 600 MHz NMR spectrometer (Switzerland).

2.2. Methods

2.2.1. Pre-formulation studies

2.2.1.1. Drug-excipients compatibility

A preliminary study was conducted to evaluate the physicochemical compatibility between the active pharmaceutical ingredient (API) and excipients before the actual formulation steps. Rifampicin (Rif) was physically mixed with human serum albumin (HSA) and with crude soybean lecithin (CSL) in a mass ratio of 1:1. The phase behaviour of the physical mixture was evaluated in comparison with pure Rif by differential scanning calorimetry (DSC). About 3 mg of each sample placed in an aluminium pan was heated from 30°C to 400°C at a flow rate of 10°C/min in an inert atmosphere saturated with nitrogen flowing at 20 ml/min. An empty aluminium pan served as the reference.

2.2.1.2. Preparation of empty liposomes

Optimization of different parameters involved in the formulation of liposomes is required not only for economic reasons but also to better control the formation of liposomes with uniform size, shape and with better encapsulation efficiency(Seth and Misra 2002).

Two series of liposomal formulation were prepared in triplicate and their particle size and polydispersity index (PDI) were evaluated by dynamic light scattering (DLS). For each series, as shown in **Table 2.1,** three independent formulation variables that could potentially influence the output variables were set at different levels. The full factorial Design of Experiment (DOE) for different parameters was generated using Minitab 17 software. The results from the evaluation of the first series (S1) of liposomes led to the choice of fixed variables for the second series (S2) of empty liposomes. The optimized formulation from the second series was then selected for drug encapsulation studies.

***Table 2.1**: Experimental design of first series (S1) and second series (S2) of preparation of empty liposomes*

Series	Parameters	Levels			
		1	2	3	4
S1	Organic/aqueous phase ratio (v/v)	6 ml:1 ml	6 ml:2 ml	6 ml:3 ml	-
	Sonication time	2.5 min	5 min	10 min	-
	Dispersing medium volume	2 ml	4 ml	6 ml	-
S2	Vortex/rotavap cycles	1 cycle	2 cycles	3 cycles	-
	Stirring time	0 min	30 min	60 min	-
	Stirring temperature	25°C	40°C	60°C	80°C

Liposomes were prepared by the reverse phase evaporation method "REV" (Seth and Misra 2002; Szoka and Papahadjopoulos 1980) according to experimental design. Briefly, 50 mg of lipid components, crude soya bean lecithin (CSL) and cholesterol (Chol) in a mass ratio of 3:1, were weighted and dissolved in 1 ml of chloroform in a clean 25 ml round bottom flask. The solvent was removed at 60°C using a rotary evaporator at 200 rotations per minute (rpm) for 5 minutes under vacuum. 6 ml of diethyl ether was added to the dried lipid in the round bottom flask. For the aqueous phase, 1 to 3 ml of Millipore water was injected and the round bottom flask was closed with a glass stopper and sonicated using a bath sonicator at 25°C for a specific time depending on the formulation. After sonication, the round bottom flask was directly attached to a rotary evaporator to remove the organic solvent at 25°C at 200 rpm for 15 min under vacuum. As per DOE, a certain volume of Millipore water was added to disperse the gel formed and the mixture was homogenized by vortex for 5 min. The suspension was again fitted to a rotary evaporator at 200 rpm and 25°C for 5 min under vacuum to remove residual organic solvent. The cycle vortex/rotavap was repeated as prescribed by the DOE. Finally, the suspension was stirred at 400 rpm and heated for 30 min at 60°C or as prescribed. The formulation was stored at 4°C until further analysis.

2.2.1.3. Evaluation of empty liposomes:

- **Particle size distribution and Zeta potential**

Particle size and PDI of the liposomal batches were appraised by DLS performed on Malvern Zetasizer Nano ZEN-3600 MAL1043132 Instrument. Water was used as dispersant and 1,497 was considered as refractive index of the material. Liposomal dispersions were placed in a clean cuvette and scattered by light at 25°C and at scattering angle of 173°. Measurements were performed in triplicate. The Zeta potential was determined for formulations with best PDI.

- **Particle shape**

The morphology of liposomes was observed by Transmission Electron Microscopy (TEM): a drop of the same sample used for DLS was placed onto a carbon-coated copper grid and the exceeding liquid was absorbed by a filter paper. The copper grid was allowed to dry overnight before microscopic observation on a Zeiss Libra-120KV TEM instrument. TEM images were also used for size confirmation of particles using ImageJ software.

2.2.1.4. Validation of the HPLC Method for quantification of rifampicin

The RP-HPLC method for quantification of Rif as described by Kumar et *al.* (2014), with few modifications in terms of HPLC equipment and column used, was validated according to the International Council for Harmonization guidelines (ICH 2005). Linearity range, accuracy, repeatability and intermediate precision were investigated to ensure that the method was suitable for use under actual experimental conditions.

For the HPLC analyses, isocratic conditions were applied for 7 min at a flow rate of 1 ml/min. The mobile phase was a 50:50 (v/v) mixture of acetonitrile and phosphate buffer adjusted to pH 3.0 using orthophosphoric acid. The injection volume was 20 µL and the wavelength for detection was set at 238 nm. To prepare the stock solution of Rif, 10 mg of the analytical standard was accurately weighted into a 10 ml clean and dry volumetric flask. Approximately 8 ml of acetonitrile was poured into the volumetric flask. The resultant mixture was sonicated to ensure complete dissolution of Rif and the volume made up to volume with acetonitrile.

- **Linearity, range and accuracy**

Five standard solutions of 10, 50, 100, 250 and 500 µg/ml Rif were prepared by serial dilution of the stock solution using acetonitrile. Each solution was injected (n = 3) onto the HPLC system. The peak areas were plotted against the respective concentration to generate a calibration curve, from which the regression equation and the correlation coefficient (R^2) were determined for linearity assessment. The percent recovery was calculated in order to assess the accuracy of the method.

- **Repeatability**

The standard solution prepared at a concentration of 30 µg/ml was injected (n = 6) into the HPLC instrument on the same day. The peak areas from the six injections were recorded and the percent relative standard deviation (%RSD) was calculated for repeatability assessment.

- **Intermediate precision**

A freshly prepared standard solution (30 µg/ml) was injected (n = 3) into the HPLC system. The experiment was repeated over five consecutive days. The %RSD of peak areas for the five days was calculated.

2.2.2. Solubility of Rif in water and HSA solution

Excess Rif was added to HPLC grade water or in aqueous HSA solutions of 10%, 20% and 40% w/v ratios. The mixture was stirred for one hour at 750 revolutions per minutes (rpm) at 25°C and then centrifuged using Eppendorf 5414 micro centrifuge at relative centrifugal force (RCF) of 15600 g for 15 min to remove any undissolved Rif particles. To evaluate the Rif content, the supernatant was subsequently treated with acetonitrile to precipitate protein and centrifuged again under the same conditions. The supernatant was filtered using a 0.22 µm simplepure^{TM} syringe filter and the Rif content in the filtrate determined using the validated HPLC method.

2.2.3. Preparation of Rif-HSA loaded liposomes

2.2.3.1. Loading of Rif-HSA saturated solution into liposomes

A factorial experimental design was used to produce nine (9) formulations that were prepared using different organic phase composition, crude soybean lecithin (CSL) to cholesterol (Chol) mass ratio, and aqueous phase as summarized in **Table 2.2**. Liposomes were prepared by the reverse phase evaporation method (REV) (Seth and Misra 2002) according to the experimental design under experimental conditions identified in pre-formulation studies.

Briefly, a total of 50 mg of the lipids and a specific amount of Rif were dissolved in 1 ml chloroform in a clean 25 ml round bottom flask. The chloroform was removed using a Rotavap set at 60°C for 5 min at 200 rpm. Subsequently, 6 ml diethyl ether was added to re-dissolve the dried product and 3 ml of a saturated aqueous solution of Rif was injected into the round bottom flask, which was then sealed with a glass stopper and sonicated for 2.5 min at 25°C. Following sonication, the organic solvent was removed by evaporation at 200 rpm at 25°C for 15 min resulting in a residual gel. The gel was dispersed into 6 ml HPLC grade water and subjected to 2 cycles of vortex-mixing (5 min) and rotary evaporation (5 min) at 25°C to homogenize the suspension and to remove trace of organic solvents. **Figure 2.1** schematically depicts the preparation of co-loaded liposomes.

The suspension of liposomes obtained was then centrifuged at a RCF of 1020 g for 5 min using a MSE Mistral-1000 to remove Rif particles (non-encapsulated drug). The supernatant following low speed centrifugation was then centrifuged at a RCF of 20000 g for 20 min at 25°C using a Beckam Coulter Allegra 64 Centrifuge. The supernatant following the second centrifugation was discarded and the remaining liposomes in the pellet were rinsed consecutively (n = 3) with approximately 15 ml HPLC grade water to wash liposomes from non-encapsulated HSA or Rif molecules. The Rif-HSA loaded liposomes (Rif-HSA-lip) were then lyophilized using a LyoLab 3000 (Apollo Scientific) and the resultant powder was stored at 4°C until required for further characterization.

Table 2.2: *Experimental design conditions for loading of Rif saturated solutions into liposomes*

Levels	CSL/Chol mass ratio (w/w)	Aqueous saturated solution in Rif	Quantity of Rif in aqueous phase (mg)	Quantity of Rif in Organic phase (mg)	Total Initial quantity of Rif (mg)
1	3:0	Water (HPLC grade)	6	27.5	33.5
2	3:1	HSA 10%	15	18.5	33.5
3	3:3	HSA 20%	21	12.5	33.5

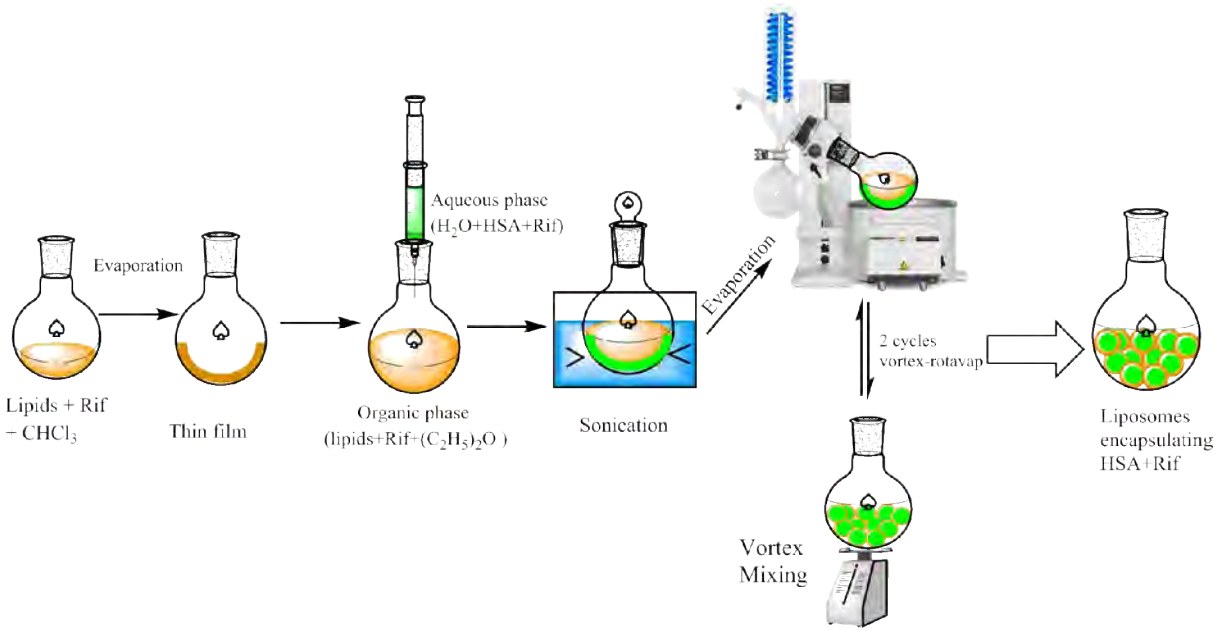

Figure 2.1*: Schematic representation of REV optimized procedure for co-loading of Rif and HSA*

2.2.3.2. Optimization of encapsulation efficiency for Rif

The formulation in which Rif was included with a 10% w/v HSA solution and a lipid composition of CSL-Chol ratio of 3:0 was selected for improvement of %EE of Rif following preliminary results of EE determination. The saturated solution of Rif in HSA 10% (Rif-HSA) was prepared as described in section **2.2.2.,** freeze-dried and stored at 4°C. The Rif content in the freeze-dried Rif-HSA was determined using the validated HPLC method.

Table 2.3 summarizes the initial quantities of Rif used at three different levels in both aqueous and organic phases. Rif-HSA loaded liposomes (Rif-HSA-lip) were prepared following the method described in section **2.2.3.1.** The aqueous phase was prepared by re-dissolving the freeze dried Rif-HSA powder in 3 ml HPLC grade water and the %EE determined using the validated HPLC method. The formulation with greatest %EE of Rif was selected for further characterization. For comparative purposes, formulations of Rif and HSA mono loaded liposomes (Rif-lip and HSA-lip respectively) were prepared using the same conditions as that for the optimized Rif-HSA-lip.

Table 2.3*: Initial parameters considered for optimization of % EE for Rif*

Formulation code	Rif repartition parameters at various levels		
	Rif in organic phase (mg)	Rif-HSA in aqueous phase (mg Rif/mg Rif-HSA)	Total Rif used (mg)
O_1	20	10/300	30
O_2	12	6/180	18
O_3	4	2/60	6

2.2.3.3. Characterization of Rif-HSA loaded liposomes

- **Determination of particle size, zeta potential and shape**

The particle size and Zeta Potential of all formulations was determined using DLS after re-dispersing the freeze-dried powder in HPLC grade water. Ordinary and capillary cuvettes were used for particle size and Zeta Potential measurements, respectively. The experiments were performed at 22°C at a scattering angle of 173°. A drop of the liposomal suspension from particle size and Zeta Potential measurement was placed on a copper grid for electron microscopy. The excess liquid was adsorbed using filter paper and the sample was allowed to dry for 24 h at room temperature (25°C). The shape of the liposomes was observed using transmission electron microscopy (TEM). The size distribution of particles was confirmed by treating TEM images with ImageJ software.

- **Determination of encapsulation efficiency of liposomes**

The encapsulation efficiency (EE) of liposomes for Rif was estimated using a direct method.

Briefly, 5 mg of the freeze-dried liposomes was accurately weighted and dispersed in 1 ml HPLC grade water by vortexing for 3 min. The suspension was made up to 5 ml with acetonitrile and the solution mixed vigorously for 5 min using a vortex-mixer to breakdown liposomal and proteinaceous structures to form a precipitate. The mixture was then filtered through a 0.45 µm and 0.22 µm simplepure™ syringe filters successively to isolate Rif from lipid and protein precipitates. The filtrate was used for quantitation of Rif using the validated HPLC method.

The following formula was used to determine the percent encapsulation efficiency (%EE):

$$\%\mathrm{EE} = \frac{\left(\frac{Rif}{excipients}\right)\text{in freeze} - \text{dried liposomes}}{\left(\frac{Rif}{excipients}\right)\text{initially used}} \mathrm{X100}$$

Where "excipients" include the lipids and HSA.

- **Proton nuclear magnetic resonance**

Proton nuclear magnetic resonance (^{1}H NMR) experiments were performed using a Bruker AMX 600 MHz NMR spectrometer. For each sample, 20 mg of the freeze-dried powder was dispersed in 0.7 ml deuterated water in specialized NMR tubes. The proton spectrum for empty liposomes (Empty-lip) was compared to the spectra of HSA-lip, Rif-lip and Rif-HSA-lip.

- **Infrared spectroscopy**

The IR spectra were obtained using an attenuated total reflection using a PerkinElmer Spectrum 100 FT-IR Spectrometer averaging 16 scans in the wavenumber range from 650 cm^{-1} to 4000 cm^{-1}. The signals from the functional groups in the freeze-dried Rif-HSA-lip were compared to those from freeze-dried Rif-lip and raw materials used (Rif, HSA and CSL).

- **Energy-Dispersive X-ray Spectroscopy**

The freeze-dried Rif-HSA-lip samples were analyzed for surface elemental analysis in comparison to Rif, Empty-lip, mono-loaded Rif-lip and HSA-lip by Energy-dispersive X-ray spectroscopy (EDX)**.**

- **Differential Scanning Calorimetry**

The polymorphism of optimized Rif-HSA-lip was studied using differential scanning calorimetry (DSC) and compared to the thermograms for equivalent empty liposomes, Rif-lip, Rif-HSA in addition to Rif, HSA and CSL. The samples (3 mg) were placed into an aluminium based pan and heated from 30°C to 400°C at a rate of 10°C/min. An empty aluminium pan was used as reference. Nitrogen gas flowing at 20 ml/min was used to saturate the atmosphere of the sample chamber. The changes in heat flow of the samples were recorded and data processed with the aid of DSC Pyris software resulting in upward endothermic peaks.

- **X-Ray Diffraction**

X-ray powder diffraction (XRD) was used to compare the crystalline nature of raw Rif and Rif in different carriers *viz*., Rif-HSA, Rif-HSA-lip and Rif-lip. Analyses were conducted using a nickel filter and Cu-Ka radiation at 1.5404 Angstrom and the scans were run at 2-θ range 10-60° with a slit width of 6.0 mm at a scanning speed of $1°min^{-1}$.

- **In vitro Release**

The in vitro release profile of Rif from optimized Rif-HSA-lip was compared to that of Rif-lip, Rif-HSA and free Rif in HPLC grade water. The Rif content and release profile studies were conducted following a procedure described by Nkanga *et al.* (2017) with slight modifications in terms of concentration and volume of suspension used.

Briefly, 10 mg of the freeze-dried sample or 1 mg of free Rif was incubated in 2 ml HPLC grade water for 30 min and the suspension gently homogenized by hand-shaking. The concentration of Rif in the suspension was determined as follows: 0.5 ml of the homogenized sample was placed in a 5 ml volumetric flask and made up to volume with acetonitrile. The volumetric flask was vortexed for 5 min to destroy the liposome/protein structure and the mixture filtered through 0.45 µm and 0.22 µm simplepure^{TM} syringe filters successively. The solution of extracted Rif was analysed using the validated HPLC method.

For release studies, 0.5 ml of the prepared suspension was transferred to a dialysis tubing membrane (Membra-Cell MD10 14X100 CLR, Sigma-Aldrich). The dialysis bag was sealed and

placed into a glass vial containing the release medium of 20 ml pH 7.4 phosphate buffer. The vial content was maintained at 37°C under stirring at 100 rpm throughout the experiment. An aliquot of 5 ml was withdrawn after 0.5, 1, 1.5, 2, 3, 4, 5, 7, 9 and 12 h and used to quantitate Rif using the validated HPLC method. After each sampling, 5 ml of fresh buffer was added to the release medium to maintain sink conditions.

- **Stability studies**

The Rif-HAS-lip and Rif-lip incubated in HPLC grade water at 4°C and the freeze-dried powders (stored on a shelf at 25°C) were subjected to stability testing over 4 weeks. The changes in Zeta Potential and average size of the incubated formulations and the freshly re-dispersed freeze dried powders were evaluated using DLS on day 1, day 7, day 14 and day 28 of the study.

- **Statistical analysis**

All experiments were run in replicate (n = 3) and the data are reported as mean ± standard deviation (SD). Statistical analysis was performed using Minitab 17 (Minitab, Ltd. UK). Where applicable, one-way ANOVA was used for comparative data analyses and differences were considered statistically significant when the value for $p < 0.05$. *DDsolver* was used to determine the release profile and ImageJ was used to process TEM images. Origin pro 8.1 and SigmaPlot 11.0 were used to plot graphs.

Chapter Three

Results and Discussion

Alain Murhimalika Bapolisi, Christian Isalomboto Nkanga, Roderick Bryan Walker, Rui Werner Maçedo Krause (2020). "Simultaneous Liposomal Encapsulation of Antibiotics and Proteins: Co-loading and Characterization of Rifampicin and Human Serum Albumin in Soy-liposomes".

(A manuscript with the above title has been submitted for publication in the International Journal of Pharmaceutics, based largely on the results from this Chapter. Professors Walker and Krause were the study supervisors, and Dr Nkanga a former PhD student who conducted some of the previous studies on the development of liposomes from soy-based lipids.)

3. RESULTS AND DISCUSSION

3.1. Pre-formulation studies

3.1.1. Drug-excipients compatibility

Figure 3.1 represents the DSC thermograms obtained with upward endothermic peaks. The DSC pattern of rifampicin Rif is characterized by three major peaks; an endothermic peak at 194°C indicating the melting point of Rif followed by another endothermic peak and with an exothermic peak at 254°C (Bhise, More, and Malayandi 2010; Panchagnula and Bhardwaj 2008; Henwood et al. 2001). In all the physical mixtures, despite a slight decrease in the intensity of the peaks there was no shift of the melting point of Rif (maximum peak at 194°C) and in addition no new peak appeared. The DSC data confirmed that there were no major physicochemical incompatibilities between the active pharmaceutical ingredient (API) and excipients.

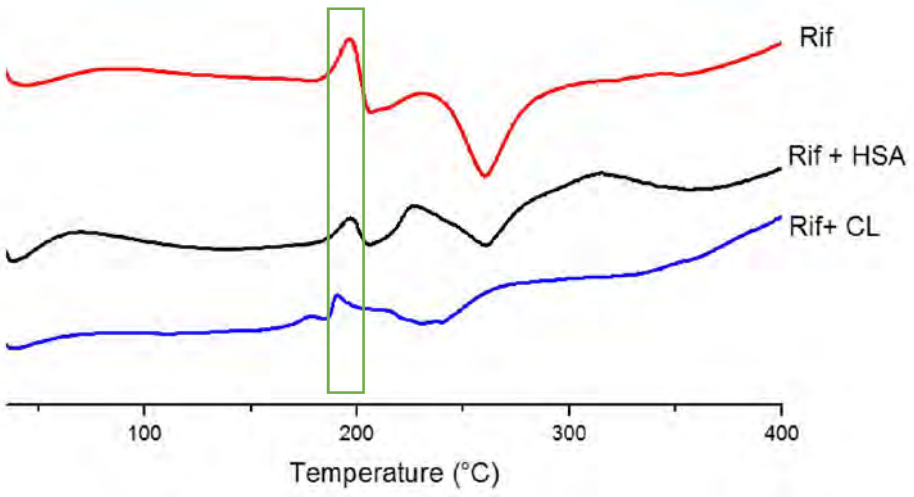

Figure 3.1: *DSC thermogram of Rif compared to the physical mixtures with the excipients*

3.1.2. Evaluation of empty liposomes

3.1.2.1. Particle size and Zeta potential

Empty liposomes prepared by reverse phase evaporation method (REV) and optimized following two series of design of experiments (DOE), as described in section **2.2.1.2.**, were evaluated by dynamic light scattering (DLS) for size distribution and Zeta potential determination.

- **First series of design of experiments**

The DLS results of the first series (S1) of design of experiments (DOE) for empty liposomes are summarized in **Table 3.1** with organic/aqueous phase ratio, sonication time and dispersing medium considered as variable parameters. As it can be observed, the formulation with the lowest PDI for the first series was F21 with 0.502 ± 0.022 (PDI ± SD) with an average particle size of 579 ± 8 nm and zeta potential of –54.4 ± 0.8 mV.

Statistical analysis of data obtained from the 27 formulations of S1 regarding the organic/aqueous phase ratio (v:v) revealed a significant difference ($p<0.05$) only for the ratio 6:1 compared to 6:2 and 6:3 (**Figure 3.2**). Generally, the ratio 6:3 yielded a better PDI and corroborates with the best formulation, F21.

The main effect of plot for PDI (**Figure 3.2**) showed a trend of having the best distribution with higher sonication time and volume of the dispersing medium, however, the difference was not statistically significant. The F21 made with 6 ml of dispersing medium was consistent with the main effect of plot but was made unexpectedly with the shortest sonication time of 2.5 min instead of 10 min. Since there was no significant difference in the sonication time, the 2.5 min seems more advantageous for cost effectiveness. In addition, as a major aim of this project was to design a system that can encapsulate proteins, longer sonication time is likely to have a greater effect on the stability of proteins (and some phospholipids) (Akbarzadeh et al. 2013; Stathopulos et al. 2004).

The formulation F21 with the best particle size distribution as shown in DLS graph (**Figure 3.3)** was made up with the following parameters: organic/aqueous phase ratio 6:3 (ml/ml), Sonication time 2.5 min and Dispersing medium 6 ml. These parameters were selected as fixed parameters for second series (S2) of DOE.

Table 3.1: *First series of empty liposomal formulations with average size and PDI values*

Formulation S1	Organic phase/aqueous phase volume ratio (ml/ml)	Sonication time (min)	Dispersing medium (ml)	Average size (nm)	PDI	Zeta potential (mV)
F1	6:1	2.5	2	735 ± 262	0.921 ± 0.119	-
F2	6:1	2.5	4	498 ± 59	0.956 ± 0.107	-
F3	6:1	2.5	6	685 ± 59	0.653 ± 0.015	-
F4	6:1	5	2	648 ± 110	0.766 ± 0.189	-
F5	6:1	5	4	598 ± 130	0.758 ± 0.189	-
F6	6:1	5	6	908 ± 332	0.653 ± 0.198	-
F7	6:1	10	2	728 ± 366	0.635 ± 0.05	-
F8	6:1	10	4	662 ± 38	0.588 ± 0.051	-
F9	6:1	10	6	632 ± 69	0.604 ± 0.026	-
F10	6:2	2.5	2	643 ± 23	0.548 ± 0.025	-
F11	6:2	2.5	4	582 ± 74	0.557 ± 0.051	-
F12	6:2	2.5	6	546 ± 78	0.576 ± 0.154	-
F13	6:2	5	2	551 ± 83	0.587 ± 0.037	-
F14	6:2	5	4	447 ± 97	0.655 ± 0.115	-
F15	6:2	5	6	702 ± 102	0.517 ± 0.097	-
F16	6:2	10	2	461 ± 162	0.604 ± 0.035	-
F17	6:2	10	4	629 ± 49	0.617 ± 0.121	-
F18	6:2	10	6	617 ± 31	0.672 ± 0.143	-
F19	6:3	2.5	2	543 ± 52	0.580 ± 0.046	-
F20	6:3	2.5	4	543 ± 21	0.613 ± 0.059	-
F21*	**6:3**	**2.5**	**6**	**579 ± 8**	**0.502 ± 0.022**	**–54.4±0.8**
F22	6:3	5	2	451 ± 63	0.697 ± 0.137	-
F23	6:3	5	4	540 ± 87	0.617 ± 0.063	-
F24	6:3	5	6	548 ± 65	0.548 ± 0.402	-
F25	6:3	10	2	533 ± 48	0.604 ± 0.087	-
F26	6:3	10	4	521 ±30	0.577 ± 0.037	-
F27	6:3	10	6	448 ± 67	0.548 ± 0.060	-

***** *formulation with best PDI in the series*

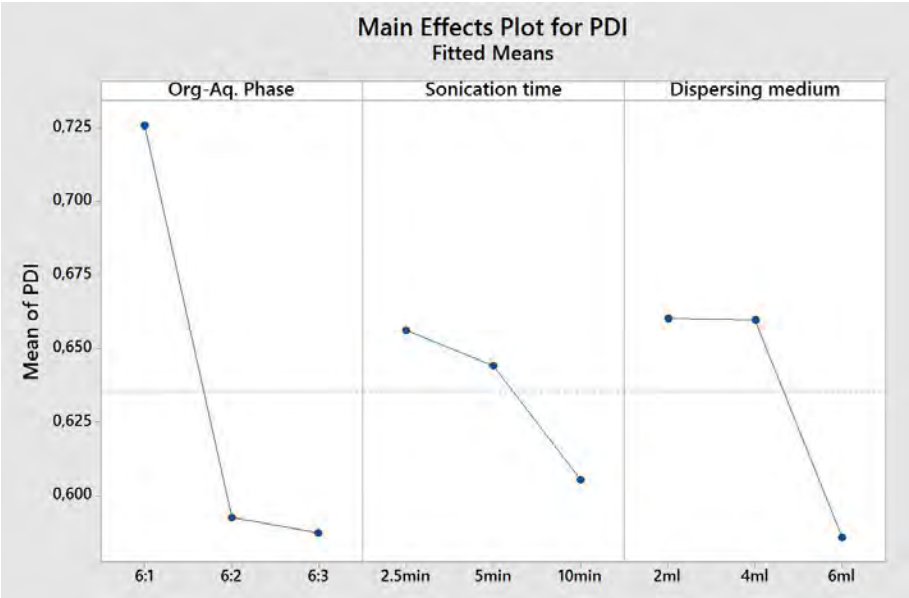

Figure 3.2: *Main Effects Plot for PDI of organic/aqueous phase ratio (ml/ml), sonication time and dispersing medium volume*

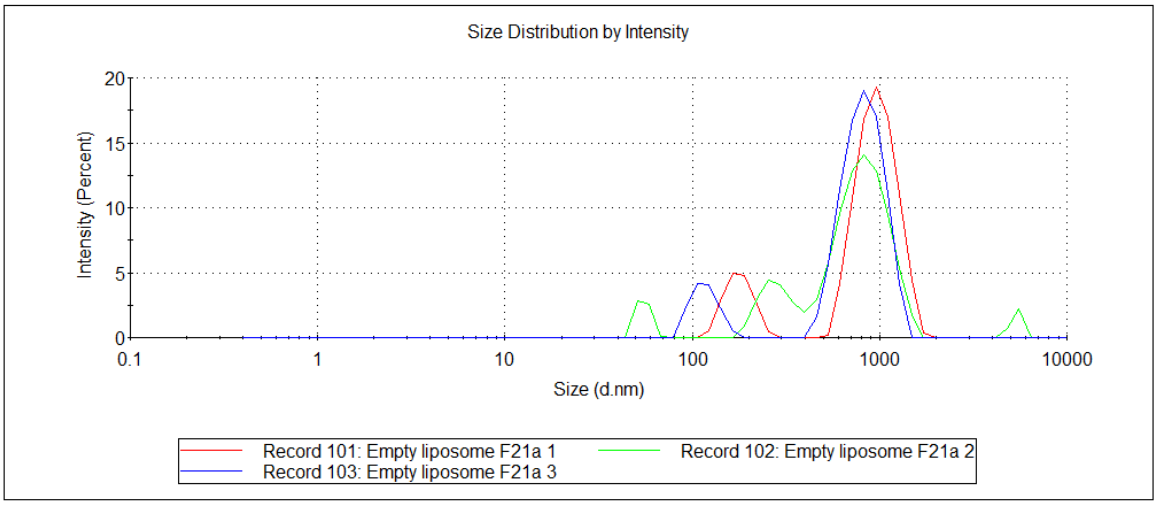

Figure 3.3*: Particle size distribution by intensity of formulation F21*

- **Second series of design of experiments**

From all the factors evaluated at this 2nd stage (vortex/rotavap cycles, stirring time, stirring temperature), none of them affected the size distribution of liposomes significantly.

However, as reported in **table 3.2**, the two best formulations for S2 were G12 and G16, with PDI values of 0.57 ± 0.039 and 0.57 ± 0.052, respectively. In addition of having similar distribution by intensity as highlighted in **Figure 3.4,** they had average particle sizes in the same range (582 ± 23 nm and 598 ± 72 nm) and were all negatively charged.

Set G12 consisted of 2 vortex/rotavap cycles and was stirred at room temperature while G16 was prepared with 3 cycles of vortex/rotavap without stirring. Interestingly, the data from the second series demonstrates that heating and stirring steps have no significant influence on the distribution of liposomes particles made by REV. Bearing in mind that temperature is the parameter that most often denatures proteins (Borzova et al. 2016; S. L. Wang et al. 2005), avoiding any heating step could be beneficial to preserve the integrity of sensitive proteins in the final formulations, and also to reduce the overall cost of preparation.

Although the main effect of plots (**Figure 3.5**) concerning the vortex/rotavap cycle shows a trend towards better PDI for one cycle, two cycles could be more suitable to remove residual organic solvents, which can affect the stability of liposomes (Cortesi et al. 1999; Szoka and Papahadjopoulos 1978). Thus in this study two cycles were subsequently chosen.

Overall, only variation of the organic phase to aqueous phase ratio could significantly have an effect upon the distribution of liposomes among the variable parameters considered in this study. This confirms the assumption that the ratio of organic phase to aqueous phase is the crucial variable that can affect the shape size and distribution of liposome in REV (Seth and Misra 2002).

***Table 3.2**: Second series of empty liposomal formulations with average size and PDI values*

Formulation S2	Vortex/rotavap cycles	Stirring time (min)	Stirring temperature (°C)	Average size (nm)	PDI	Zeta potential (mV)
G1	1	0	-	516 ± 33	0.596 ± 0.037	-
G2	1	30	25	490 ± 40	0.623 ± 0.036	-
G3	1	30	40	456 ± 29	0.632 ± 0.118	-
G4	1	30	60	468 ± 183	0.651 ± 0.177	-
G5	1	60	25	542 ± 55	0.630 ± 0.033	-
G6	1	60	40	535 ± 29	0.588 ± 0.052	-
G7	1	60	60	507 ± 37	0.601 ± 0.067	-
G8	2	0	-	487 ± 91	0.625 ± 0.155	-
G9	2	30	25	580 ± 31	0.603 ± 0.098	-
G10	2	30	40	545 ± 45	0.601 ± 0.031	-
G11	2	30	60	632 ± 120	0.600 ± 0.036	-
G12*	**2**	**60**	**25**	**582 ± 23**	**0.570 ± 0.039**	**–35.3±1.4**
G13	2	60	40	460 ± 20	0.640 ± 0.977	-
G14	2	60	60	506 ± 111	0.579 ± 0.061	-
G15	2	60	80	450 ± 18	0.591 ± 0.040	-
G16*	**3**	**0**	**-**	**598 ± 72**	**0.570 ± 0.052**	**–41.0± 1.3**
G17	3	30	25	522 ± 19	0.584 ± 0.036	-
G18	3	30	40	344 ± 25	0.794 ± 0.175	-
G19	3	30	60	610 ± 28	0.600 ± 0.040	-
G20	3	60	25	462 ± 40	0.587 ± 0.038	-
G21	3	60	40	448 ± 48	0.607 ± 0.046	-
G22	3	60	60	457 ± 44	0.666± 0.164	-
G23	3	60	80	593 ± 19	0.614 ± 0.040	-
G24	1	30	80	505 ± 81	0.586 ± 0.038	-
G25	1	60	80	533 ± 40	0.604 ± 0.019	-
G26	2	30	80	459 ± 43	0.778 ± 0.175	-
G27	3	30	80	530 ± 76	0.600 ± 0.076	-

***** *Formulation with best PDI in the series*

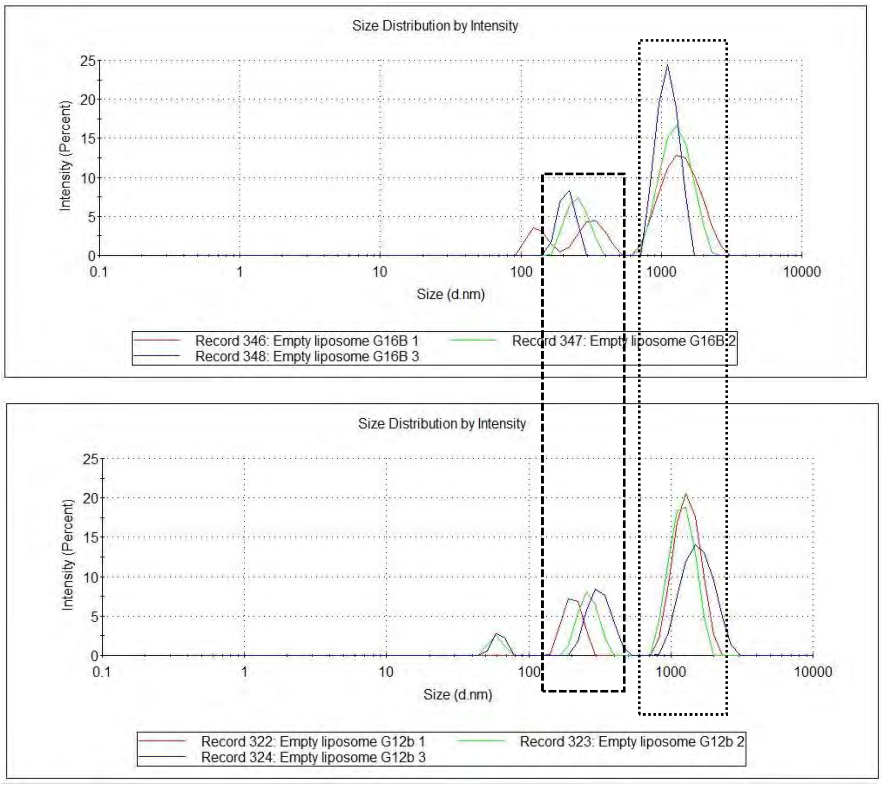

Figure 3.4: *Particle size distribution by intensity of formulation G12 and G16*

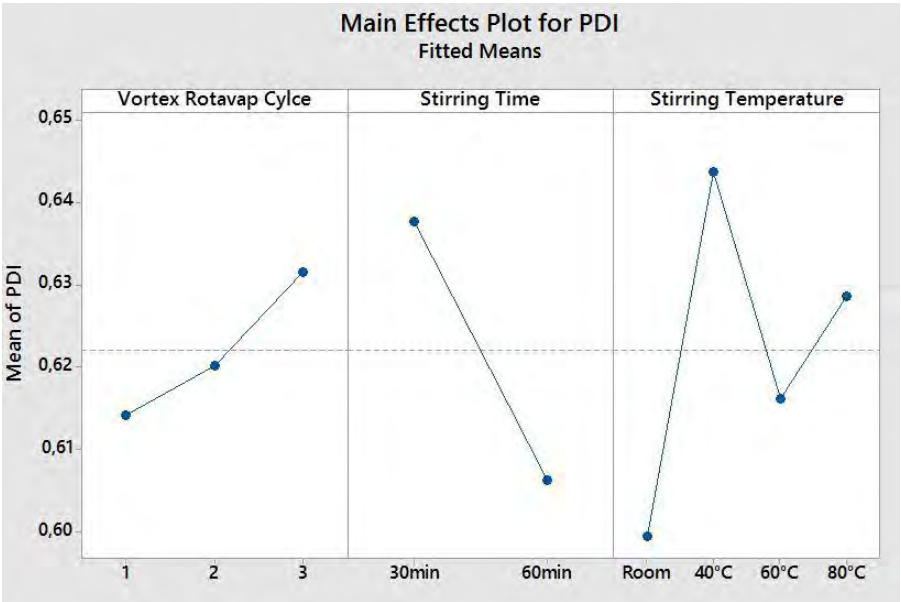

Figure 3.5: *Main Effects Plot for PDI of vortex/rotavapor cycles, stirring time and temperature*

3.1.2.2. Particle shape

Figure 3.6A shows typical TEM image of empty liposome formulation G12. The characteristic spherical shape of liposomes was observed and no aggregation of particles was detected. This could be explained by the repulsive forces between liposomes due to their highly negative surface charges (–35 mV by Zeta potential).

The size distribution of particles from the TEM image with a Gaussian distribution peak at around 60 nm (**Figure 3.6C**) correlated with the size distribution by number found in DLS (**Figure 3.6A**) for the same sample.

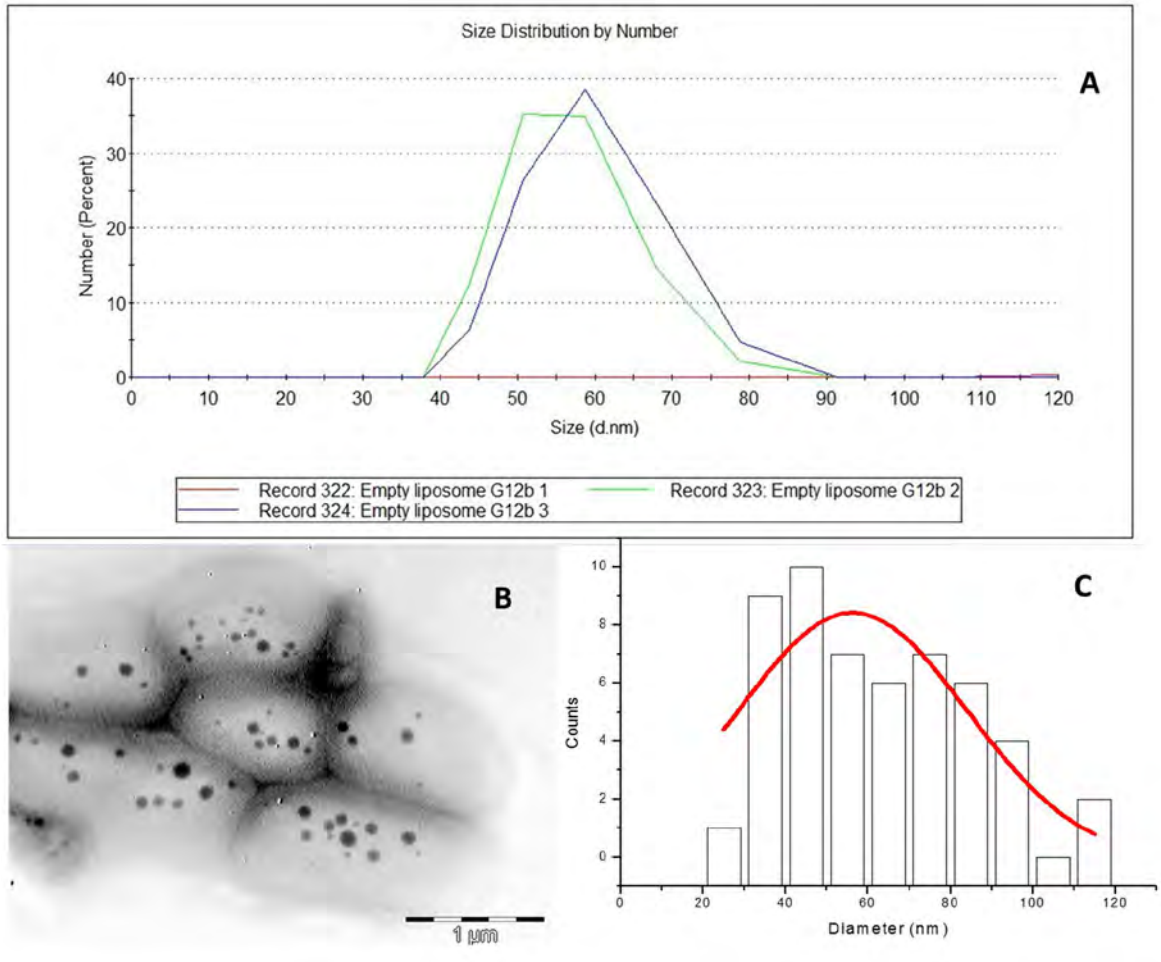

***Figure 3.6**: Empty liposomes G12: DLS distribution by number (**A**); TEM image (**B**), distribution of particles from TEM image generated by ImageJ (**C**)*

3.1.3. Validation of HPLC Method for quantification of Rif

As depicted in **Figure 3.7**, a distinct peak for Rif was observed at a retention time of approximately 5 min in the resultant chromatogram. The HPLC method was found to exhibit good precision since the RSD of the measured peak areas was ≤ 1.5% for repeatability (**Table 3.3**) and ≤ 2.0% for intermediate precision (**Table 3.4**). The method was found to be accurate, since the individual recovery values (**Table 3.5**) were within the required limits of 98.0–102.0%, with an average recovery value of 100.16%. This confirmed that experimental values were in close agreement with the nominal concentrations. The linear calibration curve (**Figure 3.8**) generated reflects a good correlation between the recorded peak areas and the concentrations of Rif, with $R^2 > 0.999$ (Kumar et al. 2014; Jimidar et al. 2007; ICH 2005).

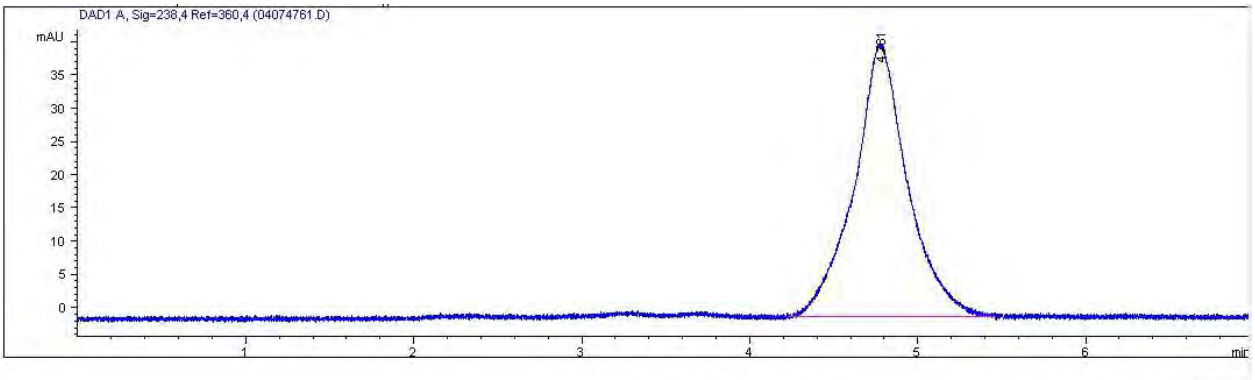

***Figure 3.7**: Typical HPLC chromatogram for a standard solution of Rif (30 µg/ml)*

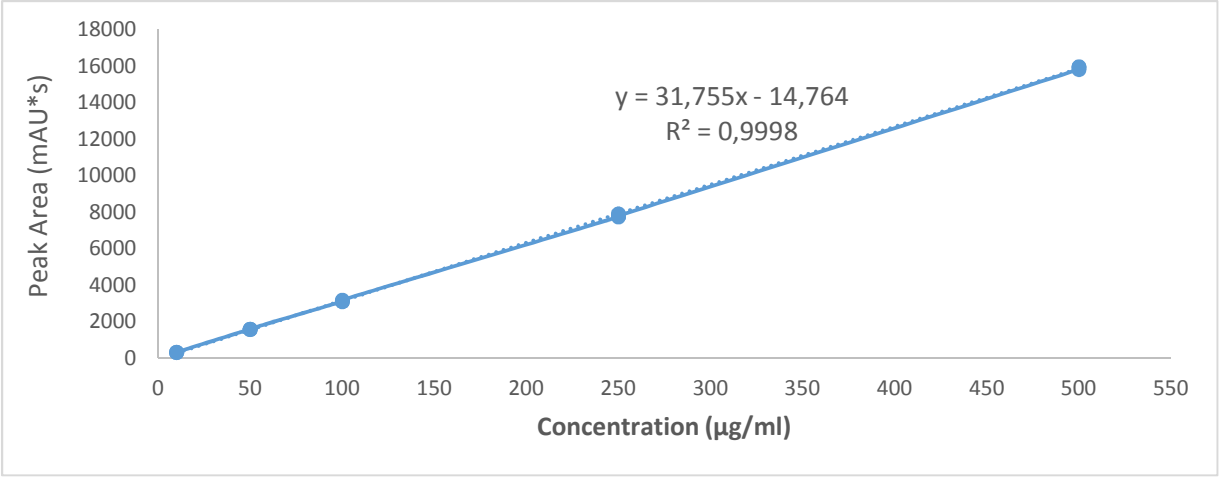

***Figure 3.8**: Standard calibration curve for Rif over the in concentration range 10-500 µg/ml*

***Table 3.3**: Results of repeatability study (Intra-day)*

Injection of Standard solution (30 µg/ml)	Peak area (mAU*s)
Injection 1	944,9
Injection 2	935,7
Injection 3	967,4
Injection 4	964,4
Injection 5	943,8
Injection 6	959,3
Average	952,6
Standard Deviation	12,8
RSD	***1,3%***

***Table 3.4**: Results of intermediate precision (inter-day)*

Standard solution (30µg/ml)	*Average peak area± SD (mAU*s)*	*RSD (%)*
Day 1	913.43 ± 9.6	**1.1**
Day 2	936.90 ± 8.9	**0.9**
Day 3	921.56 ± 13.1	**1.4**
Day 4	939.80 ± 9.1	**1.0**
Day 5	933.0 ± 13.6	**1.5**
Inter-day Precision		**1.2**

***Table 3.5**: Accuracy result for the drug Rif*

Nominal Concentration (µg/ml)	**Experimental concentration (µg/ml)**	**Accuracy (Recovery %)**
30	30.20	100.68
50	50.12	100.25
100	100.77	100.77
250	247.17	98,87
500	501.23	100,25
Average recovery		**100.16**

3.1.4. Solubility of Rif in HSA solutions and in water

Under the experimental conditions used the solubility of Rif in HPLC grade water was found to be 1.88 ± 0.07 mg/mL, which correlates with the results reported by Henwood *et al*. (2000) who found 1.74 ± 0.07 mg/mL for a mixture of crystalline form II and the amorphous form of Rif.

The bar chart in **Figure 3.9** reflects the solubility of Rif in HPLC grade water as function of HSA concentration used. It can be observed that the solubility of Rif was dramatically improved due to interaction with HSA in a concentration dependent manner, possibly due to Rif-protein hydrophobic interactions.

Hydrogen bonds, van der Waals and electrostatic forces in addition to hydrophobic interactions are the main bond types that influence protein-drug binding (L. Xu et al. 2017; C. Wang et al. 2007; Bi et al. 2004). Spontaneous binding of Rif derivatives to albumin has been demonstrated previously and were attributed primarily to hydrophobic and electrostatic interactions (O.-Y. Yu et al. 2011; C. Wang et al. 2007).

However, the data suggest the solubility of Rif increases following an arithmetic progression, with unity as the common difference *viz*., 2, 3 and 4 times whilst the increment in HSA concentration followed a geometric progression with a common ratio of 2 *viz*., 10%, 20% and 40% HSA. This could be due to folding of HSA as a result of non-polar interactions through Van der Walls forces within its molecular structure (Murray et al. 2017; Camilloni et al. 2016), which is expected to be more intense at higher concentrations and therefore reduces the number of hydrophobic binding sites for Rif. This effect underlines why highly concentrated HSA solutions such as 40% w/v appears to be less useful than lower concentrations of HSA in terms of improving Rif solubility. Hence, the saturated solutions of Rif in HPLC grade water and in HSA 10% and 20% were selected for encapsulation in liposomes.

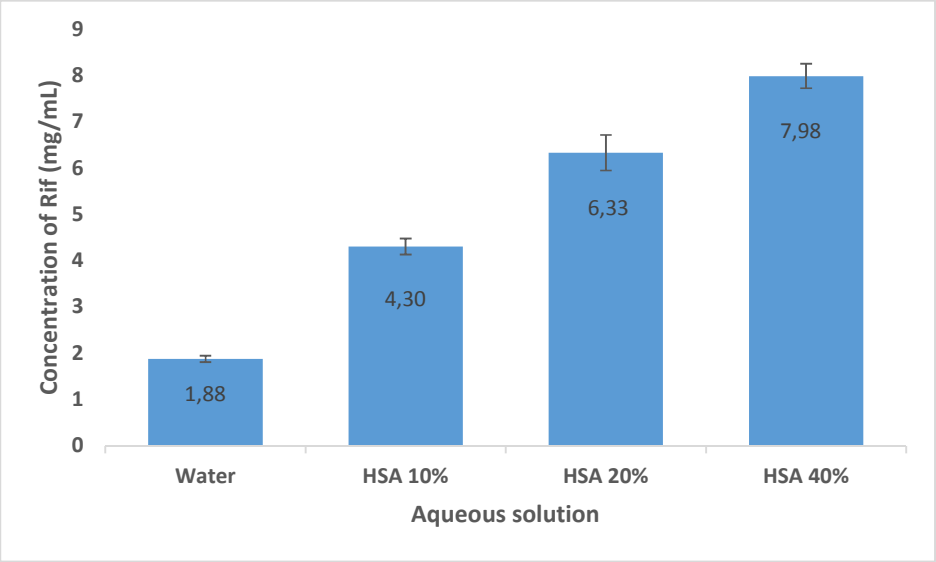

***Figure 3.9**: Solubility of Rif in HPLC grade water and HSA solution*

3.2. Preparation of Rif-HSA loaded liposomes

3.2.1. Effect of lipid and aqueous phase composition on encapsulation efficiency for Rif

Results of %EE for Rif are summarized in **Figure 3.10**. In general, it was observed that the %EE of Rif in liposomes decreased when cholesterol was present. This observation has been reported by other researchers who used lecithin to encapsulate Rif prepared using a thin film hydration method (Nkanga et al. 2019; J. S. Patil et al. 2015; Zaru et al. 2009)

Surprisingly, the liposomes made with Rif saturated HPLC grade water exhibited a significantly greater %EE (p<0.05) than formulations with Rif saturated HSA solutions. This may be explained by potential interactions between HSA and lipids within the liposomal vesicles and by the large size of HSA (Ntimenou et al. 2006; J. P. Colletier et al. 2002). HSA may therefore compete with the Rif entrapped in the lipid bilayer. However, this is less of a drawback than may initially appear, since the complexity of the structure of HSA provides several additional binding sites that may accommodate different ligands including fatty acids (Ascenzi et al. 2011), and this could be an advantage in future iterations of this system.

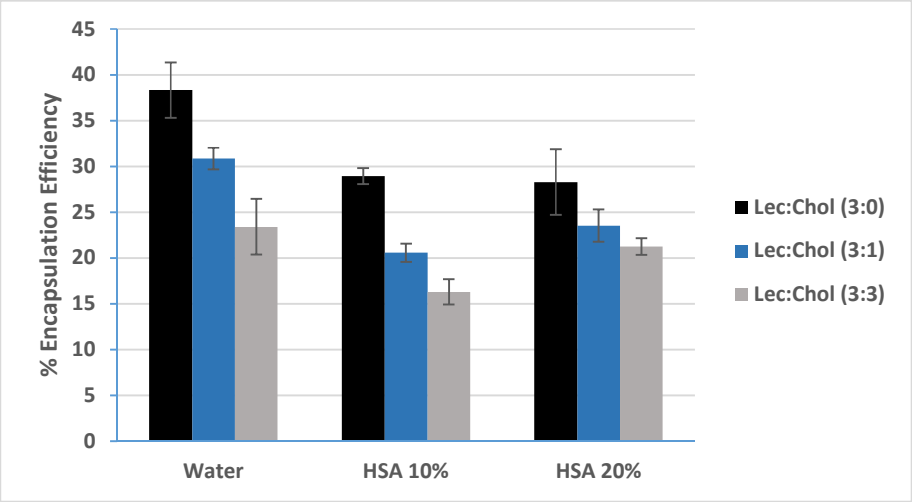

***Figure 3.10**: Comparison of encapsulation efficiency for Rif of liposomes composed of different HSA solution and lipid composition*

Moreover, the difference in %EE between the formulations with 10% or 20% HSA, of 28.9 ± 0.87% and 28.3 ± 3.6%, respectively was not statistically significant. This could be due to the fact that both the lipid bilayer and the inner aqueous core of the liposomes prepared using REV were saturated with the Rif-HSA complex. Reducing the amounts of Rif and consequently of HSA in the liposome composition is suggested to be a viable option for the optimization of %EE for Rif.

The formulation prepared with 10% HSA solution and without cholesterol was selected for further optimization studies. The reason for selecting this formulation was based on the fact that this composition results in a relatively good %EE while involving the use of fewer materials, which not only appears to be more cost-effective than preparing other formulations, but provides systems with fewer interacting components, which would be important during later spectroscopic analyses (*viz*. NMR, FTIR).

The DLS results summarized in **Table 3.6** reveal the particle size distribution as well as the Zeta potential of re-dispersed liposomes prepared without cholesterol. All formulations exhibited an acceptable polydispersity index (PDI) with the average size of liposomes varying between 500 and 750 nm. There was no particular correlation between the size of liposomes and HSA concentration used.

All the formulations exhibited negative Zeta potential values. The negative charges of liposomes observed are consistent with those observed in previous studies where CSL and thin film hydration were used for the preparation of the liposomes (Nkanga et al. 2019, 2017; Nkanga and Krause 2019).

However, the presence of HSA in the liposomes seems to affect the Zeta potential of the formulations with the results varying from –46.3 ± 0.2 mV without HSA to –57.8 ± 0.4 mV with 20% HSA. Considering the fact that free HSA has a negative Zeta potential (Larsen *et al.* 2016; Bakaeean *et al.* 2012) this change in Zeta potential suggests the presence of at least some HSA in the membrane and on the surfaces of the liposomes.

Since negatively charged particles are known to be rapidly opsonized by macrophages through scavenger receptors (Walton et al. 2010; Honary and Zahir 2013), the presence of some HSA on the surface of the liposomes or at least a more negative Zeta value may be useful for targeting intracellular infectious diseases such as tuberculosis that hijack macrophages (Teng et al. 2017).

Table 3.6*: Size distribution and Zeta potential of re-dispersed formulations after freeze-drying*

Composition aqueous phase	Lipids CSL/Chol ratio	Average size (nm)	PDI	Zeta potential (mV)
HPLC grade water	3:0	661 ± 15	0.366 ± 0.072	–46.3 ± 0.2
HSA 10%	3:0	730 ± 2	0.312 ± 0.022	–48.0 ± 2.8
HSA 20%	3:0	509 ± 74	0.473 ± 0.113	–57.8 ± 0.4

3.2.2. Optimization of encapsulation efficiency of liposomes for Rif

The %EE of formulations with different initial amount of Rif is summarized in **Table 3.7**. As can be observed formulation O_3 of Rif-HSA-lip with 6 mg total Rif loaded exhibited the best %EE of 59.2 ± 8.7%. The Rif-lip formulation prepared as a control with the same amount of Rif showed a similar %EE of 58.8 ± 11.3% as its formulation counterpart (O_3).

Considering the potential competition between Rif and HSA for sites within the lipid bilayer, one can assume that HSA occupies a larger space than Rif in the bilayer due to its larger molecular size. Therefore, the closeness in the %EE values of the two formulations prepared with and without

HSA suggests that the loading of Rif in the inner aqueous core of liposomes was considerably increased in the presence of HSA thereby compensating the resulting loss in %EE due to pure steric considerations. As recently reported by Okamoto *et al.* (2018), the improvement in loading of Rif in the aqueous core of liposomes could be attributed to drug binding properties of albumin towards hydrophobic drugs.

Table 3.7*: Encapsulation efficiency of optimized formulations*

Formulation	Rif used in organic phase (mg)	Quantity of Rif used in aqueous phase (mg)	Total Rif used (mg)	EE ± SD (%)
O_1	20	10	30	20.3 ± 0.9
O_2	12	6	18	26.1 ± 2.1
O_3	4	2	6	59.2 ± 8.7
Rif-lip	4	2	6	58.8 ± 11.3

3.2.3. Characterization of Rif-HSA loaded liposomes

3.2.3.1. Particle size and shape analysis

A typical TEM image of Rif-HSA-lip (O_3) is depicted in **Figure 3.11B**, revealing the presence of particles of with spherical shape, which is characteristic to liposomes. The size distribution of the particles from the TEM image describes a Gaussian distribution peak at around 200 nm (**Figure 3.11C).** This distribution correlated with the particle size distribution by number generated from DLS evaluation of the same sample (**Figure 3.11A)**.

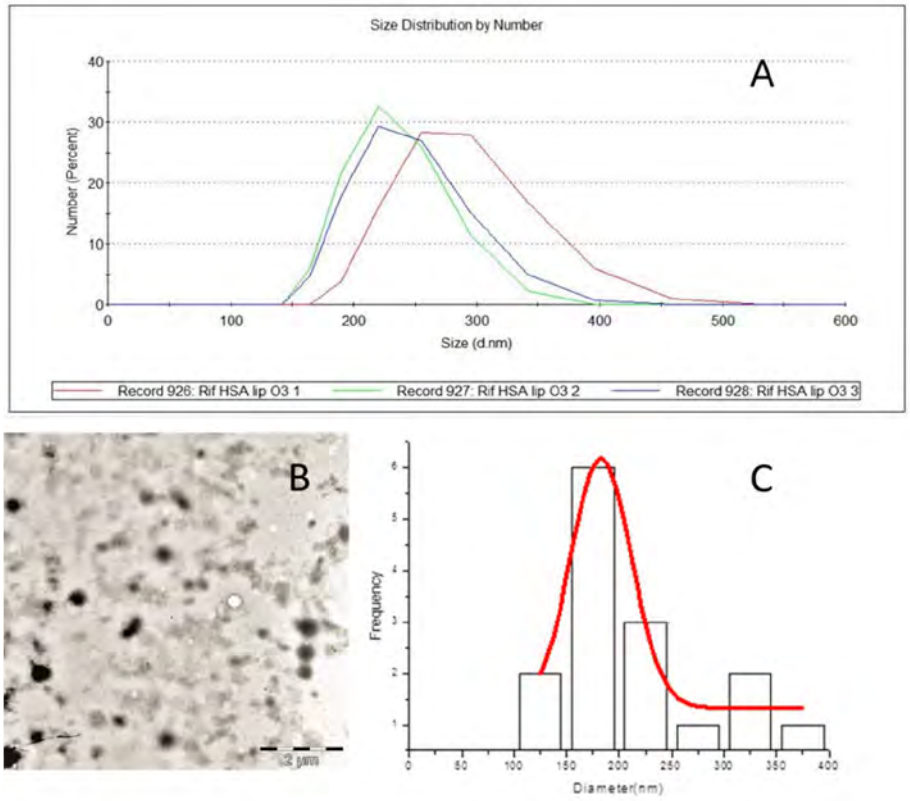

***Figure 3.11**: DLS size distribution by number (**A**); TEM image (**B**) and size distribution from TEM image generated by ImageJ (**C**) for Rif-HSA-lip O_3*

3.2.3.2. Proton nuclear magnetic resonance

NMR techniques can be used to explore intermolecular and intramolecular interactions within liposomes (Timoszyk 2017). In my study, ^{1}H NMR was used to compare the profile of empty liposomes with those of Rif-lip, HSA-lip and Rif-HSA-lip. As depicted in **Figure 3.12**, some variations in the ^{1}H NMR chemical shift (δ) of empty liposomes were observed in dual liposome (Rif-HSA-lip) and also in both mono loaded liposomes (Rif-lip and HSA lip). The shifts in the NMR signals of empty liposomes (Empty-lip) confirmed the existence of some intermolecular interactions between the lipid bilayer and the payload (Rif and HSA).

Most importantly, the shift of empty liposome proton signals at δ=2.55–2.50 ppm in mono-loaded Rif-lip and HSA-lip confirmed the existence of possible competition behaviour between Rif and HSA for sites within the liposome bilayers.

Furthermore evidence of loading of Rif in liposomes was highlighted in the partial NMR spectra (**Figure 3.12**), where Rif signals could be observed in Rif-lip and Rif-HSA-lip, unlike in Empty-lip and HSA-lip spectra where Rif was not included. These signals were visible as two broad singlets at δ=2.96 and δ=2.79 ppm corresponding to the lone methoxy group and one of the hydroxyl groups of Rif, respectively (Diehl 2008).

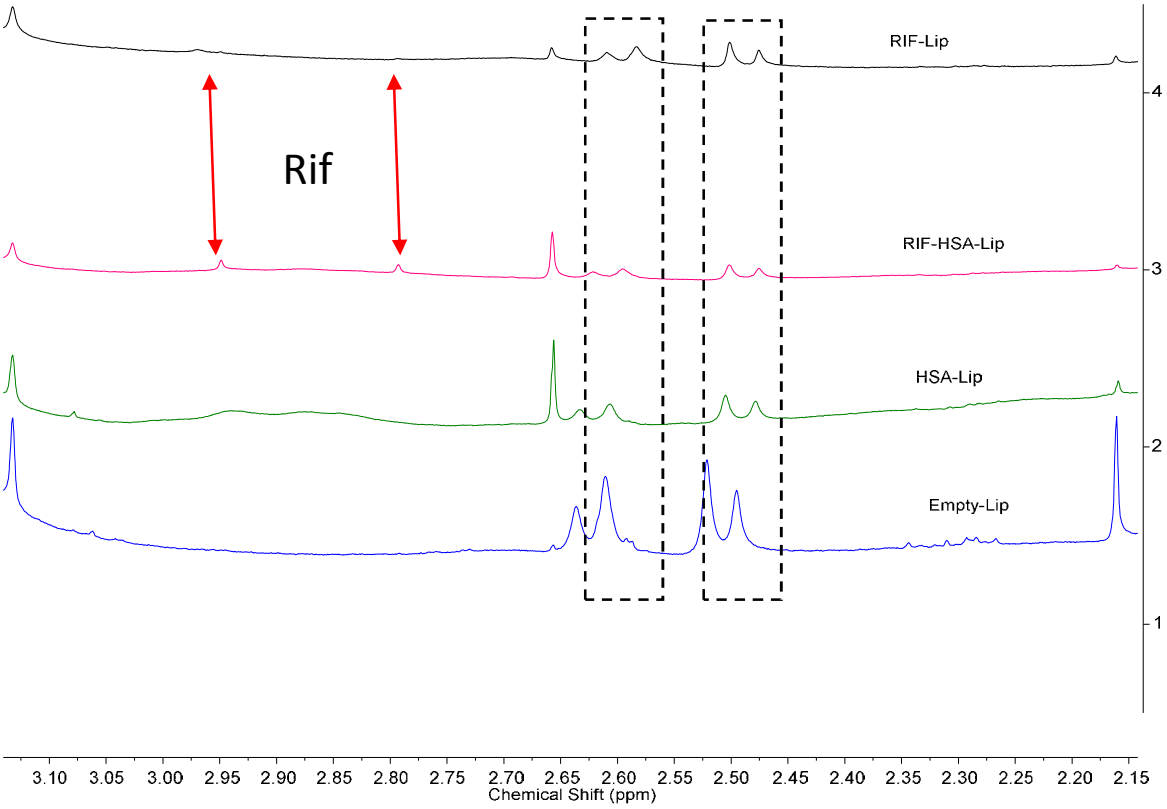

***Figure 3.12**: Partial ^{1}H NMR spectra of Empty-lip compared to Rif-HSA-lip, HSA-lip and Rif-lip*

3.2.3.3. Infrared spectroscopy

Vibrational spectroscopy FT-IR was used to generate spectra for comparison of images for raw HSA and Rif with those generated for liposomal formulations. As can be seen in **Figure 3.13**, the characteristic bands for aliphatic groups were more intense in the liposomal formulations due to the hydrophobic tails of phospholipids, with a -C-H stretch for saturated fatty acids observed at about 3000–2850 cm^{-1} and with =C-H stretch for unsaturated lipids at 3000 cm^{-1}. Although most of the typical bands for Rif coincided with peaks of HSA or Empty-lip, the single bending vibration band appearing only in the samples containing Rif at about 970 cm^{-1} permits confirmation of the presence or absence of Rif. This band may be due to the C=C bending group from the disubstituted (*trans*) alkene functions characteristic of Rif molecules (**Figure 3.14)**. Furthermore, amide bands A, I and II, characteristic of HSA at about 3280, 1641 and 1530 cm^{-1}, respectively, were only present in raw HSA and in Rif-HSA-lip, with no remarkable shifts or changes in shape. Of particular interest, the intactness of amide band I provides a hint that an unmodified secondary structure of HSA is present in liposomes (Barth and Zscherp 2002; Volkin et al. 2002). In fact, hydrophobic interactions within the lipid-protein complex have been reported to stabilize molecular conformation of large proteins (Pace et al. 2011). The IR data confirmed the co-encapsulation of Rif and HSA in Rif-HSA-lip and suggests the intactness of HSA in the liposomes, another attractive research question that need to be further investigated in using alternative techniques such as circular dichroism, DSC and/or solid state NMR.

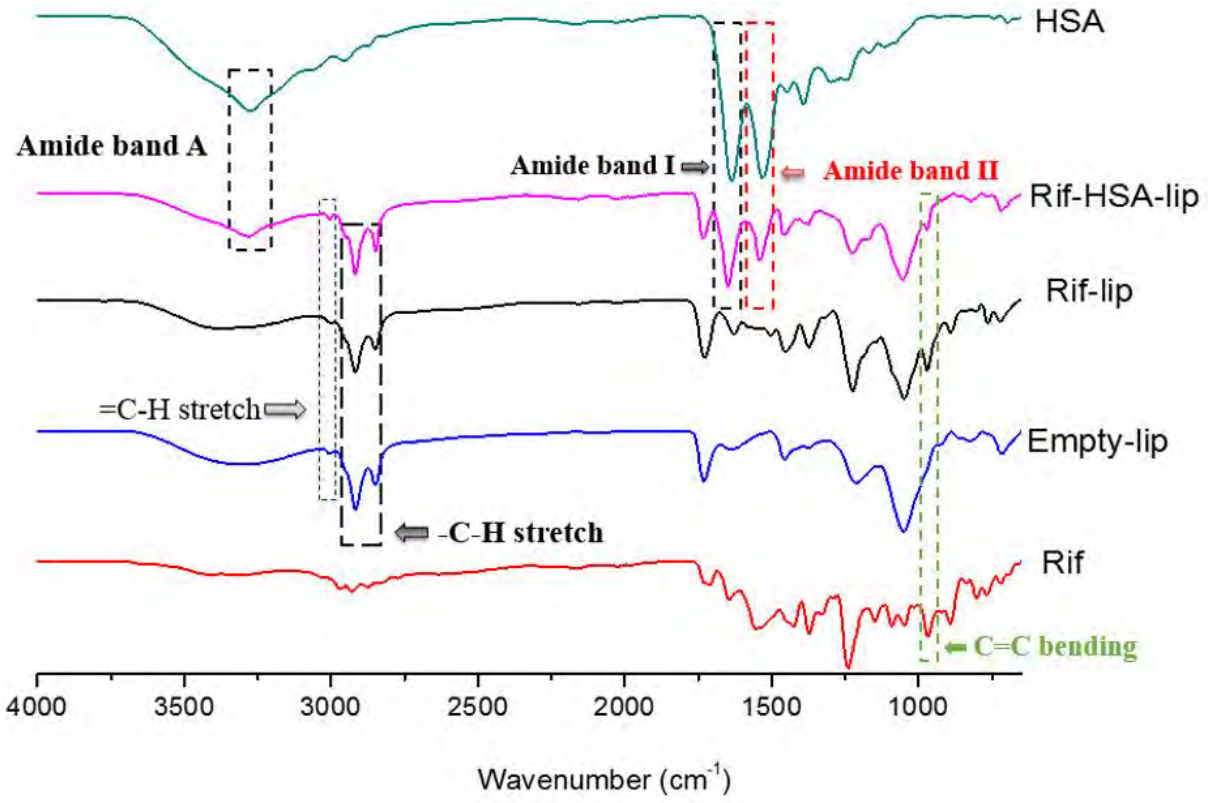

***Figure 3.13**: FT-IR spectra of different formulations compared to pure starting materials*

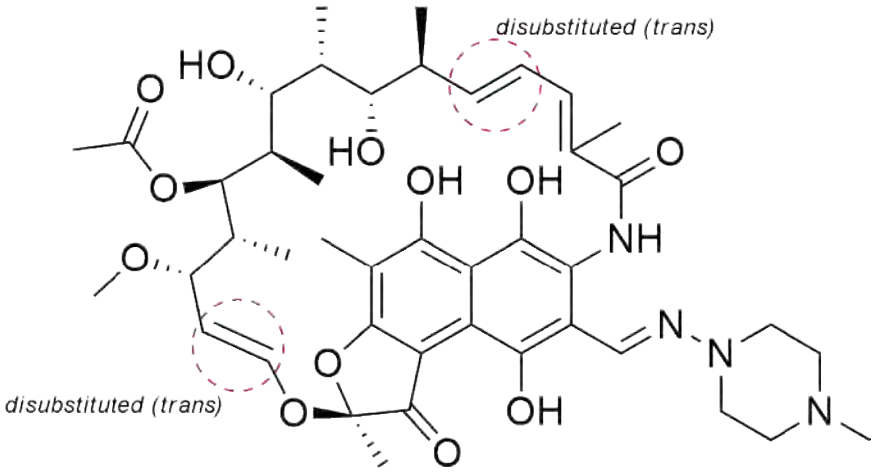

***Figure 3.14**: Rifampicin structure with disubstituted (trans) alkene functions highlighted*

3.2.3.4. Energy-dispersive X-ray spectroscopy

EDX can be used to explore the surface composition of liposomes (Nkanga and Krause 2018). In this study, the surface elemental composition of raw materials and freeze-dried formulations were compared using EDX. As illustrated in **Figure 3.15**, liposomal formulations were characterized by the presence of phosphorus, a key element in the hydrophilic heads of phospholipids, which are oriented to the surface of liposomes. Interestingly, a specific sulfur peak characteristic of HSA was detected in mono-loaded HSA-lip and in Rif-HSA-lip and can be attributed to the free HS-group of cysteine-34 that is located on the outer surface of HSA which is further exposed at the liposome surface when HSA is trapped within the lipid bilayers (Kratz 2008). The outcome of the EDX experiment confirms the presence of HSA in the liposomes confirming successful co-encapsulation of HSA and Rif in liposomes. In addition EDX results appear to be consistent with the data from Zeta Potential studies which suggest the presence of some of HSA moieties on the surface of liposomes.

The presence of HSA on the surface of liposomes can also be attributed to the formation of protein corona, resulting from the adsorption of free HSA by the liposome bilayers (Yokouchi *et al.,* 2001; Foteini *et al.*, 2019).

In fact, materials containing albumin are potent and bind naturally to neonatal Fc receptor (FcRn), which is present on the surface of epithelial, endothelial and myeloid lineages (Martins et al. 2018). Therefore, the presence of HSA on the surface of liposomes may be useful for targeted delivery applications by improving cellular uptake of Rif-HSA-lip via FcRn for the treatment of intracellular infections such as tuberculosis.

Furthermore the possible modification of albumin surfaces (e.g. maleylation) facilitates improvement of cell recognition and uptake by macrophages through scavenger receptors (Ahmed et al. 2019), promoting cell targeting features in combination with the negative surface charge of the liposomes.

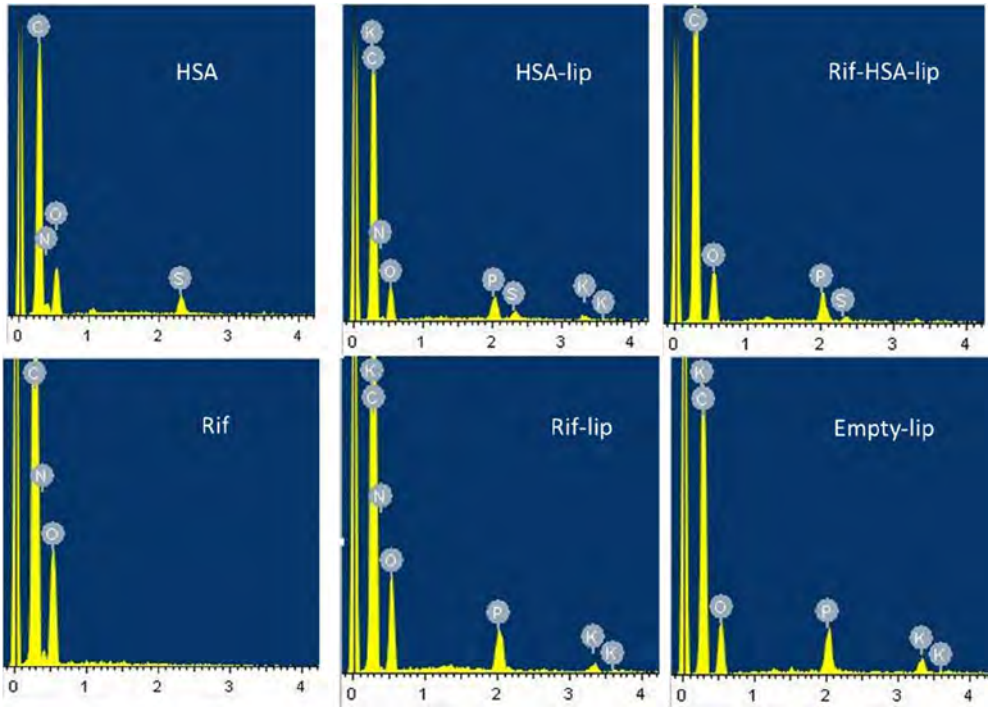

***Figure 3.15**: EDX spectra illustrating elemental surface composition of formulations and raw materials*

3.2.3.5. Differential scanning calorimetry

The thermal stability of co-loaded liposomes (Rif-HSA-lip) was compared to those of empty liposomes, mono-loaded liposomes (Rif-lip) and raw materials (Rif and HSA). The data from DSC studies are presented in **Figure 3.16**, revealing the presence of upward endothermic peaks. The DSC thermogram for Rif indicates the presence of the crystalline form II in the raw material used with the melting point (endothermic peak) at 194°C. The melting of Rif indicates transformation of Rif form II to Rif form I that is subject to decomposition characterized by an exothermic peak at 254°C (Alves et al. 2010; Bhise et al. 2010; Panchagnula and Bhardwaj 2008; Henwood et al. 2001).

The complete disappearance of the characteristic peaks for crystalline Rif in freeze-dried Rif-HSA in addition to Rif-lip and Rif-HSA-lip suggests conversion of Rif into an amorphous form, which is commonly attributed to molecular dispersion (dissolution) in carriers (Nkanga et al. 2019; J. S. Patil et al. 2015).

The HSA curve reveals the presence of an early endothermic peak with an apex at 57°C indicating denaturation of albumin (Borzova et al. 2016). The disappearance of the HSA peaks in the co-loaded liposomes suggests improved thermal stability of HSA when entrapped in the bilayers. This has been also reported when researchers have observed stabilizing effects of fatty acids on proteins, including albumin (Antoine and Souza 2007; Shrake et al. 1984). The stabilizing effect could be due to hydrophobic interactions in the lipid-protein complexes (Alzagtat and Alli 2002) .

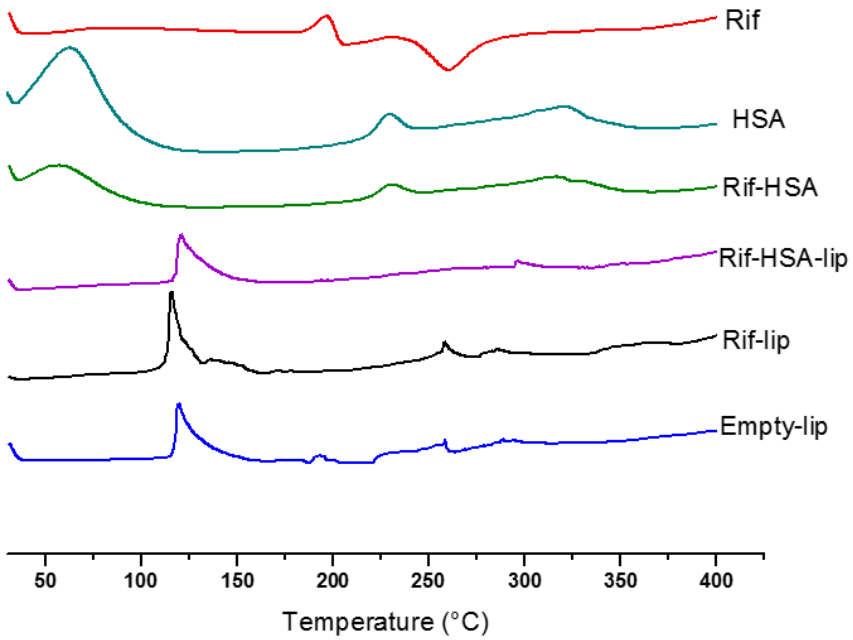

Figure 3.16: *DSC thermograms for Rif, HSA, Rif-HSA and liposomal formulations*

3.2.3.6. X-Ray Diffraction

The XRD patterns for raw Rif in comparison to Rif-HSA-lip, Rif-lip and Rif-HSA are depicted in **Figure 3.17**. The diffractogram for Rif reveals the presence of major crystalline peaks between 15° and 25°, while all carriers containing Rif exhibited broad amorphous patterns. The XRD results support DSC data and confirmed that Rif is converted into an amorphous form when incorporated in liposomes or in the presence of HSA.

The XRD profile looks promising for future investigation and application of Rif-HSA-lip, since the conversion of poorly water-soluble drugs from crystalline to amorphous forms on dispersion

in the carriers is known to ameliorate solubility and related bioavailability challenges of poorly soluble drugs (Murdande et al. 2011).

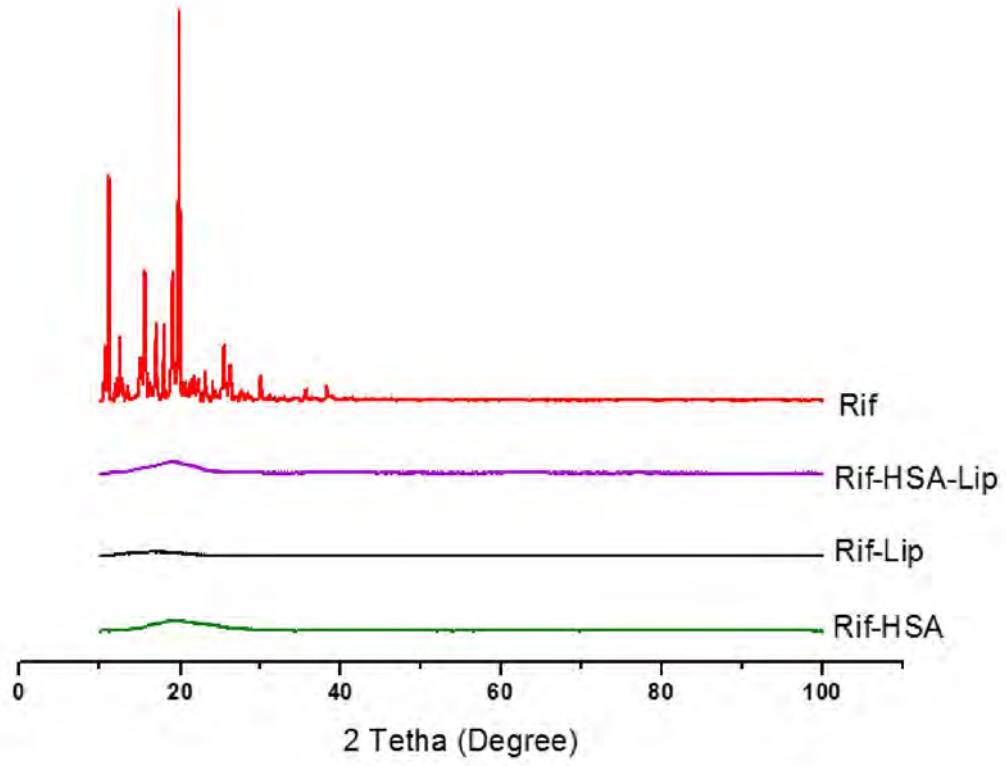

***Figure 3.17**: XRD patterns of formulations*

3.2.3.7. In vitro release studies

The release profiles of Rif from the Rif-HSA-lip, Rif-lip and Rif-HSA systems are depicted in **Figure 3.18**. Overall free Rif was relatively slow to diffuse from the dialysis bag, with an average cumulative percent released of 65% in 12 hours which may be justified by the poor aqueous solubility of Rif of 1–2 mg/ml. The dissolution profile of free Rif observed in this study appears to be similar to that observed for dissolution of Rif in phosphate buffer (Henwood et al. 2000). The release of Rif from the Rif-HSA complex was found to be more rapid than free Rif, reaching an average cumulative percent released of 85% in 12 hours that could be explained by the existence of reversible binding interactions in the Rif-HSA complex, which is known to improve the bio-distribution and bioavailability of drugs (Larsen et al. 2016). Interestingly, the release of Rif from

the liposome formulations Rif-lip and Rif-HSA-lip increased significantly with approximately 95% released after only 5 hours.

In general, the improvement of the release profile of Rif following encapsulation in different carriers (HSA and liposomes) supports the DSC and XRD data generated which suggest conversion of Rif into an amorphous form due to molecular distribution. Furthermore Rif-HSA-lip and Rif-lip exhibited similar release profiles, which indicates that the presence of HSA in the liposomes does not affect adversely Rif release. Therefore the use of HSA in liposomal encapsulation processes may add valuable properties to the delivery systems, such as antioxidant, cryoprotectant and targeted delivery features, without affecting release characteristics of the technologies.

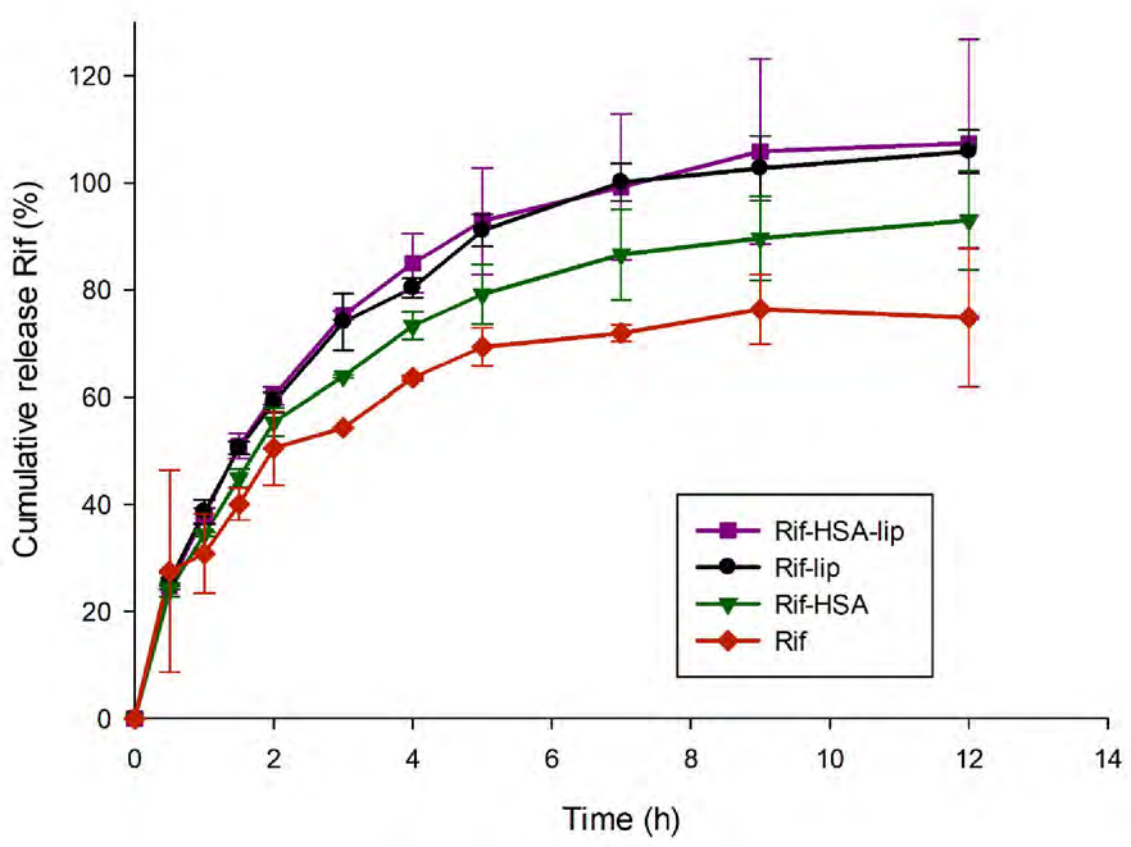

***Figure 3.18**: Comparison of In vitro release profile of free Rif, Rif-HSA, Rif-lip and Rif-HSA-lip*

Table 3.8 summarises the data of main kinetic models obtained with DDSolver software. Based on statistically higher coefficient of determination (Rsqr) and lower Akaike Information Criterion (AIC) (Bruschi 2015), Makoid-Banakar and Peppas-Sahlin are the two models describing the best the release of Rif. Noteworthy, the free Rif and the Rif-HSA adequately fitted the Makoid-Banakar model with Rsqr of 0.9921 and 0.9989, respectively. Whilst the liposomal formulations were best described by the Peppas Sahlin model (Rsqr of 0.999 for Rif-lip and of 0.9963 for Rif-HSA-lip) which indicated that the release of Rif in liposomes is governed by the combination of Fickian diffusion and case-II relaxation (Peppas and Sahlin 1989).

Table 3.8: *Release model data for Rif, Rif-HSA, Rif-lip and Rif-HSA-lip*

Release kinetic model	**Parameters**	**Formulation**			
		Rif	*Rif-HSA*	*Rif-lip*	*Rif-HSA-lip*
Zero Order	Rsqr	-0,1297	0,1934	0,3159	0,3364
	AIC	95,4375	98,0916	98,6941	99,2889
First order	Rsqr	0,6078	0,9350	0,9860	0,9922
	AIC	83,8007	70,3857	55,8978	50,4165
Higuchi	Rsqr	0,8178	0,9118	0,9369	0,9361
	AIC	75,3641	73,7417	72,4728	73,5421
Korsmeyer-Peppas	Rsqr	0,9449	0,9710	0,9715	0,9664
	n	0,352	0,360	0,389	0,395
	AIC	61,9853	63,5031	65,7350	68,4724
Hixson-Crowell	Rsqr	0,4357	0,8687	0,9567	0,9715
	AIC	87,8011	78,1205	68,3455	64,6651
Hopfenberg	Rsqr	0,6076	0,9350	0,9860	0,9922
	AIC	85,8049	72,3895	57,9091	52,4235
Baker-Lonsdale	Rsqr	0,9176	0,9858	0,9866	0,9799
	AIC	66,6345	53,6826	55,4476	60,8149
Makoid-Banakar	Rsqr	**0,9921**	**0,9989**	0,9978	0,9938
	AIC	**42,1064**	**29,5074**	37,6927	52,3051
Peppas-Sahlin	Rsqr	0,9907	0,9986	**0,9990**	**0,9963**
	AIC	43,8640	31,9361	**31,3533**	**46,2262**
Gompertz	Rsqr	0,9817	0,9899	0,9835	0,9681
	AIC	52,1143	51,9479	57,7765	67,9116

3.2.3.8. Stability studies

The electric surface properties of particles in a colloidal suspension (Zeta potential) is an important factor governing system stability. The natural tendency of particles in suspension is to aggregate and can be minimized by the presence of a surface charge, which induces repulsion effects between dispersed particles (Bakaeean *et al.*, 2012).

As can be observed in **Figure 3.19A** for the freeze-dried samples, the Zeta potential of the Rif-HSA-lip product was generally larger than that of Rif-lip. This surface feature was maintained in a plateau up to 4 weeks of storage at 25°C, whereas the Zeta potential of Rif-lip tended to decrease gradually over time. The same tendency was observed in respect of the size distribution of the same samples (**Figure 3.19C**). There was distinct variation in the size distribution of the Rif-lip between 300 and 1200 nm, while the change in average particle size of Rif-HSA-lip was maintained in the range between 300 and 700 nm.

Freeze-dried Rif-HSA-lip seems advantageous when compared to freeze dried Rif-lip in terms of stability that could be attributed to the antioxidant properties of HSA preventing lipid peroxidation (Taverna et al. 2013). In addition, HSA is known for possessing excellent cryoprotectant activity and can improve shelf-stability of nanomedicines (Tao et al. 2019).

However, for the liposomes incubated in HPLC grade water, the Zeta potential of Rif-HSA-lip and Rif-lip decreased considerably, albeit more evident for the Rif-HSA-lip (**Figure 3.19B**). Visual aggregation was observed in the formulations over time and it was more remarkable for the Rif-HSA-lip. The aggregation was confirmed by size distribution data (**Figure 3.19D**) that revealed a drastic increase in the average size of Rif-HSA-lip in suspension. The incubation time in aqueous solution of albumin have been an added factor affecting the size of the aggregates (Borzova et al. 2016).

My results contradict the findings reported by Okamoto et al. (2018) who suggested that Bovine Serum Albumin-liposomes prepared with different lipid composition *viz*., egg phosphatidylcholine, cholesterol and DSPE-PEG_{2000} were stable for at least one month in solution.

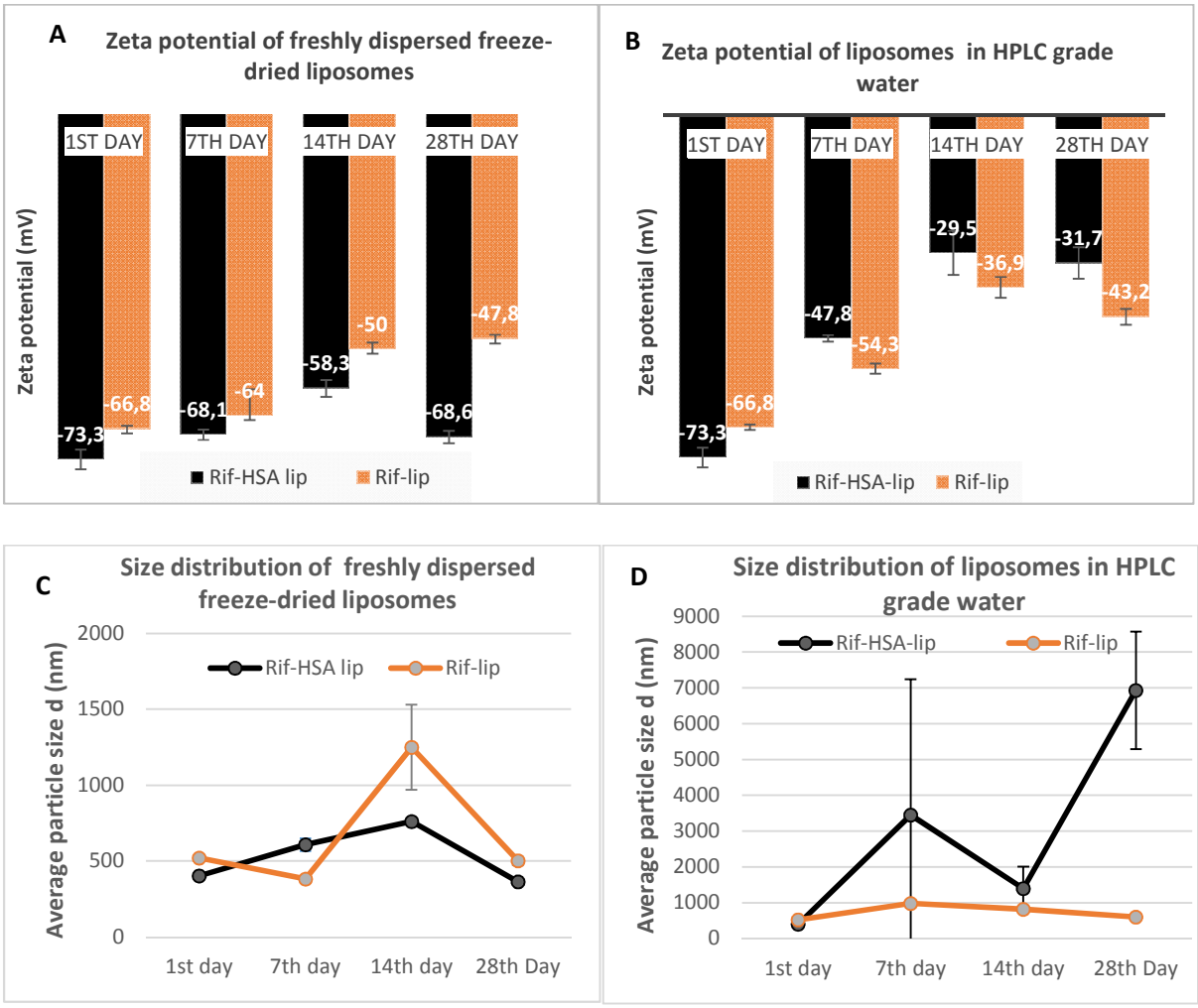

***Figure 3.19**: DLS results following stability testing of Rif-HAS-lip and Rif-lip*

Chapter Four

Conclusions

4. CONCLUSION

The main aim of this study was to design, formulate and characterize liposomes co-loaded with rifampicin (Rif), an antitubercular drug and a reasonably large protein, in this case human serum albumin (HSA). A successful simultaneous encapsulation of Rif and HSA in liposomes made of crude soybean lecithin and produced by reverse phase evaporation method (REV) is reported in this work. It was found that HSA interacts with the lipid components of the liposomes and competes with Rif for location sites within the lipid bilayers, but that this competition does not exclude Rif from being encapsulated. Far from this, there is a cooperative association between Rif and HSA that allows greater %EE than would be the case with no HSA. This is likely to be in part because the water solubility of Rif was improved in the presence of HSA which considerably increased the loading of Rif in the aqueous core of the liposomes. This aqueous stabilisation of Rif and other hydrophobic molecules may benefit from further research.

The restricted size of liposomes also assisted the conversion of Rif from a crystalline to amorphous form. This amorphous phase in the liposomes improved the *in vitro* release profile, which may lead to improved bioavailability of the encapsulated antibiotics in general.

Different characterization techniques confirmed the presence of HSA embedded in the liposomes and poking out on the surface of liposomes. This attribute could be used to improve two crucial aspects of drug delivery of the liposomes *viz.*, targeted delivery and stimuli-responsive release of the cargo. The intracellular targeted delivery could be improved through HSA specific binding receptors (such as FcRn, Scavengers) expressed on the surface of macrophages, where TB pathogens often reside. Furthermore, the breakup of liposomes could be triggered by HSA-proteases for stimuli-responsive release since proteases such as caseinolytic protease proteolytic subunits (ClpP) are known to be overexpressed in TB parasitism of the macrophage (Estorninho et al. 2010; Moreno-cinos et al. 2019).

Moreover, the presence of HSA, thanks to its potential antioxidant and cryoprotectant properties, is highly beneficial for improved shelf-stability of the freeze-dried Rif-HSA-lip. This opens an avenue to overcome the storage issue of liposomes which is one of the drawbacks preventing their wider application.

To the best of my knowledge, this study appears to be the first to report the simultaneous encapsulation of a large protein *viz*., HSA, and a hydrophobic antitubercular drug *viz*., Rif, in liposomes by means of a conventional bulk encapsulation approach (REV) and using crude soybean lecithin. The characteristics of the produced dual liposomes exhibit the potential for future biomedical investigations towards the development of effective treatments against life-threatening diseases and more particularly for TB.

Taking into consideration the fact that more effective therapeutic management of TB is a key to reduce the high morbidity and mortality rates of the disease, the development of such a new drug delivery system with targeted delivery features and improved pharmacokinetic properties holds the promise to shorten the regimen for the treatment of drug-susceptible TB and for tackling antimicrobial resistance.

Nevertheless, further studies are needed to provide additional insights into the molecular architecture and biological performance of liposomes co-loaded with therapeutic proteins and chemotherapeutic compounds for the management of intracellular infections such as tuberculosis. In particular, future investigations could include:

(i) To build on the demonstrated active targeting features of HSA liposomes for intracellular delivery of TB drugs,

(ii) To extend the therapeutic value of the developed formulation by co-loading other different anti-TB drugs and HSA,

(iii) To further investigate the stimuli response of liposomal formulation for controlled release of the cargo,

(iv) To prepare inhalable powder of liposomes for pulmonary delivery, and

(v) To evaluate the *in/ex vivo* therapeutic properties of the liposomal formulation.

An alternative novel method of preparation like supercritical fluidic techniques could be also considered so as to overcome the main drawback of REV by avoiding the use of organic solvents.

REFERENCES

Acocella, G. 1978. “Clinical Pharmacokinetics of Rifampicin.” *Clinical Pharmacokinetics* 3: 108–27. https://doi.org/10.2165/00003088-197803020-00002.

Acra, Hale Cigdem, Laura I Mosquera-giraldo, Junia M Pereira, Nammakwar Sriranganathan, Lynne S Taylor, and Kevin J Edgar. 2018. “Rifampin Stability and Solution Concentration Enhancement through Amorphous Solid Dispersion in Cellulose ω-Carboxyalkanoate Matrices.” *Journal of Pharmaceutical Sciences* 107 (1): 127–38. https://doi.org/10.1016/j.xphs.2017.05.036.

Ahmed, Mona, Roland Baumgartner, Silvia Aldi, Philip Dusart, Björn Gustafsson, and Kenneth Caidahl. 2019. “Human Serum Albumin-Based Probes for Molecular Targeting of Macrophage Scavenger Receptors.” *International Journal of Nanomedicine* 14: 3723–41. https://doi.org/http://doi.org/10.2147/IJN.S197990.

Akash, Muhammad Sajid Hamid, Kanwal Rehman, Muhammad Tariq, and Shuqing Chen. 2015. “Development of Therapeutic Proteins : Advances and Challenges Development of Therapeutic Proteins : Advances and Challenges.” *Turkish Journal of Biology* 39: 1–16. https://doi.org/10.3906/biy-1411-8.

Akbarzadeh, Abolfazl, Rogaie Rezaei-sadabady, Soodabeh Davaran, Sang Woo Joo, and Nosratollah Zarghami. 2013. “Liposome : Classification , Preparation , and Applications.” *Nanoscale Research Letters* 8 (1): 1. https://doi.org/10.1186/1556-276X-8-102.

Aktas, Meriyem, Linna Danne, Philip Möller, and Franz Narberhaus. 2014. “Membrane Lipids in Agrobacterium Tumefaciens : Biosynthetic Pathways and Importance for Pathogenesis.” *Frontier in Plant Science* 5 (109): 1–13. https://doi.org/10.3389/fpls.2014.00109.

Alves, Ricardo, Thaís Vitória, Luis Carlos, Silvia Storpírtis, Pita Mercuri, and Rosário Matos. 2010. “Thermal Behavior and Decomposition Kinetics of Rifampicin Polymorphs under Isothermal and Non-Isothermal Conditions.” *Brazilian Journal of Pharmaceutical Sciences* 46 (2): 343–51. https://doi.org/http://dx.doi.org/10.1590/S1984-82502010000200022.

Alzagtat, Ahmeda A, and Inteaz Alli. 2002. “Protein – Lipid Interactions in Food Systems : A

Review." *International Journal of Food Sciences and Nutrition* 53: 249–60. https://doi.org/10.1080/09637480220132850.

Antoine, Etou Mongo, and Comlan H. De Souza. 2007. "Study by Differential Scanning Calorimetry of the Thermal Stability of Whey Proteins Concentrate." *Biotechnology* 6 (3): 431–35. https://doi.org/10.3923/biotech.2007.431.435.

Arca, Hale Çigdem, Laura I. Mosquera-Giraldo, Junia M. Pereira, Nammalwar Sriranganathan, Lynne S. Taylor, and Kevin J. Edgar. 2018. "Rifampin Stability and Solution Concentration Enhancement Through Amorphous Solid Dispersion in Cellulose U-Carboxyalkanoate Matrices." *Journal of Pharmaceutical Sciences* 107: 127–38. https://doi.org/10.1016/j.xphs.2017.05.036.

Ascenzi, Paolo, Alessandro Bolli, Alessandra Di Masi, Grazia R. Tundo, Gabriella Fanali, Massimo Coletta, and Mauro Fasano. 2011. "Isoniazid and Rifampicin Inhibit Allosterically Heme Binding to Albumin and Peroxynitrite Isomerization by Heme-Albumin." *Journal of Biological Inorganic Chemistry* 16: 97–108. https://doi.org/10.1007/s00775-010-0706-2.

Bakaeean, Behnaz, Mona Kabiri, Hedieh Iranfar, Mohammad Reza Saberi, and Jamshidkhan Chamani. 2012. "Binding Effect of Common Ions to Human Serum Albumin in the Presence of Norfloxacin : Investigation with Spectroscopic and Zeta Potential Approaches." *Journal of Solution Chemistry* 41: 1777–1801. https://doi.org/10.1007/s10953-012-9895-3.

Bangham, A D, M M Standish, and J C Watkins. 1965. "Diffusion of Univalent Ions across the Lamellae of Swollen Phospholipids." *Journal of Molecular Biology* 13 (1): 238–52. https://doi.org/10.1016/S0022-2836(65)80093-6.

Barth, Andreas, and Christian Zscherp. 2002. "What Vibrations Tell Us about Proteins." *Quarterly Reviews of Biophysics* 35 (4): 369–430. https://doi.org/10.1017/S0033583502003815.

Bhise, Satish Balakrishna, Avinash Bhanudas More, and Rajkumar Malayandi. 2010. "Formulation and In Vitro Evaluation of Rifampicin Loaded Porous Microspheres." *Scientia Pharmaceutica* 78: 291–302. https://doi.org/10.3797/scipharm.0910-09.

Bi, Shuyun, Lan Ding, Yuan Tian, Daqian Song, Xin Zhou, Xia Liu, and Hanqi Zhang. 2004.

"Investigation of the Interaction between Flavonoids and Human Serum Albumin." *Journal of Molecular Structure* 703: 37–45. https://doi.org/10.1016/j.molstruc.2004.05.026.

Bomsel, Morgane, Daniela Tudor, Anne-sophie Drillet, Annette Alfsen, Yonatan Ganor, Nicolas Mouz, Mario Amacker, et al. 2011. "Immunization with HIV-1 Gp41 Subunit Virosomes Induces Mucosal Antibodies Protecting Nonhuman Primates against Vaginal SHIV Challenges." *Immunity* 34: 269–80. https://doi.org/10.1016/j.immuni.2011.01.015.

Borzova, Vera A., Kira A. Markossian, Natalia A. Chebotareva, Sergey Yu. Kleymenov, Nikolay B. Poliansky, Konstantin O. Muranov, Vita A. Stein-Margolina, Vladimir V. Shubin, Denis I. Markov, and Boris I. Kurganov. 2016. "Kinetics of Thermal Denaturation and Aggregation of Bovine Serum Albumin." *Plos One* 11 (4): 1–29. https://doi.org/10.1371/journal.pone.0153495.

Bouwstra, J.A., G.S. Gooris, W. Bras, and H. Talsma. 1993. "Small Angle X-Ray Scattering : Possibilities and Limitations in Characterization of Vesicles." *Chemistry and Physics of Lipids* 64: 83–98. https://doi.org/https://doi.org/10.1016/0009-3084(93)90059-C.

Bozzuto, Giuseppina, and Agnesse Molinari. 2015. "Liposomes as Nanomedical Devices." *International Journal of Nanomedicine* 10: 975–99. https://doi.org/10.2147/IJN.S68861.

Braun, A, O Couteau, K Franks, V Kestens, G Roebben, A Lamberty, and T P J Linsinger. 2011. "Validation of Dynamic Light Scattering and Centrifugal Liquid Sedimentation Methods for Nanoparticle Characterisation." *Advanced Powder Technology* 22 (6): 766–70. https://doi.org/10.1016/j.apt.2010.11.001.

Brgles, Marija, Darija Jurašin, Maja Dutour Sikirić, Ruža Frkanec, and Jelka Tomašić. 2008. "Entrapment of Ovalbumin into Liposomes — Factors Affecting Entrapment Efficiency , Liposome Size , and Zeta Potential." *Journal of Liposome Research* 18 (3): 235–48. https://doi.org/10.1080/08982100802312762.

Bruschi, Marcos Luciano. 2015. "Mathematical Models of Drug Release." In *Strategies to Modify the Drug Release from Pharmaceutical Systems*, edited by Marcos Luciano Bruschi, 63–86. Elsevier. https://doi.org/10.1016/B978-0-08-100092-2.00005-9.

Bulbake, Upendra, Sindhu Doppalapudi, Nagavendra Kommineni, and Wahid Khan. 2017.

"Liposomal Formulations in Clinical Use: An Updated Review." *Pharmaceutics* 9 (2): 1–33. https://doi.org/10.3390/pharmaceutics9020012.

Çağdaş, Melis, Ali Demir Sezer, and Seyda Bucak. 2014. "Liposomes as Potential Drug Carrier Systems for Drug Delivery." In *Application of Nanotechnology in Drug Delivery*, edited by Ali Demir Sezer, 1–50. IntechOpen. https://doi.org/http://dx.doi.org/10.5772/58459.

Camilloni, Carlo, Daniela Bonet, Angela Morrone, Rajanish Giri, Christopher M Dobson, Maurizio Brunori, Stefano Gianni, and Michele Vendruscolo. 2016. "Towards a Structural Biology of the Hydrophobic Effect in Protein Folding." *Scientific Reports* 6 (28285): 1–9. https://doi.org/10.1038/srep28285.

Caracciolo, Giulio. 2015. "Liposome – Protein Corona in a Physiological Environment : Challenges and Opportunities for Targeted Delivery of Nanomedicines." *Nanomedicine: Nanotechnology, Biology, and Medicine* 11 (3): 543–57. https://doi.org/10.1016/j.nano.2014.11.003.

Casi, Giulio, and Dario Neri. 2012. "Antibody – Drug Conjugates : Basic Concepts , Examples and Future Perspectives." *Journal of Controlled Release* 161 (2): 422–28. https://doi.org/10.1016/j.jconrel.2012.01.026.

Castelli, Francesco, Carmelo Puglia, Maria Grazia, Luisa Rizza, and Francesco Bonina. 2005. "Characterization of Indomethacin-Loaded Lipid Nanoparticles by Differential Scanning Calorimetry." *International Journal of Pharmaceutics* 304: 231–38. https://doi.org/10.1016/j.ijpharm.2005.08.011.

Chauhan, Ashish, and Priyanka Chauhan. 2014. "Powder XRD Technique and Its Applications in Science and Technology." *Journal of Analytical and Bioanalytical Techiques* 5 (5): 1–5. https://doi.org/10.4172/2155-9872.1000212.

Chetanachan, P, P Akarachalanon, D Worawirunwong, P. Dararutana, A. Bangtrakulnonth, M. Bunjop, and S. Kongmuang. 2008. "Ultrastructural Characterization of Liposomes Using Transmission Electron Microscope." *Advanced Materials Research* 55–57: 709–11. https://doi.org/10.4028/www.scientific.net/AMR.55-57.709.

Chi, Eva Y, Sampathkumar Krishnan, Theodore W Randolph, and John F Carpenter. 2003.

"Physical Stability of Proteins in Aqueous Solution : Mechanism and Driving Forces in Nonnative Protein Aggregation." *Pharmaceutical Research* 20 (9): 1325–36. https://doi.org/https://doi.org/10.1023/A:1025771421906.

Colletier, Jacques-philippe, Barnabé Chaize, Mathias Winterhalter, and Didier Fournier. 2002. "Protein Encapsulation in Liposomes : Efficiency Depends on Interactions between Protein and Phospholipid Bilayer ." *BMC Biotechnology* 2 (9). https://doi.org/https://doi.org/10.1186/1472-6750-2-9.

Colletier, Jacques Philippe, Barnabé Chaize, Mathias Winterhalter, and Didier Fournier. 2002. "Protein Encapsulation in Liposomes: Efficiency Depends on Interactions between Protein and Phospholipid Bilayer." *BMC Biotechnology* 2: 1–8. https://doi.org/10.1186/1472-6750-2-9.

Cortesi, R., E. Esposito, S. Gambarin, P. Telloli, E. Menegatti, and C. Nastruzzi. 1999. "Preparation of Liposomes by Reverse-Phase Evaporation Using Alternative Organic Solvents." *Journal of Microencapsulation* 16 (2): 251–56. https://doi.org/10.1080/026520499289220.

Costa, Antonio P., Xiaoming Xu, and Diane J Burgess. 2014. "Freeze-Anneal-Thaw Cycling of Unilamellar Liposomes : Effect on Encapsulation Efficiency." *Pharmaceutical Research* 31: 97–103. https://doi.org/10.1007/s11095-013-1135-z.

Cudahy, Patrick, and Sheela Shenoi. 2016. "Diagnostics for Pulmonary Tuberculosis." *Postgrad Med J.* 92 (1086): 187–93. https://doi.org/10.1136/postgradmedj-2015-133278.Diagnostics.

Daraee, Hadis, Ali Etemadi, Mohammad Kouhi, Samira Alimirzalu, and Abolfazl Akbarzadeh. 2016. "Application of Liposomes in Medicine and Drug Delivery." *Artificial Cells, Nanomedicine, and Biotechnology* 44 (1): 381–91. https://doi.org/10.3109/21691401.2014.953633.

Dash, Suvakanta, Padala Narasimha Murthy, Lilakanta Nath, and Prassanta Chowdhury. 2010. "Kinetic Modeling on Drug Release from Controlled Drug Deliery Systems." *Acta Poloniae Pharmaceutica -Drug Research* 67 (3): 217–23. https://www.ptfarm.pl/pub/File/Acta_Poloniae/2010/3/217.pdf.

Diamantis, Nikolaos, and Udai Banerji. 2016. “Antibody-Drug Conjugates — an Emerging Class of Cancer Treatment.” *British Journal of Cancer* 114: 362–67. https://doi.org/10.1038/bjc.2015.435.

Diehl, Bernd. 2008. “Principles in NMR Spectroscopy.” In *NMR Spectroscopy in Pharmaceutical Analysis*, edited by Ulrike Holzgrabe, Iwona Wawer, and Bernd Diehl, 528. Elsevier. https://doi.org/https://doi.org/10.1016/B978-0-444-53173-5.X0001-7.

Dimitrov, Dimiter S. 2012. “Therapeutic Proteins: Methods and Protocols.” In *Methods in Molecular Biology*, edited by V. Voynov and J. Caravella, 899:1–26. Humana Press, Totowa, NJ. https://doi.org/10.1007/978-1-61779-921-1.

Dorofeev, G A, A N Streletskii, I V Povstugar, A V Protasov, and E P Elsukov. 2012. “Determination of Nanoparticle Sizes by X Ray Diffraction.” *Colloid Journal* 74 (6): 710–20. https://doi.org/10.1134/S1061933X12060051.

Drummond, Daryl C, Monia Zignani, and Jean-christophe Leroux. 2000. “Current Status of PH-Sensitive Liposomes in Drug Delivery.” *Progress in Lipid Research* 39: 409–60. https://doi.org/10.1016/s0163-7827(00)00011-4.

Eaton, P, P Quaresma, C Soares, C Neves, M P De Almeida, E Pereira, and P West. 2017. “A Direct Comparison of Experimental Methods to Measure Dimensions of Synthetic Nanoparticles.” *Ultramicroscopy* 182: 179–90. https://doi.org/10.1016/j.ultramic.2017.07.001.

Edwards, Katie A., and Antje J. Baeumner. 2006. “Analysis of Liposomes.” *Talanta* 68 (5): 1432–41. https://doi.org/10.1016/j.talanta.2005.08.031.

Ekins, Sean. 2014. “Hacking into the Granuloma : Could Antibody Antibiotic Conjugates Be Developed for TB ?” *Tuberculosis* 94 (6): 715–16. https://doi.org/10.1016/j.tube.2014.08.009.

Elzoghby, Ahmed O, Wael M Samy, and Nazik A Elgindy. 2012. “Albumin-Based Nanoparticles as Potential Controlled Release Drug Delivery Systems.” *Journal of Controlled Release* 157 (2): 168–82. https://doi.org/10.1016/j.jconrel.2011.07.031.

Estorninho, Megan, Hilde Smith, Jelle Thole, Jose Harders-westerveen, Andrzej Kierzek, Rachel

E Butler, Olivier Neyrolles, and Graham R Stewart. 2010. “ClgR Regulation of Chaperone and Protease Systems Is Essential for Mycobacterium Tuberculosis Parasitism of the Macrophage.” *Microbiology* 156: 3445–55. https://doi.org/10.1099/mic.0.042275-0.

Fissan, Heinz, Simon Ristig, Heinz Kaminski, Christof Asbach, and Matthias Epple. 2014. “Analytical Methods Comparison of Di Ff Erent Characterization Methods for Nanoparticle Dispersions before and after Aerosolization.” *Analytical Methods* 6: 7324–34. https://doi.org/10.1039/C4AY01203H.

Floss, Heinz G, and Tin-wein Yu. 2005. “Rifamycin - Mode of Action, Resistance, and Biosynthesis.” *Chemical Reviews* 105 (2): 621–32. https://doi.org/10.1021/cr030112j.

Forget, Eric J, and Dick Menzies. 2006. “Adverse Reactions to First-Line Antituberculosis Drugs.” *Expert Opinion on Drug Safety* 5 (2): 231–49. https://doi.org/doi:10.1517/14740338.5.2.231.

Foteini, Papageorgiou, Pippa Natassa, Naziris Nikolaos, and Demetzos Costas. 2019. “Physicochemical Study of the Protein-Liposome Interactions: Influence of Liposome Composition and Concentration on Protein Binding.” *Journal of Liposome Research* 7. https://doi.org/10.1080/08982104.2018.1468774.

Fröhlich, Margret, Volker Brecht, and Regine Peschka-Süss. 2001. “Parameters Influencing the Determination of Liposome Lamellarity by 31P-NMR.” *Chemistry and Physics of Lipids* 109: 103–12. https://doi.org/10.1016/s0009-3084(00)00220-6.

Fu, L.M., and C.S. Fu-Liu. 2002. “Is Mycobacterium Tuberculosis a Closer Relative to Gram-Positive or Gram – Negative Bacterial Pathogens ?” *Tuberculosis* 82 (2/3): 85–90. https://doi.org/10.1054/tube.328.

Gaur, Praveen Kumar, Shikha Mishra, Vipin Bihari Gupta, Mahendra Singh Rathod, Suresh Purohit, and Bhavin A. Savla. 2010. “Targeted Drug Delivery of Rifampicin to the Lungs: Formulation, Characterization, and Stability Studies of Preformed Aerosolized Liposome and in Situ Formed Aerosolized Liposome.” *Drug Development and Industrial Pharmacy* 36 (6): 638–46. https://doi.org/10.3109/03639040903410300.

Ge, Zhaohui, Rong Ma, Guangxian Xu, Zhen Chen, Dangfeng Zhang, Qian Wang, Long Hei,

and Wei Ma. 2018. “Development and In Vitro Release of Isoniazid and Rifampicin-Loaded Bovine Serum Albumin Nanoparticles.” *Medical Science Monitor : International Medical Journal of Experimental and Clinical Research* 24: 473–78. https://doi.org/10.12659/MSM.905581.

Ghanbarzadeh, Saeed, and Sanam Arami. 2013. “Enhanced Transdermal Delivery of Diclofenac Sodium via Conventional Liposomes , Ethosomes , and Transfersomes.” *BioMed Research International* 2013 (616810): 1–7. https://doi.org/http://dx.doi.org/10.1155/2013/616810.

Giron, D. 2002. “Applications of Thermal Analysis and Coupled Techniques in Pharmaceutical Industry.” *Journal of Thermal Analysis and Calorimetry* 68: 335–57. https://doi.org/https://doi.org/10.1023/A:1016015113795.

Gomez, Azucena Gonzalez, Saifuddin Syed, Kenji Marshall, and Zeinab Hosseinidoust. 2019. “Liposomal Nanovesicles for Efficient Encapsulation of Staphylococcal Antibiotics.” Research-article. *ACS Omega* 4: 10866–76. https://doi.org/10.1021/acsomega.9b00825.

Hafez, Ismail M, and Pieter R Cullis. 2000. “Cholesteryl Hemisuccinate Exhibits PH Sensitive Polymorphic Phase Behavior.” *Biochimica et Biophysica Acta* 1463: 107–14. https://doi.org/https://doi.org/10.1016/S0005-2736(99)00186-8.

Heemskerk, Dorothee, Maxine Caws, Ben Marais, and Jeremy Farrar. 2015. *Tuberculosis in Adults and Children*. Springer. https://doi.org/10.1007/978-3-319-19132-4.

Henwood, S Q, Wilna Liebenberg, Lourens R Tiedt, Antonie P Lötter, and Melgardt M De Villiers. 2001. “Characterization of the Solubility and Dissolution Properties of Several New Rifampicin Polymorphs , Solvates , and Hydrates.” *Drug Development and Industrial Pharmacy* 27 (10): 1017–30. https://doi.org/10.1081/DDC-100108364.

Henwood, S Q, M M De Villiers, and W Liebenberg. 2000. “Solubility and Dissolution Properties of Generic Rifampicin Raw Materials.” *Drug Development and Industrial Pharmacy* 26 (4): 403–8. https://doi.org/10.1081/ddc-100101246.

Honary, Soheyla, and Foruhe Zahir. 2013. “Effect of Zeta Potential on the Properties of Nano-Drug Delivery Systems - A Review (Part 2).” *Tropical Journal of Pharmaceutical Research* 12 (2): 265–73. https://doi.org/http://dx.doi.org/10.4314/tjpr.v12i2.20 Effect.

Huebner, Robin E, Maybelle F Schein, John B Bass, and Jr. 1993. “The Tuberculin Skin Test.” *Clinical Infectious Diseases* 17 (6): 968–75. https://doi.org/10.1093/clinids/17.6.968.

Hussain, Afzal, Sima Singh, Sabya Sachi Das, Keshireddy Anjireddy, Subramanian Karpagam, and Faiyaz Shakeel. 2019. “Nanomedicines as Drug Delivery Carriers of Anti-Tubercular Drugs: From Pathogenesis to Infection Control.” *Current Drug Delivery* 16: 400–429. https://doi.org/10.2174/1567201816666190201144815.

ICH. 2005. “Validation of Analytical Procedures : Text and Methodology Q2(R1).” *ICH Harmonised Tripartite Guideline*. https://doi.org/http://www.ich.org/fileadmin/Public_Web_Site/ICH_Products/Guidelines/Quality/Q2_R1/Step4/Q2_R1__Guideline.pdf.

Immordino, Maria Laura, Franco Dosio, and Luigi Cattel. 2006. “Stealth Liposomes : Review of the Basic Science , Rationale , and Clinical Applications , Existing and Potential.” *International Journal of Nanomedicine* 1 (3): 297–315. https://www.ncbi.nlm.nih.gov/pmc/articles/PMC2426795/pdf/nano-0103-297.pdf.

Ingen, Jakko Van, Zeaur Rahim, Arnout Mulder, Martin J Boeree, Roxane Simeone, Roland Brosch, and Dick Van Soolingen. 2012. “Characterization of Mycobacterium Orygis as M. Tuberculosis Complex Subspecies.” *Emerging Infectious Diseases* 18 (4): 653–55. https://doi.org/http://dx.doi.org/10.3201/eid1804.110888.

Jimidar, M. Ilias, Patrick Heylen, and Maurits De Smet. 2007. “Method Validation.” In *HPLC Method Development for Pharmaceuticals*, edited by Satinder Ahuja and Henrik Rasmussen, 8:441–58. London: Academic press. https://doi.org/10.1016/S0149-6395(07)80022-5.

Kalepu, Sandeep, and Sudheer Betha. 2013. “Liposomal Drug Delivery System - A Comprehensive Review.” *Internationl Journal of Drug Development & Research* 5 (4): 62–75. http://www.ijddr.in/drug-development/liposomal-drug-delivery-system--a-comprehensive-review.pdf.

Kamboj, Sunil, Vipin Saini, Nancy Magon, Suman Bala, and Vikas Jhawat. 2013. “Vesicular Drug Delivery Systems : A Novel Approach for Drug Targeting.” *International Journal of*

Drug Delivery 5: 121–30. https://www.arjournals.org/index.php/ijdd/article/view/969/pdf.

Karanth, H, and R S R Murthy. 2007. "PH-Sensitive Liposomes — Principle and Application in Cancer Therapy." *Journal of Pharmacy and Pharmacology* 59: 469–83. https://doi.org/10.1211/jpp.59.4.0001.

Kaur, Kamaljeet, Preeti Kush, Ravi Shankar, and Jitender Madan. 2015. "Stealth Lipid Coated Aquasomes Bearing Recombinant Human Interferon- a -2b Offered Prolonged Release and Enhanced Cytotoxicity in Ovarian Cancer Cells." *Biomedicine & Pharmacotherapy* 69: 267–76. https://doi.org/10.1016/j.biopha.2014.12.007.

Kaur, Manpreet, Tarun Garg, and R. K. Narang. 2016. "A Review of Emerging Trends in the Treatment of Tuberculosis." *Artificial Cells, Nanomedicine, and Biotechnology* 44: 478–84. https://doi.org/10.3109/21691401.2014.962745.

Kim, S.J. 2005. "Drug-Susceptibility Testing in Tuberculosis: Methods and Reliability of Results." *European Respiratory Journal* 25: 564–69. https://doi.org/10.1183/09031936.05.00111304.

Kintzing, James R, Maria V Filsinger Interrante, and Jennifer R Cochran. 2016. "Emerging Strategies for Developing Next-Generation Protein Therapeutics for Cancer Treatment." *Trends in Pharmacological Sciences* 37 (12): 993–1008. https://doi.org/10.1016/j.tips.2016.10.005.

Kirby, Christopher, Jacqui Clarke, and Gregory Gregoriadis. 1980. "Effect of the Cholesterol Content of Small Unilamellar Liposomes on Their Stability in Vivo and in Vitro." *Biochemichal Journal* 186: 591–98. https://doi.org/10.1042/bj1860591.

Kirtansinh, N Gohil, M Patel Piyushbhai, and M Patel Natubhai. 2011. "Application of Analytical Techniques in Preformulation Study : A Review." *International Journal of Pharmaceutical Studies and Biological Archives* 2 (5): 1319–26.

Koyama, T M, C R Stevens, E J Borda, K J Grobe, and D A Cleary. 1999. "Characterizing the Gel to Liquid Crystal Transition in Lipid-Bilayer Model Systems." *Chemical Educator* 4: 12–15. https://doi.org/https://doi.org/10.1007/s00897990273a.

Kratz, Felix. 2008. "Albumin as a Drug Carrier: Design of Prodrugs, Drug Conjugates and

Nanoparticles." *Journal of Controlled Release* 132 (3): 171–83. https://doi.org/10.1016/j.jconrel.2008.05.010.

Krop, Ian, and Eric P Winer. 2014. "Trastuzumab Emtansine : A Novel Antibody – Drug Conjugate for HER2-Positive Breast Cancer." *Clinical Cancer Research* 20 (1): 15–20. https://doi.org/10.1158/1078-0432.CCR-13-0541.

Kruyff, B. De, R. A. Demel, and L.L.M. Van Deenen. 1971. "The Effect of Cholesterol and Epicholesterol Incorporation on the Permeability and on the Phase Transition of Intact Acholeplasma Liadlawii Cell Membranes and Derived Liposomes." *Biochemica et Biophysica Acta* 255 (1972): 331–47. https://doi.org/https://doi.org/10.1016/0005-2736(72)90032-6.

Kudarha, Ritu R, and Krutika K Sawant. 2017. "Albumin Based Versatile Multifunctional Nanocarriers for Cancer Therapy : Fabrication , Surface Modi Fi Cation , Multimodal Therapeutics and Imaging Approaches." *Materials Science & Engineering C* 81 (June): 607–26. https://doi.org/10.1016/j.msec.2017.08.004.

Kumar, S Ashutosh, Manidipa Debnath, J V L N Seshagiri Rao, B Chaitanya, A Durga, G P Sri Ramya, M Ujjwala, P R N Govinda Raj, and P Ganesh Babu. 2014. "Rapid and Sensitive RP-HPLC Analytical Method Development & Validation for Estimation of Rifampicin in Bulk As Well As in Pharmaceutical Formulation By Using Pda Detector." *Indo American Journal of Pharmaceutical Research* 4 (03): 1561–72.

Lagassé, H A Daniel, Aikaterini Alexaki, Vijaya L Simhadri, Nobuko H Katagiri, Wojciech Jankowski, Zuben E Sauna, and Chava Kimchi-sarfaty. 2017. "Recent Advances in (Therapeutic Protein) Drug Development." *F1000 Faculty Rev* 6 (113): 1–17. https://doi.org/10.12688/f1000research.9970.1.

Laouini, A., C. Jaafar-Maalej, I. Limayem-Blouza, C. Sfar, C. Charcosset, and H. Fessi. 2012. "Preparation , Characterization and Applications of Liposomes : State of the Art." *Journal of Colloid Science and Biotechnology* 1: 147–68. https://doi.org/10.1166/jcsb.2012.1020.

Larsen, Maja Thim, Matthias Kuhlmann, Michael Lykke Hvam, and Kenneth A Howard. 2016. "Albumin-Based Drug Delivery : Harnessing Nature to Cure Disease." *Molecular and*

Cellular Therapies 4 (3): 1–12. https://doi.org/10.1186/s40591-016-0048-8.

Leader, Benjamin, Quentin J Baca, and David E Golan. 2008. "Protein Therapeutics: A Summary and Pharmacological Classification." *Nature Reviews Drug Discovery* 7: 21–39. https://doi.org/10.1038/nrd2399.

Lehar, Sophie M, Thomas Pillow, Min Xu, Leanna Staben, Kimberly K Kajihara, Richard Vandlen, Laura Depalatis, et al. 2015. "Novel Antibody – Antibiotic Conjugate Eliminates Intracellular S. Aureus." *Nature* 527: 323–28. https://doi.org/10.1038/nature16057.

Levin, Margaret E, and Graham F Hatfull. 1993. "Mycobacterium Smegmatis RNA Polymerase : DNA Supercoiling , Action of Rifampicin and Mechanism of Rifampicin Resistance." *Molecular Microbiology* 8 (2): 277–85. https://doi.org/10.1111/j.1365-2958.1993.tb01572.x.

Li, Jing, Xuling Wang, Ting Zhang, Chunling Wang, and Zhenjun Huang. 2015. "A Review on Phospholipids and Their Main Applications in Drug Delivery Systems." *Asian Journal of Pharmaceutical Sciences* 10 (2): 81–98. https://doi.org/10.1016/j.ajps.2014.09.004.

Lila, Amr Selim Abu, and Tatsuhiro Ishida. 2017. "Liposomal Delivery Systems : Design Optimization and Current Applications." *Biological and Pharmaceutical Bulletin* 40 (1): 1–10. https://doi.org/10.1248/bpb.b16-00624.

Liu, Zhao, Shuiming Li, Haiyang Wang, Min Tang, Mi Zhou, Jia Yu, Shunjie Bai, Pengfei Li, Jian Zhou, and Peng Xie. 2017. "Proteomic and Network Analysis of Human Serum Albuminome by Integrated Use of Quick Crosslinking and Two-Step Precipitation." *Scientific Reports* 7 (1): 1–11. https://doi.org/10.1038/s41598-017-09563-w.

Lodish, Harvey, Arnold Berk, S Lawrence Zipursky, Paul Matsudaira, David Baltimore, and James Darnell. 2000. *Molecular Cell Biology, 4th Edition*. Edited by W.H. Freeman. New York.

Lopez-Pinto, J.M., M.L. Gonzalez-Rodrıguez, and A.M. Rabasco. 2005. "Effect of Cholesterol and Ethanol on Dermal Delivery from DPPC Liposomes." *International Journal of Pharmaceutics* 298: 1–12. https://doi.org/10.1016/j.ijpharm.2005.02.021.

Machado, A R, Leticia Marques De Assis, Maria Inês Rodrigues Machado, and Leonor Almeida

De Souza-Soares. 2014. “Importance of Lecithin for Encapsulation Processes.” *African Journal of Food Science* 8 (April): 176–83. https://doi.org/10.5897/AJFS2013.1092.

Maherani, B, E. Arab-Tethrany, M R Mozafari, C Gaiani, and M Linder. 2011. “Liposomes : A Review of Manufacturing Techniques and Targeting Strategies.” *Current Nanoscience* 7 (3): 436–52. https://doi.org/10.2174/157341311795542453.

Mariathasan, Sanjeev, and Man-wah Tan. 2017. “Antibody – Antibiotic Conjugates : A Novel Therapeutic Platform against Bacterial Infections.” *Trends in Molecular Medicine* 23 (2): 135–49. https://doi.org/10.1016/j.molmed.2016.12.008.

Martins, João P, Roberto D Auria, Dongfei Liu, Flavia Fontana, Mónica P A Ferreira, Alexandra Correia, Marianna Kemell, et al. 2018. “Engineered Multifunctional Albumin-Decorated Porous Silicon Nanoparticles for FcRn Translocation of Insulin.” *Small* 1800462: 1–11. https://doi.org/10.1002/smll.201800462.

Meloun, B., L. Moravek, and V. Kostka. 1975. “Complete Amino Acid Sequence of Human Serum Albumin.” *FEBS Letters* 58 (1): 134–37. https://doi.org/10.1016/0014-5793(75)80242-0.

Meulen, Jan. 2011. “Monoclonal Antibodies in Infectious Diseases : Clinical Pipeline in 2011.” *Infectious Disease Clinics of NA* 25 (4): 789–802. https://doi.org/10.1016/j.idc.2011.07.006.

Milán-Segovia, R. C., A. M. Domínguez-Ramírez, H. Jung-Cook, M. Magaña-Aquino, M. C. Romero-Méndez, S. E. Medellín-Garibay, M. Vigna-Pérez, and S. Romano-Moreno. 2010. “Relative Bioavailability of Rifampicin in a Three-Drug Fixed-Dose Combination Formulation.” *International Journal of Tuberculosis and Lung Disease* 14 (11): 1454–60.

Moreno-cinos, Carlos, Kenneth Goossens, Irene G Salado, Pieter Van Der Veken, Hans De Winter, and Koen Augustyns. 2019. “ClpP Protease , a Promising Antimicrobial Target.” *International Journal of Molecular Sciences* 20 (2232): 1–19. https://doi.org/10.3390/ijms20092232.

Mozafari, M R. 2005. “Liposomes: An Overview of Manufactring Techniques.” *Cellular and Molecular Biology Letters* 10: 711–19. http://www.cmbl.org.pl/pdf/Vol10_p711.pdf.

———. 2010. “Nanoliposomes : Preparation and Analysis.” In *Liposomes. Methods in*

Molecular Biology, edited by N.J. Clifton, Weissig V., 605:29–59. Humana Press. https://doi.org/10.1007/978-1-60327-360-2.

Murdande, Sharad B, Michael J Pikal, Ravi M Shanker, and Robin H Bogner. 2011. "Aqueous Solubility of Crystalline and Amorphous Drugs : Challenges in Measurement." *Pharmaceutical Development and Technology* 16 (3): 187–200. https://doi.org/10.3109/10837451003774377.

Murray, J E, N Laurieri, and R Delgoda. 2017. "Proteins." In *Pharmacognosy: Fundamentals, Applications and Strategies*, edited by Simone Badal and Rupika Delgoda, 477–94. Elsevier Inc. https://doi.org/10.1016/B978-0-12-802104-0.00024-X.

Nahid, Payam, Susan E Dorman, Narges Alipanah, Pennan M Barry, Jan L Brozek, Adithya Cattamanchi, Lelia H Chaisson, et al. 2016. "Official American Thoracic Society / Centers for Disease Control and Prevention / Infectious Diseases Society of America Clinical Practice Guidelines : Treatment of Drug-Susceptible Tuberculosis." *Clinical Infectious Diseases* 63: 853–67. https://doi.org/10.1093/cid/ciw566.

Nasiruddin, Mohammad, Md. Kausar Neyaz, and Shilpi Das. 2017. "Nanotechnology-Based Approach in Tuberculosis Treatment." *Tuberculosis Research and Treatment* 2017: 1–12. https://doi.org/10.1155/2017/4920209.

Nisini, Roberto, Noemi Poerio, Sabrina Mariotti, Federica De Santis, and Maurizio Fraziano. 2018. "The Multirole of Liposomes in Therapy and Prevention of Infectious Diseases." *Frontiers in Immunology* 9: 1–23. https://doi.org/10.3389/fimmu.2018.00155.

Nkanga, C.I., and Rui Werner Maçedo Krause. 2018. "Conjugation of Isoniazid to a Zinc Phthalocyanine via Hydrazone Linkage for PH-Dependent Liposomal Controlled Release." *Applied Nanoscience* 8 (6): 1313–1323. https://doi.org/https://doi.org/10.1007/s13204-018-0776-y.

———. 2019. "Encapsulation of Isoniazid- Conjugated Phthalocyanine-In- Cyclodextrin-In-Liposomes Using Heating Method." *Scientific Reports* 9: 1–16. https://doi.org/10.1038/s41598-019-47991-y.

Nkanga, C.I., Rui Werner Krause, Xavier Siwe Noundou, and Roderick Bryan Walker. 2017.

"Preparation and Characterization of Isoniazid- Loaded Crude Soybean Lecithin Liposomes." *International Journal of Pharmaceutics* 526 (1–2): 466–73. https://doi.org/10.1016/j.ijpharm.2017.04.074.

Nkanga, C.I., Xavier S Noundou, Roderick B Walker, and Rui W M Krause. 2019. "Co-Encapsulation of Rifampicin and Isoniazid in Crude Soybean Lecithin Liposomes." *South African Journal of Chemistry* 72: 80–87. https://doi.org/https://doi.org/10.17159/0379-4350/2019/v72a11.

Ntimenou, Vassiliki, Spyridon Mourtas, Emmanouil V Christodoulakis, Miltiadis Tsilimbaris, and Sophia G Antimisiaris. 2006. "Stability of Protein-Encapsulating DRV Liposomes After Freeze-Drying : A Study with BSA and t-PA." *Journal of Liposome Research* 16 (4): 403–16. https://doi.org/10.1080/08982100600993003.

Ohline, Shane M, Mary L Campbell, Marilyn T Turnbull, and Susan J Kohler. 2001. "Differential Scanning Calorimetric Study of Bilayer Membrane Phase Transitions A Biophysical Chemistry Experiment." *Journal of Chemical Education* 78 (9): 1251–56. https://doi.org/10.1021/ed078p1251.

Okamoto, Yuko, Kazuaki Taguchi, Keishi Yamasaki, Mina Sakuragi, Shun Kuroda, and Masaki Otagiri. 2018. "Albumin-Encapsulated Liposomes : A Novel Drug Delivery Carrier With Hydrophobic Drugs Encapsulated in the Inner Aqueous Core." *Journal of Pharmaceutical Sciences* 107 (1): 436–45. https://doi.org/10.1016/j.xphs.2017.08.003.

Omwoyo, Wesley Nyaigoti, Bernhards Ogutu, Florence Oloo, Hulda Swai, Paula Melariri, Geoffrey Maroa Mahanga, and Jeremiah Waweru Gathirwa. 2014. "Preparation, Characterization and Optimization of Primaquine-Loaded Solid Lipid Nanoparticles." *International Journal of Nanomedicine* 9: 3865–74. https://doi.org/https://doi.org/10.2147/IJN.S62630.

Pace, C Nick, Hailong Fu, Katrina Lee Fryar, John Landua, Saul R Trevino, A Bret, Marsha Mcnutt Hendricks, et al. 2011. "Contribution of Hydrophobic Interactions to Protein Stability." *Journal of Molecular Biolo* 408 (3): 514–28. https://doi.org/10.1016/j.jmb.2011.02.053.

Paecharoenchai, Orapan, Nattisa Niyomtham, Auayporn Apirakaramwong, Tanasait Ngawhirunpat, Theerasak Rojanarata, Boon-ek Yingyongnarongkul, and Praneet Opanasopit. 2012. "Structure Relationship of Cationic Lipids on Gene Transfection Mediated by Cationic Liposomes." *AAPS PharmSciTech* 13 (4): 1302–8. https://doi.org/10.1208/s12249-012-9857-5.

Pai, Madhukar, Marcel A Behr, David Dowdy, Keertan Dheda, Maziar Divangahi, Catharina C Boehme, Soumya Swaminathan, et al. 2016. "Tuberculosis." *Natural Reviews Disease Primers* 2 (1): 1–23. https://doi.org/10.1038/nrdp.2016.76.

Palomino, Juan Carlos, and Anandi Martin. 2014. "Drug Resistance Mechanisms in Mycobacterium Tuberculosis." *Antibiotics* 3: 317–40. https://doi.org/10.3390/antibiotics3030317.

Panahi, Yunes, Masoud Farshbaf, Majid Mohammadhosseini, Mozhdeh Mirahadi, Rovshan Khalilov, Siamak Saghfi, and Abolfazl Akbarzadeh. 2017. "Recent Advances on Liposomal Nanoparticles : Synthesis , Characterization and Biomedical Applications." *Artificial Cells, Nanomedicine, and Biotechnology* 45 (4): 788–99. https://doi.org/10.1080/21691401.2017.1282496.

Panchagnula, Ramesh, and Vivekanand Bhardwaj. 2008. "Effect of Amorphous Content on Dissolution Characteristics of Rifampicin." *Drug Development and Industrial Pharmacy* 34: 642–49. https://doi.org/10.1080/03639040701842451.

Panowski, Siler, Sunil Bhakta, Helga Raab, Paul Polakis, and Jagath R Junutula. 2014. "Site-Specific Antibody Drug Conjugates for Cancer Therapy." *MAbs* 6 (1): 34–45. https://doi.org/10.4161/mabs.27022.

Patel, Nishith, and Subhranshu Panda. 2012. "Liposome Drug Delivery System : A Critic Review." *Journal of Pharmaceutical and BioSciences Resaearch* 2 (4): 169–75.

Patil, Jagadevappa S, V Kusum Devi, Kshama Devi, and S Sarasija. 2015. "A Novel Approach for Lung Delivery of Rifampicin - Loaded Liposomes in Dry Powder Form for the Treatment of Tuberculosis." *Lung India* 32 (4): 331–38. https://doi.org/10.4103/0970-2113.159559.

Patil, Yogita P, and Sameer Jadhav. 2014. “Novel Methods for Liposome Preparation.” *Chemistry and Physics of Lipids* 177: 8–18. https://doi.org/10.1016/j.chemphyslip.2013.10.011.

Pattni, Bhushan S, Vladimir V Chupin, and Vladimir P Torchilin. 2015. “New Developments in Liposomal Drug Delivery.” *Chemical Reviews* 115: 10938–66. https://doi.org/10.1021/acs.chemrev.5b00046.

Peppas, Nikolaos A, and Jennifer J Sahlin. 1989. “A Simple Equation for the Description of Solute Release. III. Coupling of Diffusion and Relaxation.” *International Journal of Pharmaceutics* 57: 169–72. https://doi.org/https://doi.org/10.1016/0378-5173(89)90306-2.

Petsko, Gregory A, and Dagmar Ringe. 2004. *Protein Structure and Function*. Edited by Eleanor Lawrence and Miranda Robertson. London: New Science Press Ltd.

Prathyusha, K, M Muthukumaran, and B Krishnamoorthy. 2013. “Liposomes as Targetted Drug Delivery Systems Present and Future Prospectives: A Review.” *Journal of Drug Delivery* 3 (4): 195–201. https://doi.org/10.22270/jddt.v3i4.355.

PubChem. 2019. “Rifampicin (Compound).” PubChem. 2019. https://pubchem.ncbi.nlm.nih.gov/compound/Rifampicin.

Randles, Edward G, and Peter R Bergethon. 2013. “A Photodependent Switch of Liposome Stability and Permeability.” *Langmuir* 29: 1490–97. https://doi.org/dx.doi.org/10.1021/la303526k.

Rani, Dash Tapaswi. 2013. “Liposome as a Potential Drug Delivery System: A Review.” *International Research Journal of Pharmacy* 4 (1): 6–12. https://irjponline.com/admin/php/uploads/1559_pdf.pdf.

Riaz, Muhammad Kashif, Muhammad Adil Riaz, Xue Zhang, Congcong Lin, Ka Hong Wong, Xiaoyu Chen, Ge Zhang Id, Aiping Lu, and Zhijun Yang. 2018. “Surface Functionalization and Targeting Strategies of Liposomes in Solid Tumor Therapy : A Review.” *International Journal of Molecular Sciences* 19 (195): 1–27. https://doi.org/10.3390/ijms19010195.

Ruttala, Hima Bindu, and Young Tag Ko. 2015. “Liposome Encapsulated Albumin-Paclitaxel Nanoparticle for Enhanced Antitumor Efficacy.” *Pharmaceutical Research* 32: 1002–16.

https://doi.org/10.1007/s11095-014-1512-2.

Sensi, P. 1983. “History of the Development of Rifampin.” *Reviews of Infectious Diseases* 5 (3): S402–6. https://doi.org/10.1093/clinids/5.supplement_3.s402.

Seth, Avinash Kumar, and Ambikanandan Misra. 2002. “Mathematical Modelling of Preparation of Acyclovir Liposomes: Reverse Phase Evaporation Method.” *Journal of Pharmacy and Pharmaceutical Sciences* 5 (3): 285–91. https://sites.ualberta.ca/~csps/JPPS5(3)/A.Misra2/acyclovir.pdf.

Shrake, A, J S Finlayson, and P D Ross. 1984. “Thermal Stability of Human Albumin Measured by Differential Scanning Calorimetry.” *Vox Sang* 47: 7–18. https://doi.org/10.1111/j.1423-0410.1984.tb01556.x.

Shukla, Anshuman, Bhupinder Singh, and O P Katare. 2011. “Significant Systemic and Mucosal Immune Response Induced on Oral Delivery of Diphtheria Toxoid Using Nano-Bilosomes.” *British Journal of Pharmacology* 164: 820–27. https://doi.org/10.1111/j.1476-5381.2011.01452.x.

Silverman, Jeffrey A, and Steven R Deitcher. 2013. “Marqibo® (Vincristine Sulfate Liposome Injection) Improves the Pharmacokinetics and Pharmacodynamics of Vincristine.” *Cancer Chemother Pharmacol* 71: 555–64. https://doi.org/10.1007/s00280-012-2042-4.

Singh, Charan, L V Seshu Kumar, Arti Singh, and Sarasija Suresh. 2015. “Novel Potential for Optimization of Antitubercular Therapy : Pulmonary Delivery of Rifampicin Lipospheres.” *Asian Journal of Pharmaceutical Sciences* 10 (6): 549–62. https://doi.org/10.1016/j.ajps.2015.08.003.

Sleep, Darrell. 2015. “Albumin and Its Application in Drug Delivery.” *Expert Opinion on Drug Delivery* 12 (5): 1–20. https://doi.org/10.1517/17425247.2015.993313.

Spicer, Christopher D, Coline Jumeaux, Bakul Gupta, and Molly M Stevens. 2018. “Peptide and Protein Nanoparticle Conjugates : Versatile Platforms for Biomedical Applications.” *Chemical Society Reviews* 47: 3574–3620. https://doi.org/10.1039/c7cs00877e.

Sriwongsitanont, Supaporn, and Masaharu Ueno. 2011. “Effect of Freeze-Thawing Process on the Size and Lamellarity of PEG-Lipid Liposomes.” *The Open Colloid Science Journal* 4:

1–6. https://doi.org/10.2174/1876530001104010001.

Stathopulos, Peter B, Guenter A Scholz, Young-mi Hwang, Jessica A O Rumfeldt, James R Lepock, and Elizabeth M Meiering. 2004. “Sonication of Proteins Causes Formation of Aggregates That Resemble Amyloid.” *Protein Science* 13: 3017–27. https://doi.org/10.1110/ps.04831804.Protein.

Stop TB partnership. 2015. “The Global Plan to End TB.” Geneva. http://www.stoptb.org/assets/documents/global/plan/GlobalPlanToEndTB_TheParadigmShift_2016-2020_StopTBPartnership.pdf.

Szoka, Francis, and Demetrios Papahadjopoulos. 1978. “Procedure for Preparation of Liposomes with Large Internal Aqueous Space and High Capture by Reverse-Phase Evaporation.” *Proc. Natl. Acad. Sci. USA* 75 (9): 4194–98. https://doi.org/10.1073/pnas.75.9.4194.

———. 1980. “Comparative Properties and Methods of Preparation of Lipid Vesicles (Liposomes).” *Annual Review of Biophysics and Bioengineering* 9 (1): 467–508. https://doi.org/10.1146/annurev.bb.09.060180.002343.

Tao, Chao, Yon Jin Chuah, Chenjie Xu, and Dong-An Wang. 2019. “Albumin Conjugates and Assemblies as Versatile Bio-Functional Additives and Carriers for Biomedical Applications.” *Journal of Materials Chemistry B* 7: 357–67. https://doi.org/10.1039/c8tb02477d.

Taverna, Myriam, Anne-lise Marie, Jean-paul Mira, and Bertrand Guidet. 2013. “Specific Antioxidant Properties of Human Serum Albumin.” *Annals of Intensive Care* 3 (4): 1–7. https://doi.org/10.1186/2110-5820-3-4.

Taylor, K.M.G., G. Taylor, I.W. Kellaway, and J. Stevens. 1990. “Drug Entrapment and Release from Multilamellar and Reverse-Phase Evaporation Liposomes.” *International Journal of Pharmaceutics* 58: 49–55. https://doi.org/https://doi.org/10.1016/0378-5173(90)90286-D.

Teng, Ooiean, Candice Ke, En Ang, and Xue Li Guan. 2017. “Macrophage – Bacteria Interactions — A Lipid-Centric Relationship.” *Frontiers in Immunology* 8 (1836): 1–17. https://doi.org/10.3389/fimmu.2017.01836.

Timoszyk, Anna. 2017. “Application of Nuclear Magnetic Resonance Spectroscopy (NMR) to

Study the Properties of Liposomes." In *Liposomes*, edited by Angel Catala, 95–126. Rijeka: IntechOpen. https://doi.org/http://dx.doi.org/10.5772/intechopen.68522.

Torchilin, Vladimir P. 2005. "Recent Advances with Liposomes as Pharmaceutical Carriers." *Nature Reviews/Drug Discovery* 4: 145–60. https://doi.org/10.1038/nrd1632.

Velayati, Ali AKbar, and Parissa Farnia. 2017. *The Species Concept*. *Atlas of Mycobacterium Tuberculosis*. Elsevier. https://doi.org/10.1016/B978-0-12-803808-6.00001-3.

Vemuri, Sriram, and C T Rhodes. 1995. "Preparation and Characterization of Liposomes as Therapeutic Systems : A Review." *Pharmaceutca Acta Helvetiae* 70: 95–111. https://doi.org/https://doi.org/10.1016/0031-6865(95)00010-7.

Vhora, Imran, Sushilkumar Patil, Priyanka Bhatt, and Ambikanandan Mirsa. 2015. "Protein – and Peptide – Drug Conjugates : An Emerging Drug Delivery Technology." *Advances in Protein Chemistry and Structural Biology* 98: 1–55. https://doi.org/10.1016/bs.apcsb.2014.11.001.

Volkin, David B, Gautam Sanyal, Carl J Burke, and C Russell Middaugh. 2002. "Preformulation Studies as an Essential Guide to Formulation Development and Manufacture of Protein Pharmaceuticals." In *Development and Manufacture of Protein Pharmaceuticals*, edited by S.L. Nail and M.J. Akers, 1–46. New York: Kluwer Academic/Plenum Publishers. https://doi.org/https://doi.org/10.1007/978-1-4615-0549-5_1.

Walton, Brian L, Monika Leja, Kasey C Vickers, Monica Estevez-fernandez, Angela Sanguino, Elizabeth Wang, Fred J Clubb Jr, Joel Morrisett, and Gabriel Lopez-berestein. 2010. "Delivery of Negatively Charged Liposomes into the Atheromas of Watanabe Heritable Hyperlipidemic Rabbits." *Vascular Medicine* 15 (4): 307–13. https://doi.org/10.1177/1358863X10374118.

Wang, Cong-xia, Fang-fei Yan, Yi-xuan Zhang, and Ling Ye. 2007. "Spectroscopic Investigation of the Interaction between Rifabutin and Bovine Serum Albumin." *Journal of Photochemistry and Photobiology A: Chemistry* 192: 23–28. https://doi.org/10.1016/j.jphotochem.2007.04.032.

Wang, Shun Li, Shan Yang Lin, Mei Jane Li, Yen Shan Wei, and Tzu Feng Hsieh. 2005.

"Temperature Effect on the Structural Stability, Similarity, and Reversibility of Human Serum Albumin in Different States." *Biophysical Chemistry* 114 (2–3): 205–12. https://doi.org/10.1016/j.bpc.2004.12.004.

Wanger, Audrey, Violeta Chavez, Richard S.P. Huang, Amer Wahed, Jeffrey K. Actor, and Amitava Dasgupta. 2017. "Overview of Bacteria." In *Microbiology and Molecular Diagnosis in Pathology 1st Edition*, 75–117. Elsevier. https://doi.org/10.1016/B978-0-12-805351-5.00006-5.

Weiner, George J. 2015. "Building Better Monoclonal Antibody-Based Therapeutics." *Nature Review Cancer* 15 (6): 361–70. https://doi.org/10.1038/nrc3930.

World Health Organization, (WHO). 2010. "Treatment of Tuberculosis: Guidelines." Fourth edi. Geneva. https://apps.who.int/iris/bitstream/handle/10665/44165/9789241547833_eng.pdf?sequence=1.

———. 2016. "WHO Treatment Guidelines for Drug- Resistant Tuberculosis 2016 Update." Geneva. https://apps.who.int/iris/bitstream/handle/10665/250125/9789241549639-eng.pdf?sequence=1.

———. 2018. "Latent Tuberculosis Infection: Updated and Consolidated Guidelines for Programmatic Management." Geneva. https://apps.who.int/iris/bitstream/handle/10665/260233/9789241550239-eng.pdf?sequence=1.

———. 2019. "Global Tuberculosis Report." Geneva. https://apps.who.int/iris/bitstream/handle/10665/329368/9789241565714-eng.pdf?ua=1.

Xu, Huan, Yi-hui Deng, Kai-qian Wang, and Da-wei Chen. 2012. "Preparation and Characterization of Stable PH-Sensitive Vesicles Composed of α -Tocopherol Hemisuccinate." *AAPS PharmSciTech* 13 (4). https://doi.org/10.1208/s12249-012-9863-7.

Xu, Huan, Yihui Deng, Dawei Chen, Jing Qin, Jianfang Liu, Li Shi, and Yi Lu. 2008. "Preparation and Characterization of PH-Sensitive Vesicles Made of Cholesteryl Hemisuccinate." *Drug Development and Industrial Pharmacy* 34: 134–41.

https://doi.org/10.1080/03639040701410903.

Xu, Liang, Yan-xi Hu, Jin Li, Yu-feng Liu, Li Zhang, Hai-xin Ai, and Hong-sheng Liu. 2017. "Probing the Binding Reaction of Cytarabine to Human Serum Albumin Using Multispectroscopic Techniques with the Aid of Molecular Docking." *Journal of Photochemistry & Photobiology, B: Biology* 173: 187–95. https://doi.org/10.1016/j.jphotobiol.2017.05.039.

Yadav, Durgavati, Kumar Sandeep, Deepak Pandey, and Ranu Kumari Dutta. 2017. "Liposomes for Drug Delivery." *Journal of Biotechnology & Biomaterials* 7 (4). https://doi.org/10.4172/2155-952X.1000276.

Yokota, D, M Moraes, and S C Pinho. 2012. "Characterization of Lyophilized Liposomes Produced with Non-Purified Soy Lecithin: A Case Study of Casein Hydrolysate Microencapsulation." *Brazilian Journal of Chemical Engineering* 29 (02): 325–35. https://doi.org/http://dx.doi.org/10.1590/S0104-66322012000200013.

Yokouchi, Yumiko, Tadashi Tsunoda, Tomohiro Imura, Hitoshi Yamauchi, Shoko Yokoyoma, Hideki Sakai, and Masahiko Abe. 2001. "Effect of Adsorption of Bovine Serum Albumin on Liposomal Membrane Characteristics." *Colloids and Surfaces B: Biointerfaces* 20: 95–103. https://doi.org/https://doi.org/10.1016/S0927-7765(00)00176-4.

Yu, Ou-Yang, Yi-Feng Cheng, Shi-Yan Huang, Ai-Min Bai, and Yan-Jun Hu. 2011. "Probing the Binding of Rifampicin to Bovine Serum Albumin in Aqueous Solution." *Journal of Solution Chemistry* 40: 1711–23. https://doi.org/10.1007/s10953-011-9747-6.

Yu, Xiang, Lina Du, Yu Li, Guiying Fu, and Yiguang Jin. 2015. "Improved Anti-Melanoma Effect of a Transdermal Mitoxantrone Ethosome Gel." *Biomedicine and Pharmacotherapy* 73: 6–11. https://doi.org/10.1016/j.biopha.2015.05.002.

Yuksel, Nilufer, Zerrin Sezgin, Elif Aksakal, and A Tanju Ozcelikay. 2016. "In Situ Niosome Forming Maltodextrin Proniosomes of Candesartan Cilexetil : In Vitro and in Vivo Evaluations." *International Journal of Biological Macromolecules* 82: 453–63. https://doi.org/10.1016/j.ijbiomac.2015.10.019.

Zaru, Marco, Chiara Sinico, Alessandro De Logu, Carla Caddeo, Francesco Lai, Maria Letizia

Manca, and Anna Maria Fadda. 2009. “Rifampicin-Loaded Liposomes for the Passive Targeting to Alveolar Macrophages : In Vitro and in Vivo Evaluation.” *Journal of Liposome Research* 19 (1): 68–76. https://doi.org/10.1080/08982100802610835.

Zijenah, Lynn S. 2018. “The World Health Organization Recommended TB Diagnostic Tools.” In *Tuberculosis*, edited by Jean Marie Ntumba Kayembe, 71–90. London: IntechOpen. https://doi.org/http://dx.doi.org/10.5772/intechopen.73070.

Zumla, Alimuddin, Payam Nahid, and Stewart T Cole. 2013. “Advances in the Development of New Tuberculosis Drugs and Treatment Regimens.” *Nature Reviews Drug Discovery* 12 (5): 388–404. https://doi.org/10.1038/nrd4001.